

Transactions in Theoretical and Mathematical Physics

Publisher: Qom University of Technology

ISSN: 3041-8984

Volume: 2, Issue 4, 2025

Available online: <https://ttmp.qut.ac.ir>

Table of Contents

A classical vector method for the curved space–time analysis

Nitin Ramchandra Gadrea

Pages 165-177

Some new considerations about the v-function

Dušan Popov

Pages 178-192

Infinitely Many Fast Homoclinic Solutions for Nonlinear Damped Systems

Mohsen Timoumi

Pages 193-203

The existence of solutions for two types of nonlinear equations on locally finite graphs

Zidong Qiu

Pages 204-218

Elliptic coordinates: applications from geodesy

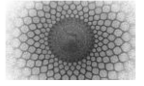
Borzoo Nazzari, Zeinab Nazari Doliskani

Pages 219-224

A splitting operator-based finite difference method for the solution of 2D Fokker-Planck equations

Neena A S, Dominic P Clemence-Mkhope Ashish Awasthi

Pages 225-233



A classical vector method for the curved space–time analysis

Nitin Ramchandra Gadre^{a,1}

¹Vaikunth Mehta Institute, University Road, Pune (India) 411007

Received: 17 August 2025 / Accepted: 22 November 2025 / Published: 26 November 2025

Abstract In flat space, the classical vectors such as a position vector are bilocal (“point for head and point for tail”). The four-dimensional curved-space Schwarzschild metric is mathematically similar to the metric of a sphere surface in three-dimensional flat space, where we can write an incremental displacement vector at a point on surface but cannot write position vectors along the curved surface. Similarly, in curved space, we can write an incremental displacement vector based on the curved-space metric, even if writing a position vector is difficult. We suggest a classical vector method based on this incremental vector which gives all the desired mathematical results including various identities, similar to conventional tensor analysis. We examine whether this mathematical similarity between a curved space and a sphere surface in flat space can also lead to geometrical similarity, but we encounter some difficulties. Therefore, the curved space-time requires discarding bilocal vectors and defining vectors called local vectors. Changing the definition of vectors can overcome the difficulties but introduces new concerns. This Newtonian vector method is an easier mathematical alternative to conventional tensor analysis in curved multidimensional space, and it also illuminates geometrical concerns. We can also establish a relationship between the three-dimensional Lagrangian method and the four-dimensional Geodesic analysis, both giving the same results.

1 Introduction

Classically, there are three important aspects of nature: (a) particles and (b) the empty space around them, and this empty space is filled with a conceptual material called (c) the field, which exerts forces on the particles. The force is a vector. In this article, we try to understand and compare the geometrical pictures of the vectors described in a classical

^ae-mail: nitingadre@gmail.com

approach and in general relativity. In the flat-space classical analysis, we can write a position vector connecting two points in space. Even in this flat space, we cannot write a curved-path position vector between two points on the surface of a sphere, as the directions of unit vectors change along the path. However, we can always write an incremental displacement (position) vector at any point on the sphere. This incremental vector can give a metric corresponding to the sphere surface, in spherical coordinates. We can also write an incremental displacement vector corresponding to the Schwarzschild metric, similar to the incremental displacement vector on the surface of a sphere. We can establish a mathematical similarity of the four-dimensional curved-space metric with the metric for the curved surface of the sphere in a flat space. We shall obtain results identical to those from the tensor analysis in general relativity [1]. We examine whether this mathematical similarity can also lead to a similarity between the classical geometrical pictures. The scheme of this analysis is as follows: (a) initially, we show that the classical vector analysis gives all the desired results, identical to the tensor analysis based on scalar components of tensors; (b) to list all the geometrical difficulties associated with the classical picture; (c) to examine how general relativity can overcome these difficulties by defining a new version of vectors; (d) to present a table giving concerns, if any, about this new definition based on our analysis.

Note that we are attempting to draw a classical geometrical picture of vectors in the multidimensional curved space. Finally, Sec. 5.2 discusses the significance of the vector method.

2 Geometrical aspects of the space

In this section, we revisit the Cartesian and spherical coordinate systems in flat space. We attempt to relate the

mathematical conditions obtained from the geometry of flat space to those of curved space.

2.1 Geometrical requirements for the Christoffel symbol symmetry

The Cartesian coordinate system is a “flat-space, linear coordinate system.” Flat space allows us to write a position vector connecting any two points in space because the directions of unit vectors remain the same along the linear path connecting the two points. The Cartesian coordinates are orthogonal to each other, and the position vector connecting the origin with a point in space is given by $\vec{s} = x \hat{x} + y \hat{y} + z \hat{z}$. This is a bilocal vector connecting two points in space, in the “point for the head and point for the tail” format. The incremental displacement vector is $d\vec{s} = \hat{x} dx + \hat{y} dy + \hat{z} dz = \vec{e}_i dx^i$, where \vec{e}_i denotes the basis vectors. This system is suitable for studying a line segment or a cube. The three-dimensional Cartesian coordinate metric is $ds^2 = dx^2 + dy^2 + dz^2 = \vec{e}_i \cdot \vec{e}_j dx^i dx^j$.

It is often easier to study spherical shapes, such as a sphere, in the spherical coordinate system. This represents a change in the mathematical and geometrical approach, although the physical nature of space itself is not expected to change. We can call this coordinate system a “flat-space, curved coordinate system.” We can write a position vector using the radial coordinate, as the direction of the radial unit vector remains unchanged: $\vec{s} = r \hat{r}$. We define a covariant basis vector $\vec{e}_r = \hat{r}$. It is difficult to specify a precise point in space with this expression, since the direction of the basis vector is a function of position. However, our interest lies in the incremental displacement vector. Because the space is flat in both coordinate systems, we can compare the geometrical pictures of the two to write the spherical unit vectors \hat{r} , $\hat{\theta}$, and $\hat{\phi}$ in terms of the unit vectors of the Cartesian coordinates, such as $\hat{r} = \hat{x} \sin \theta \cos \phi + \hat{y} \sin \theta \sin \phi + \hat{z} \cos \theta$. These relations connect the geometries of the two coordinate systems with mathematics, allowing any mathematical expression to be transformed from one coordinate system to another.

In the spherical coordinate system, an infinitesimally small increment ($ds \rightarrow 0$) of this position vector can be written by differentiating the position vector:

$$\begin{aligned} d\vec{s} &= \vec{e}_r dr + r \times \left(\frac{\partial \vec{e}_r}{\partial r} dr + \frac{\partial \vec{e}_r}{\partial \theta} d\theta + \frac{\partial \vec{e}_r}{\partial \phi} d\phi \right) \\ &= \vec{e}_r dr + \vec{e}_\theta d\theta + \vec{e}_\phi d\phi. \end{aligned} \quad (1)$$

The geometry of the coordinate system gives the other basis vectors, and we can write:

$$\begin{aligned} \frac{\partial \vec{e}_r}{\partial r} &= 0, \quad r \left(\frac{\partial \vec{e}_r}{\partial \theta} \right) = \vec{e}_\theta = r \hat{\theta}, \\ r \left(\frac{\partial \vec{e}_r}{\partial \phi} \right) &= \vec{e}_\phi = r \sin \theta \hat{\phi}. \end{aligned} \quad (2)$$

Hence, the incremental vector is

$$d\vec{s} = \hat{r} dr + r d\theta \hat{\theta} + r \sin \theta d\phi \hat{\phi}. \quad (3)$$

The three-dimensional flat-space metric then follows as $ds^2 = d\vec{s} \cdot d\vec{s} = dr^2 + r^2 d\theta^2 + r^2 \sin^2 \theta d\phi^2$. Suppose $A(r_1, \theta_1)$ and $B(r_2, \theta_2)$ are two very close positions in space, and the difference between the position vectors at B and A is $d\vec{s}$. We can travel along a straight line from A to B ; alternatively, we may first move along the \hat{r} direction and then along the $\hat{\theta}$ direction, or first along $\hat{\theta}$ and then \hat{r} , to reach the same position B . In a flat space, the displacement vector $d\vec{s}$ should be identical irrespective of the path taken. This condition expresses the *path independence* property of the incremental displacement vector:

$$\frac{\partial^2 \vec{s}}{\partial r \partial \theta} = \frac{\partial^2 \vec{s}}{\partial \theta \partial r}. \quad (4)$$

We can write an incremental displacement vector in a generalized coordinate system as $d\vec{s} = \vec{e}_i dx^i$, and the corresponding metric as $ds^2 = \vec{e}_i \cdot \vec{e}_j dx^i dx^j = g_{ij} dx^i dx^j$, where the components of the metric are given by $g_{ij} = \vec{e}_i \cdot \vec{e}_j$. The path independence of the incremental displacement vector can then be expressed as

$$\frac{\partial^2 \vec{s}}{\partial x^j \partial x^i} = \frac{\partial^2 \vec{s}}{\partial x^i \partial x^j}. \quad (5)$$

This condition leads directly to the symmetry of the basis vectors [2].

$$\frac{\partial \vec{e}_i}{\partial x^j} = \frac{\partial \vec{e}_j}{\partial x^i}. \quad (6)$$

In a flat space, the condition (6) is supported by the geometry of the coordinate systems. Eq. (6) expresses the symmetry of the Christoffel symbols ($\Gamma_{ij}^\beta = \Gamma_{ji}^\beta$) with respect to their lower two indices, assuming a torsion-free connection.

$$\frac{\partial \vec{e}_i}{\partial x^j} = \Gamma_{ij}^\beta \vec{e}_\beta = \Gamma_{ji}^\beta \vec{e}_\beta = \frac{\partial \vec{e}_j}{\partial x^i}. \quad (7)$$

Based on these geometrical properties, we can derive the general formula for the Christoffel symbols:

$$\Gamma_{ij}^k = \frac{1}{2} g^{k\alpha} \left(\frac{\partial g_{i\alpha}}{\partial x^j} + \frac{\partial g_{j\alpha}}{\partial x^i} - \frac{\partial g_{ij}}{\partial x^\alpha} \right). \quad (8)$$

Since the metric components are zero for $i \neq j$, this reduces to

$$\Gamma_{ij}^k = \frac{g^{kk}}{2} \left(\frac{\partial g_{ik}}{\partial x^j} + \frac{\partial g_{jk}}{\partial x^i} - \frac{\partial g_{ij}}{\partial x^k} \right), \quad (\text{no sum on } k). \quad (9)$$

The derivation of the Christoffel symbol formula (8) is based on the assumption that the symmetry of the basis vectors, Eq. (6), is satisfied. This can be verified by expressing the metric components as $g_{ij} = \vec{\varepsilon}_i \cdot \vec{\varepsilon}_j$ in Eq. (8). Therefore, whenever we use the Christoffel symbols, it is implicitly presumed that the symmetry of the basis vectors (6) holds true. Now, consider the surface of a sphere. We can draw a curved line segment connecting two points on the sphere surface; however, we cannot write a single mathematical expression for a curved position vector connecting these two points, since the directions of the unit vectors change along the path. If the two points on the sphere surface are very close to each other, we can nevertheless write an incremental displacement vector at that location as $d\vec{s} = r d\theta \hat{\theta} + r \sin \theta d\phi \hat{\phi}$. The corresponding metric at that point is $ds^2 = r^2 d\theta^2 + r^2 \sin^2 \theta d\phi^2$. As $d\vec{s}$ is infinitesimally small, the small surface around it can be treated as locally flat. We obtain the same value of $d\vec{s}$ whether we first move along the $\hat{\theta}$ direction and then along $\hat{\phi}$, or vice versa, between two nearby points on the sphere surface. Therefore, this surface incremental displacement vector satisfies the path-independence property of Eq. (5). Even though writing a position vector on the sphere surface is difficult, the symmetry conditions (5) and (6) are both satisfied by the incremental displacement vector.

As the distance between the two points is very small, this infinitesimally small incremental vector $d\vec{s}$ can be mathematically termed a *local vector*. This local vector can be represented by the coordinates of any one of the two points, say (r_1, θ_1, ϕ_1) , on the sphere surface. As the small surface around this point can be mathematically treated as flat, the small vector $d\vec{s}$ on the surface is equivalent to a small tangent vector in the tangent space at that point. The path-independence property (Eq. (5)) of the vector $d\vec{s}$ on the sphere surface is important for providing geometrical support to the Christoffel-symbol symmetry in Eq. (6). We now proceed to examine the concept and geometry of the curved space.

2.2 Unit vectors and their derivatives in four-dimensional curved space

The classical total energy H for a planet moving around a large mass in a conservative gravitational field, in a three-dimensional flat space, can be written in spherical coordinates as follows. We can treat the mass of the planet as a single unit, since it does not affect the shape of the orbit. The total energy consists of kinetic energy T and potential energy U :

$$\begin{aligned} H &= T + U = K \\ &= \frac{1}{2} \left(\dot{r}^2 + r^2 \dot{\theta}^2 + r^2 \sin^2 \theta \dot{\phi}^2 \right) - \frac{a^2 M}{r}. \end{aligned} \quad (10)$$

Here M is the mass of the central body and r is the radial distance. The Lagrangian analysis ($L = T - U$) of this total-energy equation yields the Newtonian planetary orbits [3]. We can also write a corresponding four-dimensional metric that produces the same Newtonian orbits under a geodesic analysis.

$$ds^2 = dr^2 + r^2 d\theta^2 + r^2 \sin^2 \theta d\phi^2 + e^{-\mu} dt^2. \quad (11)$$

Here $e^\mu = 1 - 2M/r$, and we have introduced an additional fourth coordinate such that $t = \frac{dt}{ds} = a e^\mu$. The space remains flat; we have merely extended it by adding a temporal dimension that yields the same expressions for planetary orbits, which are relations between the distance r (or $u = 1/r$) and the azimuthal angle ϕ .

We now study the curved-space, four-dimensional Schwarzschild metric [4]:

$$ds^2 = -e^\lambda dr^2 - r^2 d\theta^2 - r^2 \sin^2 \theta d\phi^2 + e^\mu dt^2. \quad (12)$$

There is an additional coefficient e^λ that appears in the radial component. It now becomes impossible to write any position vector connecting two points in space, even using the radial coordinate (Sec. 2.3). This coordinate system can therefore be called a *curved-space, curved-coordinate system*. Mathematically, this metric can be treated analogously to the metric for the surface of a sphere in flat space (Sec. 2.1). Similarly, the incremental displacement vector (satisfying $ds^2 = d\vec{s} \cdot d\vec{s}$) corresponding to the Schwarzschild metric can be written as

$$\begin{aligned} d\vec{s} &= \vec{\varepsilon}_r dr + \vec{\varepsilon}_\theta d\theta + \vec{\varepsilon}_\phi d\phi + \vec{\varepsilon}_t dt \\ &= i e^{\lambda/2} \hat{r} dr + ir \hat{\theta} d\theta + ir \sin \theta \hat{\phi} d\phi + e^{\mu/2} \hat{t} dt. \end{aligned} \quad (13)$$

Modifying the flat-space three-dimensional metric g_{jk} to the four-dimensional curved-coordinate metric g_{jk}^m alters both the basis and the unit vectors. For simplicity, we denote this modified metric g_{jk}^m as g_{jk} . It is assumed that μ and λ are functions of r . Imaginary factors have been introduced only so that $i^2 = -1$, with the understanding that all unit vectors are real. These imaginary terms vanish when evaluating the curvature-tensor components. The modified metric coefficients are $g_{11} = -e^\lambda$, $g_{22} = -r^2$, $g_{33} = -r^2 \sin^2 \theta$, and $g_{44} = e^\mu$. The Christoffel symbols can then be calculated using Eq. (9). The modified covariant and contravariant basis vectors are

$$\begin{aligned}\vec{\varepsilon}_r &= i e^{\lambda/2} \hat{r}, & \vec{\varepsilon}_\theta &= ir \hat{\theta}, \\ \vec{\varepsilon}_\phi &= ir \sin \theta \hat{\phi}, & \vec{\varepsilon}_t &= e^{\mu/2} \hat{t},\end{aligned}\quad (14)$$

and

$$\begin{aligned}\vec{\varepsilon}^r &= -e^{-\lambda/2} i \hat{r}, & \vec{\varepsilon}^\theta &= -\frac{i}{r} \hat{\theta}, \\ \vec{\varepsilon}^\phi &= -\frac{i}{r \sin \theta} \hat{\phi}, & \vec{\varepsilon}^t &= e^{-\mu/2} \hat{t}.\end{aligned}\quad (15)$$

The unit vectors are assumed orthogonal, such that $\hat{r} \cdot \hat{r} = \hat{\theta} \cdot \hat{\theta} = \hat{\phi} \cdot \hat{\phi} = \hat{t} \cdot \hat{t} = 1$, and $\hat{r} \cdot \hat{\theta} = \hat{\theta} \cdot \hat{\phi} = \hat{r} \cdot \hat{t} = 0$. We can now obtain the derivatives of the curved-space unit vectors using the Christoffel symbols :

$$\begin{aligned}\frac{\partial \vec{\varepsilon}_t}{\partial t} &= \frac{\partial}{\partial t} (e^{\mu/2} \hat{t}) = \Gamma_{44}^1 \vec{\varepsilon}_t = \frac{1}{2} e^{\mu-\lambda} \mu' \vec{\varepsilon}_r \\ &= \frac{1}{2} e^{\mu-\lambda} \mu' (i e^{\lambda/2} \hat{r}),\end{aligned}\quad (16a)$$

$$\frac{\partial \hat{t}}{\partial t} = \frac{i}{2} \mu' e^{(\mu-\lambda)/2} \hat{r}.\quad (16b)$$

Table 1 compares the derivatives of the unit vectors for the three-dimensional flat space and the four-dimensional curved space. The derivation of the Christoffel-symbol formula (Eq. (8)) is based on the symmetry of basis vectors given by Eq. (6). This presumption continues automatically in curved space since we use the Christoffel symbols. We verify this symmetry using values from Table 1.

$$\begin{aligned}\frac{\partial \vec{\varepsilon}_r}{\partial \theta} &= \frac{\partial}{\partial \theta} (i e^{\lambda/2} \hat{r}) = i e^{\lambda/2} \frac{\partial \hat{r}}{\partial \theta} = \frac{\vec{\varepsilon}_\theta}{r} = \frac{ir \hat{\theta}}{r} \\ &= \Gamma_{r\theta}^\theta \vec{\varepsilon}_\theta = \frac{\partial (ir \hat{\theta})}{\partial r} = \frac{\partial \vec{\varepsilon}_\theta}{\partial r}.\end{aligned}\quad (17)$$

However, it is difficult to propose a clear geometrical picture that supports this symmetry in a four-dimensional curved space (Sec. 2.3). This difficulty leads to contradictory results, as noted in the comments column of Table 1:

1. Row 5: $\hat{\theta}$ is not a function of r .
2. Row 6: $\hat{\theta}$ is a function of r since $\lambda = \lambda(r)$.

We can now identify the first difficulty associated with the geometrical framework of the curved space.

Difficulty 1. It is inconsistent to obtain contradictory derivatives for the same unit vectors (Table 1) associated with the curved-space metric. Consequently, there is no purely geometrical justification for assuming the path independence (Eqs. (5) and (6)) of the incremental displacement vector $d\vec{s}$ defined by Eq. (13) in the four-dimensional curved space (see also Difficulty 3). This marks the key distinction between the geometry of the curved space defined by the Schwarzschild metric and that of a spherical surface embedded in a flat space (Sec. 2.1).

2.3 Geometry of the four-dimensional curved space

We now study the space defined by the Schwarzschild metric to see whether a position vector can be written in the curved space. In analogy with Sec. 2.1, we suggest the spatial position vector $\vec{s} = r \vec{\varepsilon}_r = r i e^{\lambda/2} \hat{r}$. Restricting to the three spatial coordinates and differentiating \vec{s} , using the Schwarzschild Christoffel symbols or the unit-vector derivatives from Table 1:

$$\begin{aligned}d\vec{s} &= \vec{\varepsilon}_r dr + r \left(\frac{\partial \vec{\varepsilon}_r}{\partial r} dr + \frac{\partial \vec{\varepsilon}_r}{\partial \theta} d\theta + \frac{\partial \vec{\varepsilon}_r}{\partial \phi} d\phi \right) \\ &= \left(1 + \frac{r\lambda'}{2} \right) \vec{\varepsilon}_r dr + \vec{\varepsilon}_\theta d\theta + \vec{\varepsilon}_\phi d\phi.\end{aligned}\quad (18)$$

Then, using $r(\partial \vec{\varepsilon}_r / \partial \theta) = \vec{\varepsilon}_\theta = ir \hat{\theta}$ and $r(\partial \vec{\varepsilon}_r / \partial \phi) = \vec{\varepsilon}_\phi = ir \sin \theta \hat{\phi}$ give the same angular basis vectors as required in Sec. 2.2. However, by inserting the entries from Table 1, one finds that this incremental displacement vector is not always path independent:

$$\frac{\partial^2 \vec{s}}{\partial r \partial \theta} \neq \frac{\partial^2 \vec{s}}{\partial \theta \partial r},\quad (19)$$

Also, the incremental vector (18) obtained by differentiating the position vector is not the desired incremental vector (13) corresponding to the Schwarzschild metric. The unit vectors are assumed to be orthogonal (Sec. 2.2) and therefore, the coordinates should be independent. But, a direct verification

of the dot and cross product rules is not possible. We can verify the dot and cross product rules through differentiation using the derivatives in Table 1:

$$(a) \quad \frac{\partial(\hat{r} \cdot \hat{r})}{\partial \theta} = 2 \hat{r} \cdot \frac{\partial \hat{r}}{\partial \theta} = 2 \hat{r} \cdot e^{-\lambda/2} \hat{\theta} = 0. \quad (20)$$

$$(b) \quad \begin{aligned} \frac{\partial(\hat{\theta} \times \hat{\phi})}{\partial \phi} &= \frac{\partial \hat{\theta}}{\partial \phi} \times \hat{\phi} + \hat{\theta} \times \frac{\partial \hat{\phi}}{\partial \phi} \\ &= \sin \theta e^{-\lambda/2} \hat{\phi} = \frac{\partial \hat{r}}{\partial \phi}. \end{aligned} \quad (21)$$

The dot and cross product rules are satisfied by the curved-space unit vectors \hat{r} , $\hat{\theta}$, and $\hat{\phi}$, similar to the unit vectors in a three-dimensional flat-space analysis. We now introduce the fourth coordinate t and suggest a position vector in the curved-space coordinate system as

$\vec{s} = r \vec{\varepsilon}_r + t \vec{\varepsilon}_t = i r e^{\lambda/2} \hat{r} + t e^{\mu/2} \hat{t}$. Differentiating \vec{s} , we obtain the incremental vector

$$\begin{aligned} d\vec{s} &= \left(\vec{\varepsilon}_r + r \frac{\partial \vec{\varepsilon}_r}{\partial r} + t \frac{\partial \vec{\varepsilon}_t}{\partial r} \right) dr + \vec{\varepsilon}_\theta d\theta + \vec{\varepsilon}_\phi d\phi \\ &+ \left(\vec{\varepsilon}_t + r \frac{\partial \vec{\varepsilon}_r}{\partial t} + t \frac{\partial \vec{\varepsilon}_t}{\partial t} \right) dt. \end{aligned} \quad (22)$$

Again, this vector $d\vec{s}$ does not satisfy the path-independence rule for all possible combinations of j and k :

$$\frac{\partial^2 \vec{s}}{\partial x^j \partial x^k} \neq \frac{\partial^2 \vec{s}}{\partial x^k \partial x^j}. \quad (23)$$

The incremental vector in Eq. (22) is not the desired incremental vector corresponding to the Schwarzschild metric given in Eq. (13). It is difficult to write any position vector \vec{s} that, upon differentiation, yields the required incremental displacement vector of Eq. (13). As discussed in Sec. 2.2, the path independence of the incremental displacement vector of Eq. (13) is only a mathematical assumption. The analysis of the curved-space metric is mathematically similar to that of a spherical surface in the flat-space spherical coordinate system (Sec. 2.1). The vector \vec{s} cannot be defined, but we can still write the vector $d\vec{s}$. The differences then arise in the geometrical interpretation. We now examine the cross and dot-product rules.

$$(c) \quad \begin{aligned} \frac{\partial(\hat{r} \cdot \hat{t})}{\partial t} &= \frac{\partial \hat{r}}{\partial t} \cdot \hat{t} + \hat{r} \cdot \frac{\partial \hat{t}}{\partial t} \\ &= -\frac{i\mu'}{2} e^{(\mu-\lambda)/2} \hat{t} \cdot \hat{t} + \frac{i\mu'}{2} e^{(\mu-\lambda)/2} \hat{r} \cdot \hat{r} = 0. \end{aligned} \quad (24)$$

$$(d) \quad \begin{aligned} \frac{\partial(\hat{r} \times \hat{\theta})}{\partial t} &= \frac{\partial \hat{r}}{\partial t} \times \hat{\theta} + \hat{r} \times \frac{\partial \hat{\theta}}{\partial t} \\ &= \frac{1}{2} \mu' e^{(\mu-\lambda)/2} i(\hat{r} \times \hat{\theta}) \\ &= \frac{i}{2} \mu' e^{(\mu-\lambda)/2} \hat{\phi}. \end{aligned} \quad (25)$$

$$(e) \quad \begin{aligned} \frac{\partial(\hat{\phi} \times \hat{r})}{\partial t} &= \frac{\partial \hat{\phi}}{\partial t} \times \hat{r} + \hat{\phi} \times \frac{\partial \hat{r}}{\partial t} \\ &= -\frac{1}{2} \mu' e^{(\mu-\lambda)/2} i(\hat{\phi} \times \hat{r}) = 0. \end{aligned} \quad (26)$$

We can now write four additional difficulties with the geometrical framework of a curved space:

Difficulty 2. The derivatives of the unit vectors \hat{r} , $\hat{\theta}$, and $\hat{\phi}$ satisfy the cross-product rules, but these derivatives should be taken only with respect to r , θ , or ϕ . When the time-like unit vector \hat{t} or the coordinate t is introduced, the cross-product rules fail. From Eq. (e) it is evident that the differentiation of a cross product of two spatial unit vectors also fails when differentiating with respect to the fourth coordinate t .

Difficulty 3. Table 1 was obtained using the Christoffel symbols in Eq. (9), not by differentiating the unit vectors. Because the flat-space unit vectors are modified in the curved space, it is not possible to write explicit expressions for \hat{r} , $\hat{\theta}$, $\hat{\phi}$, and \hat{t} that reproduce the derivatives in Table 1 directly by differentiation, owing to the contradictions noted in the comments column of that table. These coordinates can still be treated as orthogonal (Sec. 2.2), since dot products vanish [Eqs. (a), (c)], but explicit unit-vector forms corresponding to them cannot be written even locally. Hence, a clear geometrical picture of the infinitesimal local vector $d\vec{s}$ of Eq. (13) cannot be drawn (see Difficulty 1).

Difficulty 4. Explicit expressions for the unit vectors are required to write any physical vector such as the force vector. Since these expressions cannot be defined consistently, writing any bilocal (“point-for-head and point-for-tail”) vector is not possible in the curved-space geometry.

Difficulty 5. Due to Difficulty 3, it is not possible to write relationships between the unit vectors of the curved space curved coordinate system and the unit vectors of flat space, spherical or Cartesian coordinate systems (see Sec. 2.1) by comparing their geometrical pictures. Hence, it is not possible to transform either Eq. (13) or the Schwarzschild metric Eq. (12) from curved space, curved coordinate system to flat space spherical or Cartesian coordinate systems. It is not possible to suggest a correspondence between flat space spherical coordinate system and curved space curved coordinate system.

Table 1 Partial derivatives of unit vectors.

Three-dimensional flat space	Four-dimensional curved space	Comments
$\frac{\partial \hat{r}}{\partial r} = 0$	$\frac{\partial \hat{r}}{\partial r} = 0$	If zero in flat space, it remains zero in curved space.
$\frac{\partial \hat{r}}{\partial \theta} = \hat{\theta}$	$\frac{\partial \hat{r}}{\partial \theta} = e^{-\lambda/2} \hat{\theta}$	
$\frac{\partial \hat{r}}{\partial \phi} = \sin \theta \hat{\phi}$	$\frac{\partial \hat{r}}{\partial \phi} = \sin \theta e^{-\lambda/2} \hat{\phi}$	
$\frac{\partial \hat{r}}{\partial t} = 0^a$	$\frac{\partial \hat{r}}{\partial t} = -i \frac{\mu'}{2} e^{(\mu-\lambda)/2} \hat{t}$	
$\frac{\partial \hat{\theta}}{\partial r} = 0$	$\frac{\partial \hat{\theta}}{\partial r} = 0$	$\hat{\theta}$ is not a function of r .
$\frac{\partial \hat{\theta}}{\partial \theta} = -\hat{r}$	$\frac{\partial \hat{\theta}}{\partial \theta} = -e^{-\lambda/2} \hat{r}$	$\hat{\theta}$ is a function of r . as λ is a function of r .
$\frac{\partial \hat{\theta}}{\partial \phi} = \cos \theta \hat{\phi}$	$\frac{\partial \hat{\theta}}{\partial \phi} = \cos \theta \hat{\phi}$	
$\frac{\partial \hat{\theta}}{\partial t} = 0^a$	$\frac{\partial \hat{\theta}}{\partial t} = 0$	
$\frac{\partial \hat{\phi}}{\partial r} = 0$	$\frac{\partial \hat{\phi}}{\partial r} = 0$	$\hat{\phi}$ independent of r .
$\frac{\partial \hat{\phi}}{\partial \theta} = 0$	$\frac{\partial \hat{\phi}}{\partial \theta} = 0$	
$\frac{\partial \hat{\phi}}{\partial \phi} = -\sin \theta \hat{r} - \cos \theta \hat{\theta}$	$\frac{\partial \hat{\phi}}{\partial \phi} = -\sin \theta e^{-\lambda/2} \hat{r} - \cos \theta \hat{\theta}$	$\hat{\phi}$ is a function of r . as λ is a function of r .
$\frac{\partial \hat{\phi}}{\partial t} = 0^a$	$\frac{\partial \hat{\phi}}{\partial t} = 0$	
	$\frac{\partial \hat{t}}{\partial r} = 0$	\hat{t} independent of r .
	$\frac{\partial \hat{t}}{\partial \theta} = 0$	\hat{t} independent of θ .
	$\frac{\partial \hat{t}}{\partial \phi} = 0$	\hat{t} independent of ϕ .
	$\frac{\partial \hat{t}}{\partial r} = i \frac{\mu'}{2} e^{(\mu-\lambda)/2} \hat{r}$	\hat{t} is a function of r due to μ and λ .

^aThe coordinate t is not used in a three-dimensional analysis.

3 A comparison between the tensor and the vector methods

The Schwarzschild metric is given in Eq. (12). In the standard tensor formulation, one seeks to determine the functions λ and μ and the relation between them. This analysis proceeds through the evaluation of the Ricci tensor, the Einstein tensor, and the use of the Bianchi identities. Equivalently, one

can obtain the required tensor equations by taking gradients of the metric or of the basis vectors. In the following, we briefly outline the standard tensor analysis in Sec. 3.1, and then present a corresponding vector formulation in Secs. 3.2 and 3.3, which provides an alternative and more geometrically intuitive interpretation of the same results.

3.1 Tensor analysis: Riemann–Christoffel tensor

In a classical analysis, the force vector can be written as $\vec{F} = F_i \vec{e}^i$. Let us now consider an arbitrary vector $\vec{A} = A_\alpha \vec{e}^\alpha$ in a four-dimensional space. The gradient of a vector, using the summation convention, can be expressed as

$$\begin{aligned} \nabla \vec{A} &= \frac{\partial (A_\alpha \vec{e}^\alpha)}{\partial x^j} \vec{e}^j = \sum_{\alpha=1}^4 \sum_{j=1}^4 \frac{\partial (A_\alpha \vec{e}^\alpha)}{\partial x^j} \vec{e}^j \\ &= \sum_{\alpha=1}^4 \sum_{j=1}^4 \frac{\partial A_\alpha}{\partial x^j} \vec{e}^\alpha \vec{e}^j + A_\alpha \frac{\partial \vec{e}^\alpha}{\partial x^j} \vec{e}^j. \end{aligned} \quad (27)$$

Defining the gradient with respect to a specific index j ,

$$\begin{aligned} \nabla_j \vec{A} &= \sum_{\alpha=1}^4 \frac{\partial (A_\alpha \vec{e}^\alpha)}{\partial x^j} \vec{e}^j \\ &= \sum_{\alpha=1}^4 \frac{\partial A_\alpha}{\partial x^j} \vec{e}^\alpha \vec{e}^j + A_\alpha \frac{\partial \vec{e}^\alpha}{\partial x^j} \vec{e}^j, \end{aligned} \quad (28)$$

we obtain (no sum on j)

$$\begin{aligned} \nabla_j \vec{A} &= \frac{\partial (A_\alpha \vec{e}^\alpha)}{\partial x^j} \vec{e}^j = \frac{\partial A_\alpha}{\partial x^j} \vec{e}^\alpha \vec{e}^j + A_\alpha \frac{\partial \vec{e}^\alpha}{\partial x^j} \vec{e}^j, \\ &= \left(\frac{\partial A_\alpha}{\partial x^j} - A_\beta \Gamma_{j\alpha}^\beta \right) \vec{e}^\alpha \vec{e}^j. \end{aligned} \quad (29)$$

Taking a further gradient with respect to a specific index k , we define the *Riemann curvature tensor* as the measure of non-commutativity of successive covariant derivatives:

$$\begin{aligned} (\nabla_k \nabla_j - \nabla_j \nabla_k) \vec{A} &= A_\beta \left(\frac{\partial \Gamma_{\alpha k}^\beta}{\partial x^j} - \frac{\partial \Gamma_{\alpha j}^\beta}{\partial x^k} + \Gamma_{\gamma j}^\beta \Gamma_{\alpha k}^\gamma - \Gamma_{\gamma k}^\beta \Gamma_{\alpha j}^\gamma \right) \vec{e}^\alpha \vec{e}^j \vec{e}^k \\ &= A_\beta R_{\alpha j k}^\beta \vec{e}^\alpha \vec{e}^j \vec{e}^k. \end{aligned} \quad (30)$$

$$(\nabla_k \nabla_j - \nabla_j \nabla_k) \vec{A} = R_{\alpha j k}^\beta A_\beta \vec{e}^\alpha \vec{e}^j \vec{e}^k, \quad (31)$$

where

$$R_{\alpha j k}^\beta = \frac{\partial \Gamma_{\alpha k}^\beta}{\partial x^j} - \frac{\partial \Gamma_{\alpha j}^\beta}{\partial x^k} + \Gamma_{\gamma j}^\beta \Gamma_{\alpha k}^\gamma - \Gamma_{\gamma k}^\beta \Gamma_{\alpha j}^\gamma. \quad (32)$$

Thus, the curvature tensor can also be written as the difference between the covariant double derivatives of a vector:

$$\begin{aligned} A_{\alpha, j k} - A_{\alpha, k j} &= A_\beta R_{\alpha j k}^\beta \\ &= A_\beta \left(\frac{\partial \Gamma_{k\alpha}^\beta}{\partial x^j} - \frac{\partial \Gamma_{j\alpha}^\beta}{\partial x^k} + \Gamma_{j\gamma}^\beta \Gamma_{k\alpha}^\gamma - \Gamma_{k\gamma}^\beta \Gamma_{j\alpha}^\gamma \right) \end{aligned} \quad (33)$$

The quantity $R_{\alpha j k}^\beta$ is the curvature (Riemann) tensor. We can also express the difference of the double covariant derivatives of a basis vector as

$$(\nabla_k \nabla_j - \nabla_j \nabla_k) \vec{e}^\alpha = R_{i j k}^\alpha \vec{e}^i \vec{e}^j \vec{e}^k. \quad (34)$$

Any physical quantity can be expressed either as a scalar or a vector. We will give the vector analysis corresponding to this work.

3.2 Vector analysis: Gradient and partial derivatives of a vector

Consider a vector $\vec{A}(x^j, x^k) = A_\alpha \vec{e}^\alpha$ defined in space. We first move by a small distance Δx^j from the origin O to a nearby point A . Taking the gradient of this vector with respect to the specific index j , we obtain the corresponding expression for the vector at the new position:

$$\begin{aligned} \vec{A}_{0 \rightarrow j}(x^j + \Delta x^j, x^k) &= A_\alpha \vec{e}^\alpha + (\nabla_j \vec{A}) \cdot \vec{e}_j \Delta x^j \\ &= A_\alpha \vec{e}^\alpha + \frac{\partial (A_\alpha \vec{e}^\alpha)}{\partial x^j} \vec{e}^j \cdot \vec{e}_j \Delta x^j, \end{aligned} \quad (35)$$

We then travel from point A a further distance Δx^k to reach the point B .

$$\begin{aligned} \vec{A}(x^j + \Delta x^j, x^k + \Delta x^k) &= \left[A_\alpha \vec{e}^\alpha + (\nabla_j \vec{A}) \cdot \vec{e}_j \Delta x^j \right] \\ &\quad + \nabla_k \left[A_\alpha \vec{e}^\alpha + (\nabla_j \vec{A}) \cdot \vec{e}_j \Delta x^j \right] \cdot \vec{e}_k \Delta x^k, \end{aligned} \quad (36)$$

Expanding the derivatives explicitly,

$$\begin{aligned} \vec{A}(x^j + \Delta x^j, x^k + \Delta x^k) &= A_\alpha \vec{e}^\alpha + \frac{\partial (A_\alpha \vec{e}^\alpha)}{\partial x^j} \cdot \Delta x^j \\ &\quad + \frac{\partial}{\partial x^k} \left(A_\alpha \vec{e}^\alpha + \frac{\partial (A_\alpha \vec{e}^\alpha)}{\partial x^j} \cdot \Delta x^j \right) \cdot \Delta x^k. \end{aligned} \quad (37)$$

The incremental vector between the two points B and O is $\Delta\vec{A} = \Delta\vec{A}_{O \rightarrow j \rightarrow k} = \vec{A}(x^j + \Delta x^j, x^k + \Delta x^k) - \vec{A}(x^j, x^k)$. We could also reach the same final coordinates by travelling along another route: first moving by Δx^k from O to P , and then by Δx^j from P to Q . The end point B of the first route and end point Q of the second route should be same in a flat space. However, the two routes shall not reach the same point in space if the space is curved. Then, the difference in the incremental vectors will be non-zero and can be written in terms of the difference of the two partial double derivatives of the vector.

$$\Delta(\Delta\vec{A}) = (\vec{A}_{O \rightarrow j \rightarrow k} - \vec{A}_O) - (\vec{A}_{O \rightarrow k \rightarrow j} - \vec{A}_O), \quad (38)$$

$$\begin{aligned} \Delta(\Delta\vec{A}) &= \left(\frac{\partial^2 \vec{A}}{\partial x^k \partial x^j} - \frac{\partial^2 \vec{A}}{\partial x^j \partial x^k} \right) \Delta x^j \Delta x^k \\ &= A_\alpha \left(\frac{\partial^2 \vec{\varepsilon}^\alpha}{\partial x^k \partial x^j} - \frac{\partial^2 \vec{\varepsilon}^\alpha}{\partial x^j \partial x^k} \right) \Delta x^j \Delta x^k. \end{aligned} \quad (39)$$

The term in the parentheses can be written as the difference between the partial double derivatives of $\vec{\varepsilon}^\alpha$:

$$\frac{\partial \vec{\varepsilon}^\alpha}{\partial x^j} = -\Gamma_{j\beta}^\alpha \vec{\varepsilon}^\beta, \quad (40)$$

$$\vec{\varepsilon}_{/jk}^\alpha = \frac{\partial^2 \vec{\varepsilon}^\alpha}{\partial x^k \partial x^j} = -\frac{\partial \Gamma_{j\beta}^\alpha}{\partial x^k} \vec{\varepsilon}^\beta + \Gamma_{j\gamma}^\alpha \Gamma_{k\beta}^\gamma \vec{\varepsilon}^\beta, \quad (41)$$

$$\begin{aligned} \vec{\varepsilon}_{/ijk}^\alpha - \vec{\varepsilon}_{/kji}^\alpha &= \frac{\partial^2 \vec{\varepsilon}^\alpha}{\partial x^k \partial x^j} - \frac{\partial^2 \vec{\varepsilon}^\alpha}{\partial x^j \partial x^k} \\ &= \left(\frac{\partial \Gamma_{k\beta}^\alpha}{\partial x^j} - \frac{\partial \Gamma_{j\beta}^\alpha}{\partial x^k} + \Gamma_{j\gamma}^\alpha \Gamma_{k\beta}^\gamma - \Gamma_{k\gamma}^\alpha \Gamma_{j\beta}^\gamma \right) \vec{\varepsilon}^\beta \\ &= R_{\beta jk}^\alpha \vec{\varepsilon}^\beta. \end{aligned} \quad (42)$$

The scalar coefficient $R_{\beta jk}^\alpha$ of the difference between the two partial double derivatives of $\vec{\varepsilon}^\alpha$, as given by Eq. (42), is the same as the coefficient that appears in the difference of the covariant double gradients in Eq. (34). Even though the partial double derivatives $\partial^2 \vec{A} / \partial x^k \partial x^j$ and the covariant double derivatives $A_{\alpha, jk}$ of a vector \vec{A} are not the same, the coefficients of their differences are identical (Eqs. (33) and (42)). The space is curved whenever $R_{\alpha jk}^\beta \neq 0$. From Eq. (39), this implies that in a curved space the incremental vector is not path independent, and therefore $\Delta(\Delta\vec{A}) \neq 0$.

As this incremental vector $\Delta\vec{A}$ is infinitesimally small, it can be expressed using only the coordinates of the first point and may therefore be regarded as a local vector at that point.

3.3 Vector analysis: Bianchi identity

We can calculate the difference between two partial triple derivative terms, $A_{/jkl} - A_{/jlk}$, as follows:

$$\begin{aligned} \frac{\partial^3 \vec{A}}{\partial x^l \partial x^k \partial x^j} - \frac{\partial^3 \vec{A}}{\partial x^k \partial x^l \partial x^j} &= \frac{\partial A_\alpha}{\partial x^j} \left(\frac{\partial^2 \vec{\varepsilon}^\alpha}{\partial x^l \partial x^k} - \frac{\partial^2 \vec{\varepsilon}^\alpha}{\partial x^k \partial x^l} \right) \\ &+ A_\alpha \left(\frac{\partial^2}{\partial x^l \partial x^k} - \frac{\partial^2}{\partial x^k \partial x^l} \right) \frac{\partial \vec{\varepsilon}^\alpha}{\partial x^j}, \end{aligned} \quad (43)$$

$$\begin{aligned} A_{/jkl} - A_{/jlk} &= \frac{\partial A_\alpha}{\partial x^j} R_{ikl}^\alpha \vec{\varepsilon}^i - A_\alpha \Gamma_{j\beta}^\alpha R_{ikl}^\beta \vec{\varepsilon}^i. \end{aligned} \quad (44)$$

We can write two additional equations by performing cyclic permutations of the indices j, k , and l , and then adding the three resulting expressions.

$$\begin{aligned} (A_{/jkl} - A_{/jlk}) + (A_{/klj} - A_{/kjl}) + (A_{/ljk} - A_{/ljk}) &= \left(\frac{\partial A_\alpha}{\partial x^j} R_{ikl}^\alpha + \frac{\partial A_\alpha}{\partial x^k} R_{ilj}^\alpha + \frac{\partial A_\alpha}{\partial x^l} R_{ijk}^\alpha \right) \vec{\varepsilon}^i \\ &- A_\alpha \left(\Gamma_{j\beta}^\alpha R_{ikl}^\beta + \Gamma_{k\beta}^\alpha R_{ilj}^\beta + \Gamma_{l\beta}^\alpha R_{ijk}^\beta \right) \vec{\varepsilon}^i. \end{aligned} \quad (45)$$

Similarly, we can solve the following combination:

$$\begin{aligned} \vec{A}_{/jkl} - \vec{A}_{/kjl} &= \frac{\partial^3 \vec{A}}{\partial x^l \partial x^k \partial x^j} - \frac{\partial^3 \vec{A}}{\partial x^l \partial x^j \partial x^k} \\ &= \left(\frac{\partial A_\alpha}{\partial x^l} \right) R_{ijk}^\alpha \vec{\varepsilon}^i + A_\alpha \frac{\partial}{\partial x^l} \left(R_{ijk}^\alpha \vec{\varepsilon}^i \right). \end{aligned} \quad (46)$$

We write two more terms by changing the indices in a cyclic manner and adding them:

$$\begin{aligned} (A_{/jkl} - A_{/kjl}) + (A_{/klj} - A_{/ljk}) + (A_{/ljk} - A_{/jlk}) &= \left(\frac{\partial A_\alpha}{\partial x^l} R_{ijk}^\alpha + \frac{\partial A_\alpha}{\partial x^j} R_{ikl}^\alpha + \frac{\partial A_\alpha}{\partial x^k} R_{ilj}^\alpha \right) \vec{\varepsilon}^i \\ &+ A_\alpha \left(\frac{\partial (\vec{\varepsilon}^i R_{ijk}^\alpha)}{\partial x^l} + \frac{\partial (\vec{\varepsilon}^i R_{ikl}^\alpha)}{\partial x^j} + \frac{\partial (\vec{\varepsilon}^i R_{ilj}^\alpha)}{\partial x^k} \right) \end{aligned} \quad (47)$$

We subtract Eq. (45) from (47). The left hand side terms of both the equations are same.

$$A_\alpha \left[\frac{\partial R_{ijk}^\alpha}{\partial x^l} - R_{\beta jk}^\alpha \Gamma_{li}^\beta + R_{ijk}^\beta \Gamma_{l\beta}^\alpha + \frac{\partial R_{ikl}^\alpha}{\partial x^j} - R_{\beta kl}^\alpha \Gamma_{ji}^\beta + R_{ikl}^\beta \Gamma_{j\beta}^\alpha + \frac{\partial R_{ilj}^\alpha}{\partial x^k} - R_{\beta lj}^\alpha \Gamma_{ki}^\beta + R_{ilj}^\beta \Gamma_{k\beta}^\alpha \right] \vec{\varepsilon}^i = 0. \quad (48)$$

The Eq. (48) must hold for any arbitrary vector A_α , and therefore the expression inside the square brackets must vanish for every specific choice of α and i . The coefficient of the basis vector inside the square brackets in Eq. (48) is precisely the Bianchi identity. This identity was obtained by subtracting the same triple-derivative terms in Eq. (45) from those in Eq. (47); hence, the result must always be zero. The derivation does not rely on any additional geometrical or physical assumptions and therefore remains valid for any metric in any number of dimensions. A further contraction of the Bianchi identity yields the Einstein tensor equation.

$$\left(R_l^j - \frac{1}{2} \delta_l^j R \right)_{,j} = G_{l,j}^j = 0. \quad (49)$$

As the Bianchi identity is satisfied by any metric, the covariant derivative of the Einstein tensor G_l^j is always zero, irrespective of the form of the metric or the number of dimensions. We then assume that $G_l^j = 0$ outside the mass. According to general relativity, G_l^j is proportional to the stress-energy tensor, and therefore it vanishes in vacuum. A further contraction yields the Ricci tensor condition in vacuum, $R_{jl} = 0$.

3.4 Space suggested by Ricci tensor condition

We now examine the Schwarzschild metric given in Eq. (12). Using the basis vectors introduced in Sec. 2.2, we compute the Ricci tensor components by applying Eq. (42) together with the curved-space partial derivatives of the unit vectors listed in Table 1.

$$R_{kj} \vec{\varepsilon}^k = R_{kj\alpha}^\alpha \vec{\varepsilon}^k = \left(\frac{\partial^2 \vec{\varepsilon}^\alpha}{\partial x^\alpha \partial x^j} - \frac{\partial^2 \vec{\varepsilon}^\alpha}{\partial x^j \partial x^\alpha} \right). \quad (50)$$

Thus,

$$R_{112}^2 \vec{\varepsilon}^1 = R_{rr\theta}^\theta \vec{\varepsilon}^r = \left(\frac{\partial^2 \vec{\varepsilon}^\theta}{\partial \theta \partial r} - \frac{\partial^2 \vec{\varepsilon}^\theta}{\partial r \partial \theta} \right). \quad (51)$$

$$\frac{\partial \vec{\varepsilon}^\theta}{\partial \theta} = \frac{\partial}{\partial \theta} \left(\frac{-i \hat{\theta}}{r} \right) = \frac{-i}{r} \left(\frac{\partial \hat{\theta}}{\partial \theta} \right) = \left(\frac{i e^{-\lambda/2}}{r} \right) \hat{r}, \quad (52)$$

$$\begin{aligned} \frac{\partial^2 \vec{\varepsilon}^\theta}{\partial r \partial \theta} &= \frac{\partial}{\partial r} \left(\frac{i e^{-\lambda/2}}{r} \hat{r} \right) \\ &= -i e^{\lambda/2} \hat{r} \left(\frac{1}{r^2} + \frac{\lambda'}{2r} \right) = \vec{\varepsilon}^r \left(\frac{1}{r^2} + \frac{\lambda'}{2r} \right). \end{aligned} \quad (53)$$

Then, calculate $R_{rr\theta}^\theta \vec{\varepsilon}^r$. Similarly, calculate $R_{rr\phi}^\phi \vec{\varepsilon}^r$, $R_{rrt}^t \vec{\varepsilon}^r$, and $R_{rrr}^r \vec{\varepsilon}^r = 0$. Then, from Eq. (51):

$$\begin{aligned} R_{rr} \vec{\varepsilon}^r &= \left(R_{rrr}^r + R_{rr\theta}^\theta + R_{rr\phi}^\phi + R_{rrt}^t \right) \vec{\varepsilon}^r \\ &= \left(\frac{\mu''}{2} - \frac{\mu' \lambda'}{4} + \frac{\mu'^2}{4} - \frac{\lambda'}{r} \right) \vec{\varepsilon}^r. \end{aligned} \quad (54)$$

The vector analysis (Eqs. (42) and (50)) yields the same curvature tensor and Ricci tensor components as the standard tensor analysis based on the scalar components of the tensor [4]. The Ricci tensor condition $R_{rr} = 0$ gives the coefficients of the metric as $\mu = -\lambda$ and $e^\mu = 1 - \frac{2M}{r}$.

In a flat space, every curvature tensor component is zero. The Ricci tensor condition $\sum_\alpha R^\alpha_{kj\alpha} = 0$ suggests that the sum of the curvature tensor components, under this contraction, must vanish. Such a space may be described as *approximately flat*. We may write the unit-vector derivatives in this approximately flat space by setting $\lambda = -\mu$ in Table 1. However, even in such a local coordinate system, it remains difficult to write explicit unit-vector expressions (*Difficulty 3*, Sec. 2.3); consequently, constructing a geometrical picture of any classical vector (including the infinitesimal displacement vector $d\vec{s}$) is not possible. An approximately flat space is not equivalent to a flat space in the immediate neighbourhood of $d\vec{s}$ unless $\lambda = -\mu = 0$.

We now examine the behaviour of incremental vectors in the curved space.

4 Path independence property of the incremental vectors

In this section, we compare the path-independence properties of the incremental displacement vector and the incremental vector of any general vector, both in flat space and in curved space.

(a) *Flat-space scenario.*

The covariant derivative of a general vector $\vec{A} = A^\alpha \vec{\varepsilon}_\alpha$ gives a general incremental vector:

$$\begin{aligned} d\vec{A} &= dA^\alpha \vec{\varepsilon}_\alpha + A^\alpha \frac{\partial \vec{\varepsilon}_\alpha}{\partial x^j} dx^j \\ &= (dA^\alpha + A^\beta \Gamma_{\beta j}^\alpha dx^j) \vec{\varepsilon}_\alpha. \end{aligned} \quad (55)$$

In a flat space, this incremental vector of a general vector is path independent, since all curvature tensor components vanish. From Eq. (39), we therefore obtain $\Delta(\Delta\vec{A}) = 0$.

In a three-dimensional flat space (Sec. 2.1), we can write a position vector as, $\vec{A} = \vec{s} = x^\alpha \vec{\varepsilon}_\alpha = r \vec{\varepsilon}_r = r \hat{r}$. Hence, the incremental displacement vector is $d\vec{s} = \hat{r} dr + \hat{\theta} r d\theta + \hat{\phi} r \sin \theta d\phi$. Using the flat-space unit-vector derivatives from Table 1, one verifies that the mixed partial derivatives are symmetric (Eq. (5)). Therefore, the incremental displacement vector is path independent, $\Delta(\Delta\vec{s}) = 0$.

In a flat space, both the incremental vector of a general vector and the incremental displacement vector are obtained in the same way, namely by taking covariant derivatives of their original vectors (\vec{A} and \vec{s}). Hence both incremental vectors are path independent.

(b) *Curved-space scenario.*

In a curved space, some of the curvature tensor components $R_{\beta j k}^\alpha$ (Secs. 3.1 and 3.2) are non-zero. Therefore, the incremental vector of a general vector is not always path independent, $\Delta(\Delta\vec{A}) \neq 0$.

We cannot write any meaningful position vector $\vec{A} = \vec{s}$ in a curved space (Sec. 2.3), and the incremental displacement vector corresponding to the Schwarzschild metric must instead be defined by Eq. (13). The symmetry of the basis vectors has been verified in Eq. (17) using the curved-space unit-vector derivatives in Table 1. Thus, based on Eqs. (6) and (5), we conclude that the incremental displacement vector is always *assumed* to be path independent, $\Delta(\Delta\vec{s}) = 0$. This analysis assumes vanishing torsion (Sec. 2.1).

Based on this discussion, we write the last difficulty with the curved space analysis.

Difficulty 6. The general incremental vector $d\vec{A}$ is *not* always path independent, but the incremental displacement vector $d\vec{s}$ is always path independent. Thus, the two incremental vectors behave differently in the same curved space.

Finally, we summarize the main concerns associated with the four-dimensional curved space:

- It is difficult to write explicit unit-vector expressions or draw a geometrical picture of the coordinate system, as discussed in Secs. 2.2 and 2.3.
- The general incremental vector $d\vec{A}$ is not always path independent, while the incremental displacement vector $d\vec{s}$ is always path independent. Thus the two incremental vectors behave differently in the same curved space.

The Schwarzschild metric contains the coefficient $e^\mu = 1 - 2M/r$, where r is the distance from the central mass (as used in deriving planetary orbits). However, writing a position vector \vec{r} in a curved space is not possible. The tensor analysis is therefore a mathematical procedure involving relations between scalar components of tensors, rather than a construction based on classical geometric vectors.

5 Bilocal and Local vectors and significance of vector method

5.1 Geometrical difficulties with the bilocal vectors and concerns with the local vectors

The classical vector analysis adopted in this article gives all the desired results required by the general relativity. A mathematical analysis of the curved space metric in a classical manner can be treated quite similar to the curved surface of a sphere. But, any attempt to draw a similar classical picture raises some serious geometrical concerns and we have listed six important difficulties in the article. Note that, in this analysis till now, we have not given the specific difference between the three spatial dimensions and the fourth dimension. We have treated the fourth dimension very similar to the three spatial dimensions.

In initial paragraph of Sec. 2.2, we saw that we can introduce an additional fourth coordinate in a three dimensional flat space metric which gives same Newtonian planetary orbits in a four dimensional geodesic analysis as obtained by introducing potential in the three dimensional flat space Lagrangian analysis. We can also write a total energy equation for a body in motion under a conservative field, corresponding to the Schwarzschild metric. This mathematical correspondence is limited to obtaining the same planetary orbits from both the general relativistic and classical approaches. We know that physical interpretations of both approaches are different.

In a classical approach, the fourth coordinate can be introduced through an arbitrary variable, for example $i = a e^{-\mu}$. Using this definition, we may write the corresponding modified total-energy equation by assuming $\mu = -\lambda$ and $e^\mu = 1 - \frac{2M}{r}$.

$$H^m = \frac{e^{-\mu} \dot{r}^2 + r^2 \dot{\theta}^2 + r^2 \sin^2 \theta \dot{\phi}^2 - e^\mu \dot{i}^2}{2} = -\frac{1}{2}. \quad (56)$$

By inserting the expression for i into Eq. (56), we obtain a purely three-dimensional equation. Here, H^m , T^m , and U^m denote the modified total energy, kinetic energy, and potential energy, respectively, in the curved space.

$$\begin{aligned}
H^m &= \frac{e^{-\mu} \dot{r}^2 + r^2 \dot{\theta}^2 + r^2 \sin^2 \theta \dot{\phi}^2}{2} - \frac{a^2 e^{-\mu}}{2} \\
&= T^m + U^m = -\frac{1}{2}.
\end{aligned} \tag{57}$$

The Lagrangian analysis of this three-dimensional total-energy equation [3] yields the three components of the force along the spatial coordinates. Solving these equations reproduces the same planetary orbits (for $\theta = 90^\circ$) as those obtained from the general-relativistic geodesic analysis of the Schwarzschild metric. However, this analysis in curved space encounters significant geometrical difficulties. It is hard to provide geometrical support for the symmetry of the basis vectors discussed in Sec. 2.2 (Difficulty 1), even though such symmetry is also a necessary requirement of the Lagrangian formulation. As shown in Sec. 2.3, it is difficult to write explicit unit-vector expressions in curved space. We may mathematically assume that the coordinates are orthogonal (as in Sec. 2.2), but writing the force vector becomes problematic because the unit-vector expressions themselves cannot be constructed.

Thus, the classical analysis up to this point may give the impression that the four-dimensional Schwarzschild metric is mainly a mathematical structure that reproduces the correct planetary orbits, while lacking an appropriate underlying geometrical interpretation.

We now examine how general relativity provides remedies for these geometrical difficulties, remedies that require fundamental changes in the underlying geometrical concepts. In general relativity, the fourth coordinate is identified with time, and every point in the four-dimensional space-time manifold corresponds to a physical event. Consequently, the conventional notion of a vector must be modified in curved space-time (see Ref. [1]). The familiar interpretation of vectors as arrows connecting two points (a “bilocal” picture with a head and a tail) must be abandoned. In curved space-time, such a bilocal construction is not well defined. Instead, vectors must be treated as *purely local* objects. They cannot be translated physically from one point to another, and each vector is attached to a specific event on the manifold.

There is therefore no position vector on a general curved manifold. Points are labelled only by their coordinates and are not themselves vectors. Rather, vectors are elements of the tangent space at each event, and the basis vectors are given by the coordinate partial derivatives along the coordinate lines:

$$\vec{e}_i \equiv \frac{\partial}{\partial x^i}. \tag{58}$$

Modifying the three-dimensional flat space metric to the four-dimensional curved space-time metric modifies geometry

and also the interpretations of the physical phenomenon. Completely discarding the bilocal vectors, can overcome some of the difficulties listed in the article but this also raises some new concerns. Therefore, drawing the classical orbits showing the mass bodies rotating with certain velocities can still remain difficult. In a classical Newtonian picture, both bodies rotate around the center of mass by exerting forces on each other and we have to incorporate the reduced mass in calculations. This factor becomes important if the mass of the planet is not small compared with the central mass. Analysis of such situation will be quite complicated in a geodesic analysis and we normally study situations where central mass is very large. We shall list the difficulties with the classical vectors and briefly discuss how the general relativity tries to overcome these difficulties by defining a new version of vectors called the local vectors in Table 2. This modification raises some new concerns which are also briefly discussed in the Table 2.

Before proceeding, we recall the distinction between bilocal and local vectors as used in our analysis. The classical vectors \vec{s} and \vec{A} are *bilocal* vectors: they point from one point in space to another and therefore depend simultaneously on two spatial locations. Such bilocal vectors are not admissible in curved space-time (Sec. 2.3). In contrast, the infinitesimally small classical incremental vectors $d\vec{s}$ and $d\vec{A}$ can be treated mathematically as *local* vectors, since they are represented entirely by the coordinates of a single point in space (Secs. 2.1, 2.2, and 3.2). These local vectors reside in the tangent space associated with that point and do not require a bilocal construction.

5.2 Significance of the vector method

Finally, we discuss the significance of the vector method used in Sec. 3.2, Sec. 3.3 and Sec. 3.4. An element of arc $d\vec{s}$ can be written as $ds^2 = g_{ij} dx^i dx^j$. This tensor is called a metric tensor because all the metric properties of space should be completely determined by this tensor. Success of a curved space multidimensional analysis very much depends upon the intelligent choice of the metric tensor and this may not easily enlighten us about the geometrical aspects of the physical problem. However, an incremental displacement vector $d\vec{s} = \vec{e}_i dx^i$ corresponding to this multidimensional metric can be written in terms of basis vectors such that, $g_{ij} = \vec{e}_i \cdot \vec{e}_j$. The basis vector symmetry condition (6) is true for zero torsion condition. Suitable conditions will have to be written if we wish to study nonzero torsion situations. In Section 3, we have shown that the Riemann-Christoffel tensor is related to the second partial derivatives while the Bianchi identity is related to the third partial derivatives of these basis vectors. Describing the classical vectors encounters various geometrical difficulties (Sec. 2.2, Sec. 2.3, Sec. 4). The standard general relativity has tried to overcome these

Table 2. The problems, the remedies, and the concerns with the remedies

Difficulties with a classical bilocal vector in a curved space	Remedy in GR: redefine vectors as local vectors in spacetime	Concerns regarding the local-vector formulation and the geometry of spacetime
Difficulty in defining a coordinate system (Sec. 2.3): In flat space a global coordinate system can be chosen with any convenient origin to describe positions, motions, and vectors. In curved space a global coordinate system is not possible.	In curved spacetime vectors are defined as <i>local</i> . One can only attempt to define a <i>local coordinate system</i> attached to each event.	In four-dimensional curved space one cannot write unit-vector expressions corresponding to coordinates even in a local frame. Thus writing classical vector expressions becomes difficult.
Difficulty in writing classical vector expressions (Sec. 2.3): Unit vectors cannot be written, and hence classical vectors (displacement, velocity, force) cannot be expressed. A Lagrangian force-based analysis becomes inappropriate for planetary orbits.	Planets do not orbit because of forces acting on them. Instead, one writes geodesic equations; geodesics around a central mass describe planetary motion.	In the Schwarzschild geometry, r, θ, ϕ are used with the same scalar meaning as in flat space when describing orbits, but the curved-space unit vectors cannot be related to flat-space unit vectors. No geometrical picture of vectors along (r, θ, ϕ) is possible. Even the basis vectors of Eq. (58) cannot be given classical unit-vector representations.
Difficulty with path independence (Secs. 4 and 2.2): The general incremental vector $d\vec{A}$ is <i>not</i> always path independent, whereas the incremental displacement vector $d\vec{s}$ is always path independent. Thus, the two behave differently in the same curved space.	The fourth coordinate is defined as time. There are <i>no bilocal vectors</i> in curved spacetime; GR uses only local vectors attached to events. Hence the notion of “path independence of vectors” loses physical meaning.	Time is the fourth coordinate to maintain consistency with special relativity. Local vectors such as $d\vec{s}$ and $d\vec{A}$ can be defined because the second point is infinitesimally close. In flat space or on a sphere, an infinitesimal patch is nearly flat and derivatives behave symmetrically. But in curved space, the tangent space cannot be assumed flat even locally near $d\vec{s}$. Thus the assumption that $d\vec{s}$ and $d\vec{A}$ behave differently has no clear geometrical explanation.
Difficulty with symmetry of Christoffel symbols (Sec. 2.2): There is no geometrical justification for path independence of $d\vec{s}$ or symmetry of basis vectors. Thus symmetric Christoffel symbols appear as a mathematical assumption.	The symmetry of Christoffel symbols is not derived from path independence. In GR the basis vectors are defined as partial derivatives along the coordinate lines (Eq. (58)). They commute because partial derivatives commute.	Partial second derivatives of a scalar are symmetric; for vectors only in flat space. Basis vectors in curved space commute only if the space is locally flat. But even in Ricci-flat space (Sec. 3.4) one cannot write unit vectors. Thus local flatness may not guarantee commuting basis vectors. Hence symmetric Christoffel symbols are a mathematical assumption with limited geometric support.
Difficulty with cross product (Sec. 2.3): Cross products fail when the fourth coordinate is introduced.	Orthogonal cross product is meaningful only in 3D; not in 4D. The fourth coordinate is time; a cross product involving time has no geometrical meaning.	The three spatial unit vectors obey dot and cross product rules under differentiation in curved space; the time-like unit vector obeys only the dot-product rule. GR discards bilocal vectors; therefore classical geometric meaning of dot and cross products between two local vectors becomes unclear.

difficulties by (Sec. 5.1) redefining the vector [1] as a local vector (Eq. (58)) but this definition also raises some new concerns. But, note that, the vector method, based on the classical incremental vectors gives all the desired mathematical results including various identities, similar to the conventional tensor analysis based on scalar components of tensors. A vector analysis is inherently superior to a scalar analysis as a vector has both magnitude and direction. This vector method, based on a classical geometrical picture, is an easier mathematical alternative to the tensor analysis in the curved multidimensional space and also throws light on the geometrical complications, if any, in describing such curved space. This method is generic in nature as it can be applied to any metric of any dimensions. We can also establish rela-

tionship between the three-dimensional Lagrangian method and the four-dimensional Geodesic analysis, both giving the same results.

6 Conclusion

This article has initially attempted to study the geometrical representation of vectors in a curved space. The Schwarzschild metric represents a four-dimensional curved-space geometry. This metric can be mathematically compared with the metric of the surface of a sphere embedded in a three-dimensional flat space, where we can write an incremental displacement vector at a point but cannot write a position vector linking two distinct points on the surface. Likewise, in the four-

dimensional curved space it is difficult to write a position vector, but we can write an incremental displacement vector based on the four-dimensional metric. This incremental-vector-based classical approach reproduces exactly the same results as the tensor analysis of general relativity, but it faces several geometrical difficulties. We have discussed six such difficulties, which may create the impression that curved space-time lacks appropriate geometrical support. This article has examined why a new definition of vector is required in curved space-time and how it helps overcome these geometrical difficulties.

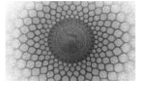
In general relativity, the fourth dimension is designated as time, so each point in space is associated with a specific event. The temptation to regard vectors as arrows linking two events has to be discarded [1]. The bilocal (head–tail) version of a vector must be replaced by a purely local version. There is no position vector on a manifold, and vectors cannot be physically transported as arrows; each vector must be attached to a specific local event. The difficulties encountered by classical (bilocal) vectors become the basis for assigning the peculiar characteristics of vectors in curved space-time. We can redefine the geometrical picture only because the fourth dimension represents time and is distinct from the spatial dimensions. Using this new definition, one may attempt to draw the geometrical picture of planetary motion in four-dimensional space-time. However, the new definition also raises additional geometrical concerns, especially when one tries to visualize vectors. It is accepted that we can not write bilocal vectors such as a position vector \vec{s} or a general vector \vec{A} in the curved space-time. But we realize that their incremental vectors $d\vec{s}$ and $d\vec{A}$ exhibit different path-independence properties in the same curved space and it is not possible to provide any geometrical justification for this behaviour. Such characteristics are evident only from a vector analysis.

However, we can still adopt the vector method, which is based on the classical incremental vectors to get all the desired mathematical results including various identities, similar to the conventional tensor analysis. This geometrical vector method can work as an easier mathematical alternative to the tensor analysis in the curved multidimensional space and also throws light on the geometrical concerns, if any, in describing such curved space. This Newtonian analysis is generic in nature as it can be applied to any metric of any dimensions. We can also establish relationship between the three-dimensional Lagrangian method and the four-dimensional Geodesic analysis, both giving the same results.

Acknowledgements The mathematical analysis in this article, especially the tensor and vector algebra, is based on lectures by Dr. V. R. Marathe (Professor (Retd.), Tata Institute of Fundamental Research, Mumbai). Dr. A. P. Sathe (Professor (Retd.), Institute of Science, Mumbai) gave valuable suggestions regarding the final draft. This article would not have been possible without the support and guidance of my esteemed professors.

References

1. C.W. Misner, K.S. Thorne, J.A. Wheeler, *Gravitation*, W.H. Freeman, San Francisco (1973)
2. G. Arfken, *Mathematical Methods for Physicists*, Academic Press, New York (1985)
3. K.R. Symon, *Mechanics*, Addison–Wesley, Massachusetts (1964)
4. I.S. Sokolnikoff, *Tensor Analysis: Theory and Applications*, John Wiley & Sons, London (1951)



Some new considerations about the ν -function

Dušan Popov^{1,2,a}

¹ University Politehnica Timișoara, Department of Physical Foundations of Engineering,
Bd. V. Pârvan No. 2, 300223 Timișoara, Romania

² Serbian Academy of Nonlinear Sciences (SANS), Belgrade, Serbia

Received: 27 July 2025 / Accepted: 26 November 2025 / Published: 26 November 2025

Abstract In this work, we construct a new family of coherent states associated with generalized hypergeometric functions. These hypergeometric coherent states are introduced through an appropriate choice of weight factors in the Fock space expansion. We analyze their mathematical structure, normalization and completeness, and we examine the corresponding photon number distribution and statistical properties. The results show that the hypergeometric coherent states exhibit both classical-like and non-classical features, such as sub-Poissonian statistics and quadrature squeezing. This framework provides a unifying approach to a broad class of coherent states and may open pathways for new applications in quantum optics and related areas of mathematical physics.

Furthermore, we focus on generalized hypergeometric coherent states (GH-CSs) for a continuous spectrum. We establish their basic mathematical properties (normalization, completeness, overlaps) and investigate their statistical characteristics (photon distribution, sub-Poissonian behavior). We also point out possible applications in quantum mechanics, as well as in quantum optics and related domains, where these states may serve as useful models for non-classical light. The formalism of such coherent states naturally leads to a mathematical “feedback”: one is led to obtain and solve integrals involving ν -functions, thereby enlarging the range of applications of these functions.

1 Introduction

In this work, we focus on a new family of coherent states based on generalized hypergeometric functions. Hypergeometric functions appear naturally in many areas of mathematical physics, including solutions of differential equations, special function theory, and representations

of orthogonal polynomials. By employing hypergeometric functions in the definition of coherent states, we aim to unify and extend several previously studied classes of states within a single framework. The purpose of this paper is to construct and analyze these hypergeometric coherent states, to establish their mathematical properties such as normalization and completeness, and to investigate their statistical characteristics, including photon number distribution, sub-Poissonian behavior, and quadrature squeezing. We also highlight possible applications in quantum optics and related domains, where these states may serve as useful models for non-classical light. The purpose of this paper is to construct and analyze these generalized hypergeometric coherent states (GHCSs) for continuous spectrum, to establish some mathematical properties (normalization, completeness, overlap), and to investigate their statistical characteristics (photon distribution, sub-Poissonian behavior). We also highlight some possible applications in quantum mechanics, as well as in quantum optics and related domains, where these states may serve as useful models for non-classical light. Also, the formalism of this type of CSs implicitly leads to a mathematical feedback: obtaining and solving integrals involving the ν -functions, which implicitly means an expansion of the applications that use these functions.

As is well known, for some function $f(E)$, the Laplace transform is defined by the integral

$$\mathcal{L}\{f\}(s) = \int_0^{\infty} dE e^{-sE} f(E), \quad (1)$$

where s is a complex number.

On the other hand, the reciprocal gamma function can be written as

^ae-mail: dusan_popov@yahoo.co.uk

$$f(E+1) = \frac{1}{\Gamma(E+1)}. \quad (2)$$

By combining Eqs. (1) and (2), we obtain

$$\mathcal{L}\{f\}(e^{-s}) = \int_0^\infty dE \frac{e^{-sE}}{\Gamma(E+1)}. \quad (3)$$

If we set

$$e^{-s} = z, \quad z = |z|e^{i\varphi}, \quad 0 \leq |z| \leq R_c \leq \infty, \quad (4)$$

where R_c is the radius of convergence of the power series in the variable $|z|$, then Eq. (3) becomes

$$\nu(z) \equiv \mathcal{L}\{f\}(s) = \int_0^\infty dE \frac{z^E}{\Gamma(E+1)}. \quad (5)$$

A new function $\nu(z)$ thus appears on the right-hand side. This is the so-called ν -function, which may be regarded as a generalization of the Laplace transform of the reciprocal gamma function. The ν -function was introduced by Volterra in 1916 [1]. Apart from a few classical monographs [1, 2], there are relatively few references in the literature dealing explicitly with $\nu(z)$.

A further generalization is the function $\nu(z, \alpha)$, defined by [1]

$$\nu(z, \alpha) = \int_0^\infty dE \frac{z^{E+\alpha}}{\Gamma(E+1+\alpha)}, \quad (6)$$

which reduces to $\nu(z)$ for $\alpha = 0$. The relation between these two functions can be expressed in terms of derivatives with respect to z as

$$\frac{d^n}{dz^n} \nu(z) = \nu(z, -n), \quad (7)$$

so that higher-order derivatives of $\nu(z)$ generate the family $\nu(z, \alpha)$.

On the other hand, one may consider the most general form of coherent states (CSs) in quantum mechanics, expanded in the Fock basis $\{|n\rangle, n = 0, 1, 2, \dots, n_{\max} \leq \infty\}$. These are the generalized hypergeometric coherent states (GH-CSs), defined by [3]

$$|z\rangle = \frac{1}{\sqrt{{}_pF_q(\{a_i\}_1^p, \{b_j\}_1^q; |z|^2)}} \sum_{n=0}^{n_{\max} \leq \infty} \frac{z^n}{\sqrt{\rho_{p,q}(n)}} |n\rangle, \quad (8)$$

where p, q are non-negative integers and $\{a_i\}, \{b_j\}$ are parameter sets entering the generalized hypergeometric functions. We adopt the notation $\{x_i\}_{i=1}^m \equiv (x_1, x_2, \dots, x_m)$.

The Pochhammer symbols $(a_i)_n$ appear in the structure constants. The name ‘‘generalized hypergeometric coherent states’’ comes from the fact that their normalizing function ${}_pF_q(\{a_i\}_{i=1}^p; \{b_j\}_{j=1}^q; |z|^2)$ is a generalized hypergeometric function. Moreover, the positive constants $\rho_{p,q}(n)$ are assumed to arise as the moments of a probability distribution [4], and for GH-CSs they are defined as follows [5]:

$$\rho_{p,q}(n) \equiv n! \frac{\prod_{j=1}^q (b_j)_n}{\prod_{i=1}^p (a_i)_n}, \quad (9)$$

so that the normalization function can be written as [6]

$$\begin{aligned} & {}_pF_q(\{a_i\}_{i=1}^p; \{b_j\}_{j=1}^q; |z|^2) \\ &= \sum_{n=0}^{\infty} \frac{\prod_{i=1}^p (a_i)_n}{\prod_{j=1}^q (b_j)_n} \frac{|z|^{2n}}{n!} = \sum_{n=0}^{\infty} \frac{|z|^{2n}}{\rho_{p,q}(n)}. \end{aligned} \quad (10)$$

Any family of coherent states must satisfy the well-known Klauder prescriptions [7]:

- Normalization and non-orthogonality:

$$\langle z | z' \rangle = \begin{cases} 1, & \text{if } z = z', \\ \neq 0, & \text{if } z \neq z'. \end{cases} \quad (11)$$

- Continuity in the label z :

$$\lim_{z' \rightarrow z} \|z - z'\| = 0. \quad (12)$$

- Resolution of the identity:

$$\int d\mu(z) |z\rangle\langle z| = \hat{I} = \sum_{n=0}^{\infty} |n\rangle\langle n|, \quad (13)$$

where $d\mu(z) = \frac{d^2z}{\pi} = \frac{d\rho}{2\pi} d(|z|^2) h(|z|^2)$ is a measure with a positive weight function $h(|z|^2)$, to be determined for each family of coherent states.

Although at first glance there seems to be no connection between the two concepts introduced above, namely the ν -function $\nu(z)$ and the generalized coherent states (GH-CSs) $|z\rangle$, it was shown in Ref. [8] that such a connection does exist. This may be regarded as the first physical application of the ν -function. In the present paper we aim to deepen this connection, leading to a series of new properties of the ν -function $\nu(z)$ that do not appear in the specialized literature.

In Ref. [8] we also examined the transition from a discrete spectrum (d) to a continuous spectrum (c) for a given quantum system. We found that if a certain limiting procedure—referred to as the discrete–continuous limit $d \rightarrow c$ —is applied, any quantity associated with a system possessing a discrete spectrum is mapped to the corresponding quantity associated with the continuous spectrum.

There exist quantum systems whose spectra include both discrete and continuous parts. A well-known example is the diatomic molecule, whose internuclear potential is accurately represented by the Morse potential. This potential supports a finite number of discrete energy levels corresponding to bound states. For sufficiently large values of the vibrational quantum number n , i.e. for energies exceeding the dissociation energy D_e , the molecule dissociates under external influences such as increasing temperature. In this regime the two nuclei (together with their electrons) behave as free particles, and the spectrum becomes continuous.

Let us emphasize that, for a given quantum system, two types of coherent states can be defined: (a) Barut–Girardello (BG) coherent states, introduced as the eigenstates of an annihilation operator [9]; and (b) Klauder–Perelomov (KP) coherent states, obtained by applying a displacement operator to the vacuum state [10]. Although their expansions in the Fock basis differ, the two families are dual. This duality manifests itself in the fact that the indices p and q and the corresponding parameter sets $\{a_i\}_{i=1}^p$ and $\{b_j\}_{j=1}^q$ can be interchanged [11]. However, when the discrete–continuous limit $d \rightarrow c$ is applied, both families converge to the same mathematical structure, identical to that of the coherent states of the one-dimensional harmonic oscillator (HO–1D). For this reason, and in light of the aims of the present work, we shall restrict our atten-

tion to the Barut–Girardello type coherent states as our starting point [11].

2 The main results from Ref. [8]—in short

To begin with, let us consider a dimensionless Hamiltonian \mathcal{H} with a non-degenerate continuous spectrum, together with a corresponding set of dimensionless eigenstates $|E\rangle$ (where $\hbar\omega = 1$ is assumed). The energies lie in the interval $0 \leq E < \infty$ and the eigenstates are normalized in the sense of Dirac delta functions:

$$\mathcal{H}|E\rangle = E|E\rangle, \quad \langle E|E'\rangle = \delta(E - E'). \quad (14)$$

The closure, or completeness relation, for a continuous spectrum takes the form

$$\int_0^{\infty} dE |E\rangle\langle E| = \hat{I}, \quad (15)$$

and therefore

$$\int_0^{\infty} dE \langle E'|E\rangle\langle E|E''\rangle = \delta(E' - E''). \quad (16)$$

The coherent states corresponding to the continuous spectrum can be obtained by applying a suitable limiting procedure, which we refer to as the discrete–continuous limit $d \rightarrow c$ (for brevity). This limit has been introduced and discussed in detail in Ref. [13]; see also Ref. [8].

$$X_c(E) = \lim_{n \rightarrow E} X_d(n, n_{\max}) \equiv \lim_{d \rightarrow c} X_d(n, n_{\max}), \quad (17)$$

$$\begin{array}{l} n_{\max} \rightarrow \infty \\ \sum_0^{\infty} \rightarrow \int_0^{\infty} \\ p=q \\ \{a_i\} = \{b_j\} \end{array}$$

and

$$\sum_{n=0}^{n_{\max}} X_d(n, n_{\max}) \longrightarrow \int_0^{\infty} dE X_c(E). \quad (18)$$

Thus, establishing the correspondence between the observables (or quantities) of the discrete spectrum, X_d , and those of the continuous spectrum, X_c , requires the following operations: (a) the discrete quantum number n must be replaced by the dimensionless energy E ; (b) the maximal number of bound states must tend to infinity,

$n_{\max} \rightarrow \infty$; (c) simultaneously, the summation over n must be replaced by an integral over E ; (d) the indices p and q of the generalized hypergeometric functions, as well as the parameter sets $\{a_i\}_{i=1}^p$ and $\{b_j\}_{j=1}^q$, must be taken equal.

Consequently, we obtain the following limits:

$$\lim_{d \rightarrow c} \rho_{p,q}(n) = \lim_{d \rightarrow c} n! \frac{\prod_{j=1}^q (b_j)_n}{\prod_{i=1}^p (a_i)_n} = \Gamma(E+1), \quad (19)$$

$$\begin{aligned} \lim_{d \rightarrow c} {}_pF_q(\{a_i\}_{i=1}^p; \{b_j\}_{j=1}^q; |z|^2) \\ = \lim_{d \rightarrow c} \sum_{n=0}^{\infty} \frac{|z|^{2n}}{\rho_{p,q}(n)} \\ = \int_0^{\infty} \frac{|z|^{2E}}{\Gamma(E+1)} dE = \nu(|z|^2). \end{aligned} \quad (20)$$

This leads to the following limit for GH-CSs:

$$|z\rangle = \lim_{d \rightarrow c} |z\rangle = \frac{1}{\sqrt{\nu(|z|^2)}} \int_0^{\infty} \frac{z^E}{\sqrt{\Gamma(E+1)}} |E\rangle dE. \quad (21)$$

The expression of coherent states (CSs) for a continuous spectrum was first obtained—by different methods and considerations—for the Gazeau–Klauder coherent states in Ref. [4], and later reconsidered in Refs. [13] and [14].

The overlap of two coherent states follows immediately and is given by

$$\langle z | z' \rangle = \lim_{d \rightarrow c} \langle z | z' \rangle = \frac{\nu(z^* z')}{\sqrt{\nu(|z|^2) \nu(|z'|^2)}}. \quad (22)$$

Observation: To avoid overloading the notation, we keep the same complex variable z for both the discrete and the continuous spectra; in other words, $\lim_{d \rightarrow c} z = z$. Whenever necessary, and only in order to avoid ambiguity, we will explicitly indicate the indices d or c .

Using the Mellin transform of the Meijer G -function [1],

$$\begin{aligned} \int_0^{\infty} x^{s-1} G_{p,q}^{m,n} \left(\omega x \left| \begin{matrix} \{a_i\}_{i=1}^n; \{a_i\}_{i=n+1}^p \\ \{b_j\}_{j=1}^m; \{b_j\}_{j=m+1}^q \end{matrix} \right. \right) dx \\ = \omega^{-s} \frac{\prod_{j=1}^m \Gamma(b_j + s) \prod_{i=1}^n \Gamma(1 - a_i - s)}{\prod_{j=m+1}^q \Gamma(1 - b_j - s) \prod_{i=n+1}^p \Gamma(a_i + s)}. \end{aligned} \quad (23)$$

The integration measure of a GH-CS, as defined in Eq. (6), for a discontinuous spectrum was obtained in Ref. [15], and it is given by

$$\begin{aligned} d\mu_{p,q}^{(d)}(z) = \frac{d\varphi d(|z|^2)}{2\pi} \frac{\prod_{i=1}^p \Gamma(a_i)}{\prod_{j=1}^q \Gamma(b_j)} \\ \times F_{p,q}(\{a_i\}_{i=1}^p; \{b_j\}_{j=1}^q; |z|^2) \\ \times G_{p,q+1}^{q+1,0} \left(|z|^2 \left| \begin{matrix} /; & \{a_i - 1\}_{i=1}^p \\ 0, \{b_j - 1\}_{j=1}^q; & / \end{matrix} \right. \right). \end{aligned} \quad (24)$$

so that its limit is

$$\lim_{d \rightarrow c} d\mu_{p,q}^d(z) = \frac{d\varphi d(|z|^2)}{2\pi} e^{-|z|^2} \nu(|z|^2) \equiv d\mu^c(z). \quad (25)$$

where we have used the specialized value of the Meijer G -function, namely $G_{0,1}^{1,0}(|z|^2 | 0) = e^{-|z|^2}$, see Ref. [6].

In this context, the following relationship is also valid

$$\begin{aligned} \lim_{d \rightarrow c} \int d\mu_{p,q}^d(z) |z\rangle \langle z| \\ = \int d\mu^c(z) |z\rangle \langle z| = \int_0^{\infty} dE |E\rangle \langle E| = \hat{I}. \end{aligned} \quad (26)$$

In performing the demonstration through the corresponding substitutions, after the angular integration, we used a fundamental integral:

$$\begin{aligned}
& \int_0^\infty d(|z|^2) (|z|^2)^E \\
& \times G_{p,q+1}^{q+1,0} \left(\begin{matrix} |z|^2 \\ 0, \{b_j - 1\}_{j=1}^q \end{matrix} \middle| \begin{matrix} /; & \{a_i - 1\}_{i=1}^p \\ / & \end{matrix} \right) \\
& = \Gamma(E+1) \frac{\prod_{j=1}^q \Gamma(b_j + E)}{p} = \frac{\prod_{j=1}^p \Gamma(b_j)}{q} \rho_{p,q}(E), \\
& \prod_{i=1}^q \Gamma(a_i + E) \quad \prod_{i=1}^p \Gamma(a_i)
\end{aligned} \tag{27}$$

which will be useful in the following.

As we showed previously in Ref. [5], the GH-CSs are generated by a pair of creation and annihilation operators, \mathcal{A}_+ and \mathcal{A}_- . A new operational ordering procedure, called DOOT (the diagonal ordering operation technique), can be applied to these operators. This approach leads to several new results, both for the discontinuous spectrum [15] and for the continuous one [8].

The pair operators are $(\mathcal{A})^+ = \mathcal{A}_+$ and satisfy the following equations:

$$\begin{aligned}
\mathcal{A}^- |n\rangle &= \sqrt{n} |n-1\rangle, \\
\mathcal{A}^+ |n\rangle &= \sqrt{n+1} |n+1\rangle, \\
\mathcal{A}^+ \mathcal{A}^- |n\rangle &= |n\rangle.
\end{aligned} \tag{28}$$

Their action on the vectors $|E\rangle$ follows from applying the discrete-continuous limit $d \rightarrow c$ to their discrete counterparts:

$$\begin{aligned}
\mathcal{A}_- |E\rangle &= E |E-1\rangle, \\
\mathcal{A}_+ |E\rangle &= (E+1) |E+1\rangle, \\
\mathcal{A}_+ \mathcal{A}_- |E\rangle &= E |E\rangle.
\end{aligned} \tag{29}$$

In Ref. [8], for the continuous spectrum we introduced a real, dimensionless energy parameter $\varepsilon > 0$, which is not a quantum number but may be interpreted as a suitable “unit jump” in the energy scale of continuous spectra. By choosing $\varepsilon = 1$, the system energy can be written simply as $E = m$. If we apply the raising operator \mathcal{A}_+ successively m times to the ground (vacuum) state $|0\rangle$, then for the continuous spectrum we obtain

$$\begin{aligned}
|E\rangle &= \frac{1}{\Gamma(E+1)} (\mathcal{A}_+)^E |0\rangle, \\
\langle E| &= \frac{1}{\Gamma(E+1)} \langle 0| (\mathcal{A}_-)^E.
\end{aligned} \tag{30}$$

Starting from Eqs (14)-(15) and applying the DOOT rules (for details, see Refs. [12],[15]), we obtain the expression of the vacuum-state projector for the continuous spectrum, $|0\rangle\langle 0|$:

$$\begin{aligned}
\int_0^\infty dE |E\rangle\langle E| &= |0\rangle\langle 0| \int_0^\infty \frac{\# (\mathcal{A}_+ \mathcal{A}_-)^E \#}{\Gamma(E+1)} dE \\
&= |0\rangle\langle 0| \# \nu(\mathcal{A}_+ \mathcal{A}_-) \# = 1,
\end{aligned} \tag{31}$$

$$|0\rangle\langle 0| = \frac{1}{\# \nu(\mathcal{A}_+ \mathcal{A}_-) \#}. \tag{32}$$

The symbol $\# \cdot \#$ denotes the normal (diagonal) ordering of operators within the DOOT formalism.

Consequently, the projector in the energy eigenvector basis, $|E\rangle\langle E|$, is given by

$$|E\rangle\langle E| = \# \frac{(\mathcal{A}_+ \mathcal{A}_-)^E}{\Gamma(E+1)} \frac{1}{\nu(\mathcal{A}_+ \mathcal{A}_-)} \#. \tag{33}$$

With the above relations and the DOOT rules, the CSs for the continuous spectrum becomes:

$$\begin{aligned}
|z\rangle &= \frac{1}{\sqrt{\nu(|z|^2)}} \int_0^\infty dE \frac{(z \mathcal{A}_+)^E}{\Gamma(E+1)} |0\rangle \\
&= \frac{1}{\sqrt{\nu(|z|^2)}} \nu(z \mathcal{A}_+) |0\rangle.
\end{aligned} \tag{34}$$

and similarly for their dual counterparts, so that the projector onto the coherent state $|z\rangle$ is given by

$$|z\rangle\langle z| = \frac{1}{\nu(|z|^2)} \# \frac{\nu(z \mathcal{A}_+) \nu(z^* \mathcal{A}_-)}{\nu'(\mathcal{A}_+ \mathcal{A}_-)} \#. \tag{35}$$

The correctness of this expression can be verified by using the completeness relation for coherent states, Eq. (25).

$$\begin{aligned}
& \int d\mu^c(z) |z\rangle\langle z| \\
&= \# \frac{1}{\nu(\mathcal{A}_+\mathcal{A}_-)} \# \int_0^\infty d(|z|^2) e^{-|z|^2} \\
& \int_0^{2\pi} \frac{d\varphi}{2\pi} \# \nu(z\mathcal{A}_+) \nu(z^*\mathcal{A}_-) \# = 1.
\end{aligned} \tag{36}$$

because the angular integral is

$$\begin{aligned}
& \int_0^{2\pi} \frac{d\varphi}{2\pi} \# \nu(z\mathcal{A}_+) \nu(z^*\mathcal{A}_-) \# \\
&= \int_0^\infty dE \frac{\# (\mathcal{A}_+\mathcal{A}_-)^E \#}{[\Gamma(E+1)]^2} |z|^{2E}.
\end{aligned} \tag{37}$$

On the other hand, the probability density for the transition from the energy eigenstate $|E\rangle$ to the coherent state $|z\rangle$ is given by

$$P(|z|^2) \equiv |\langle z | E \rangle|^2 = \frac{1}{\nu(|z|^2)} \frac{|z|^{2E}}{\Gamma(E+1)}. \tag{38}$$

If we apply the inverse limit, that is, the continuous–discrete limit $c \rightarrow d$, we recover precisely the Poisson probability density function corresponding to the discrete case.

$$\begin{aligned}
\lim_{c \rightarrow d} \nu(|z|^2) &= \lim_{E \rightarrow n} \int_0^\infty dE \frac{|z|^{2n}}{\Gamma(E+1)} \\
& \int \rightarrow \sum \\
&= \sum_{n=0}^\infty \frac{|z|^{2n}}{\Gamma(n+1)} = e^{|z|^2},
\end{aligned} \tag{39}$$

$$\begin{aligned}
\lim_{c \rightarrow d} P(|z|^2) &= \lim_{E \rightarrow n} P(|z|^2) \\
& \int \rightarrow \sum \\
&= e^{-|z|^2} \frac{|z|^{2n}}{n!} \equiv P_n^{\text{Poiss}}(|z|^2).
\end{aligned} \tag{40}$$

This result shows that the coherent states $|z\rangle$ obey sub-Poissonian statistics, i.e. they exhibit non-classical features.

From the relations above, it is clear that the ν -function, $\nu(|z|^2)$, naturally appears in the description of the continuous spectrum of a quantum system. To the best of our knowledge, this represents the first application of the ν -function $\nu(|z|^2)$ in a non-mathematical scientific context, namely in quantum mechanics and, more specifically, in quantum optics.

3 The generalized discrete–continuous limit $d \rightarrow c$

Let us now generalize the main results obtained in Ref. [8] and examine the practical consequences of this generalization. Compared with the limit used in this paper, Eqs (17)–(18), we will now adopt a less restrictive limit, namely:

$$\begin{aligned}
X_c(E) &= \lim_{n \rightarrow E} X_d(n, n_{\max}) \\
& \lim_{n_{\max} \rightarrow \infty} \sum_{n=0}^\infty \rightarrow \int_0^\infty dE \\
&\equiv \lim_{d \rightarrow c} X_d(n, n_{\max}) \\
\sum_{n=0}^{n_{\max}} X_d(n, n_{\max}) &\rightarrow \int_0^\infty X_c(E) dE.
\end{aligned} \tag{41}$$

This means that all observables X_c that characterize a system with a continuous spectrum are obtained as limiting cases of the corresponding observables X_d of the discrete spectrum, through the following three operations: (a) replacing the discrete quantum number n by the dimensionless energy E ; (b) extending the upper bound $n_{\max} \rightarrow \infty$; (c) simultaneously replacing the sum over n by an integral over E .

For this reason, we shall refer to this transformation as the *generalized discrete–continuous limit* $d \rightarrow c$, or simply the *Gd–cL*. In what follows, we also introduce the notation *d-GH-CSs* for the generalized hypergeometric coherent states associated with the discrete spectrum, and *c-GH-CSs* for those associated with the continuous spectrum.

Let us now apply the Gd–cL to the objects that characterize the discontinuous spectrum.

$$\begin{aligned}
\lim_{d \rightarrow c} \rho_{p,q}(n) &= \lim_{d \rightarrow c} n! \frac{\prod_{j=1}^q (b_j)_n}{\prod_{i=1}^p (a_i)_n} \\
&= \Gamma(E+1) \frac{\prod_{j=1}^q (b_j)_E}{\prod_{i=1}^p (a_i)_E} \equiv \rho_{p,q}(E).
\end{aligned} \tag{42}$$

where the Pochhammer symbols are defined by $(x)_E = \frac{\Gamma(x+E)}{\Gamma(x)}$.

$$\begin{aligned}
 \lim_{d \rightarrow c} \mathcal{F}(\{a\}_p; \{b\}_q; |z|^2) &= \lim_{d \rightarrow c} \sum_{n=0}^{\infty} \frac{\prod_{i=1}^p (a_i)_n}{\prod_{j=1}^q (b_j)_n} \frac{|z|^{2n}}{n!} \\
 &= \int_0^{\infty} dE \frac{\prod_{i=1}^p (a_i)_n}{\prod_{j=1}^q (b_j)_n} \frac{|z|^{2E}}{\Gamma(E+1)} \\
 &= \int_0^{\infty} dE \frac{|z|^{2E}}{\rho_{p,q}(E)} \\
 &\equiv {}_p\mathcal{F}_q(\{a\}_1^p; \{b\}_1^q; |z|^2) = \nu_{p,q}(|z|^2).
 \end{aligned} \tag{43}$$

It is observed that a function similar to the generalized hypergeometric function is obtained, but defined not by a sum, but by an integral. We will call this new object the *integral generalized hypergeometric function* (int-GHF), and we denote it by ${}_p\mathcal{F}_q(\{a\}_1^p; \{b\}_1^q; |z|^2)$, which is precisely the ν -function in the continuous formulation. Let us note that the last integral has the same structure as the ordinary ν -function $\nu(|z|^2)$, but in a much more general form, in accordance with Eq. (27). For this reason we call it the *generalized ν -function* ($G\nu$), $\nu_{p,q}(|z|^2)$, which is in fact equal to the integral generalized hypergeometric function (int-GHF) ${}_p\mathcal{F}_q(\{a\}_1^p; \{b\}_1^q; |z|^2)$.

$$\begin{aligned}
 \nu_{p,q}(|z|^2) &\equiv \int_0^{\infty} \frac{|z|^{2E}}{\rho_{p,q}(E)} dE \\
 &= \int_0^{\infty} dE \frac{\prod_{i=1}^p (a_i)_E}{\prod_{j=1}^q (b_j)_E} \frac{|z|^{2E}}{\Gamma(E+1)} \\
 &\equiv {}_p\mathcal{F}_q(\{a\}_1^p; \{b\}_1^q; |z|^2).
 \end{aligned} \tag{44}$$

In the special case $p = q = 0$, we have

$$\begin{aligned}
 \nu_{0,0}(|z|^2) &\equiv \nu(|z|^2) \\
 &= \int_0^{\infty} \frac{|z|^{2E}}{\Gamma(E+1)} dE \\
 &\equiv {}_0\mathcal{F}_0(;; |z|^2) = \exp(|z|^2).
 \end{aligned} \tag{45}$$

In this context, we may state that the function $\nu(|z|^2)$ is an *integral exponential function*, namely the integral representation of $\exp(|z|^2)$.

Note: This integral exponential function $\exp(|z|^2)$ must not be confused with the *exponential integral* $\text{Ei}(x)$, for real x , which is a special function defined on the complex plane by

$$\text{Ei}(x) = - \int_{-x}^{\infty} \frac{e^{-t}}{t} dt = \int_{-\infty}^x \frac{e^t}{t} dt. \tag{46}$$

Consequently, the Gd-cl of the GH-CSs is

$$\begin{aligned}
 \lim_{d \rightarrow c} |z\rangle &\equiv |z\rangle \\
 &= \frac{1}{\sqrt{\nu_{p,q}(|z|^2)}} \int_0^{\infty} \frac{z^E}{\sqrt{\rho_{p,q}(E)}} |E\rangle dE.
 \end{aligned} \tag{47}$$

Since the construction involves the same complex variable z , we keep the same notation as before for the GH-CSs in the continuous spectrum, namely $|z\rangle$.

The overlap of two GH-CSs for the continuous spectrum is, consequently,

$$\langle z | z'\rangle = \frac{\nu_{p,q}(z^* z')}{\sqrt{\nu_{p,q}(|z|^2)} \sqrt{\nu_{p,q}(|z'|^2)}}. \tag{48}$$

Using the action of the generalized creation and annihilation operators, together with the DOOT rules, the projector onto the coherent state $|z\rangle$ is

$$\begin{aligned}
 |z\rangle\langle z| &= \frac{1}{\nu_{p,q}(|z|^2)} \\
 &\times \int_0^{\infty} dE \frac{z^E |E\rangle}{\sqrt{\rho_{p,q}(E)}} \int_0^{\infty} dE' \frac{(z^*)^{E'} \langle E'|}{\sqrt{\rho_{p,q}(E')}}.
 \end{aligned} \tag{49}$$

Following the same calculation procedure as before, it will be obtained that the measure of integration in the continuous space will be

$$\begin{aligned}
 d\mu^c(z) &= \frac{d\varphi}{2\pi} d(|z|^2) \frac{\prod_{i=1}^p \Gamma(a_i)}{\prod_{j=1}^q \Gamma(b_j)} \nu_{p,q} |z|^2 \\
 &\times G_{p,q+1}^{q+1,0} \left(|z|^2 \middle| \begin{matrix} /; & \{a_i - 1\}_{i=1}^p \\ 0, \{b_j - 1\}_{j=1}^q; & / \end{matrix} \right),
 \end{aligned} \tag{50}$$

where we took into account that the angular integral has the value

$$\int_0^{2\pi} \frac{d\varphi}{2\pi} z^E (z^*)^{E'} = |z|^{2E} \delta(E - E'), \quad (51)$$

and we have also used the fundamental integral, Eq. (27), that is, the general formula for reducing a classical integral to a single Meijer G -function [6], together with the completeness relation for the energy eigenvectors $|E\rangle$:

$$\int_0^\infty |E\rangle\langle E| dE = 1. \quad (52)$$

In this context, it is confirmed that the c-GH-CSs associated with a continuous spectrum admit an expansion in the energy basis $\{|E\rangle\}$, of the form

$$|z\rangle = \frac{1}{\sqrt{\nu_{p,q}(|z|^2)}} \int_0^\infty \frac{z^E}{\sqrt{\rho_{p,q}(E)}} |E\rangle dE. \quad (53)$$

Therefore, this integration measure ensures the validity of the completeness relationship of the unit operator:

$$\int d\mu^c(z) |z\rangle\langle z| = 1. \quad (54)$$

It is observed that the difference between the mathematical expressions of $\nu(|z|^2)$, Eq. (5), and the generalized form $\nu_{p,q}(|z|^2)$, Eq. (3.13), lies in the fact that in the denominator, instead of $\Gamma(E + 1)$, one now finds $\rho_{p,q}(E)$, where $\nu(|z|^2) \equiv \nu_{0,0}(|z|^2)$.

After applying the discrete–continuous generalized limit $d \rightarrow c$, the actions of the generalized creation and annihilation operators on the vacuum state lead to the relations:

$$|E\rangle = \frac{1}{\sqrt{\rho_{p,q}(E)}} (\mathcal{A}_+)^E |0\rangle, \quad (55a)$$

$$\langle E| = \frac{1}{\sqrt{\rho_{p,q}(E)}} \langle 0| (\mathcal{A}_-)^E. \quad (55b)$$

In general, the pair of operators \mathcal{A}_- and \mathcal{A}_+ acts on the vectors $|E\rangle$ in a manner that follows directly from the application of the discrete–continuous limit $d \rightarrow c$:

$$\mathcal{A}_- |E\rangle = \sqrt{\rho_{p,q}(E)} |E - 1\rangle, \quad (56a)$$

$$\mathcal{A}_+ |E\rangle = \sqrt{\rho_{p,q}(E + 1)} |E + 1\rangle, \quad (56b)$$

$$\mathcal{A}_+ \mathcal{A}_- |E\rangle = \rho_{p,q}(E) |E\rangle, \quad (56c)$$

$$\# (\mathcal{A}_+ \mathcal{A}_-)^E \# |E\rangle = [\rho_{p,q}(E)]^E |E\rangle. \quad (56d)$$

or, equivalently

$$\mathcal{A}_- = \int_0^\infty \sqrt{\rho_{p,q}(E)} |E - 1\rangle\langle E| dE, \quad (57a)$$

$$\mathcal{A}_+ = \int_0^\infty \sqrt{\rho_{p,q}(E + 1)} |E + 1\rangle\langle E| dE, \quad (57b)$$

$$\mathcal{A}_+ \mathcal{A}_- = \int_0^\infty \rho_{p,q}(E) |E\rangle\langle E| dE, \quad (57c)$$

$$\# (\mathcal{A}_+ \mathcal{A}_-)^E \# = \int_0^\infty [\rho_{p,q}(E)]^E |E\rangle\langle E| dE. \quad (57d)$$

Similarly, by applying the DOOT rules, we obtain the expression for the generalized projector of the vacuum state associated with the continuous spectrum:

$$\begin{aligned} \int_0^\infty |E\rangle\langle E| dE &= |0\rangle\langle 0| \int_0^\infty \frac{\# (\mathcal{A}_+ \mathcal{A}_-)^E \#}{\rho_{p,q}(E)} dE \\ &= |0\rangle\langle 0| \# \nu_{p,q}(\mathcal{A}_+ \mathcal{A}_-) \# = 1, \end{aligned} \quad (58)$$

$$|0\rangle\langle 0| = \frac{1}{\# \nu_{p,q}(\mathcal{A}_+ \mathcal{A}_-) \#}. \quad (59)$$

The projector onto the state $|z\rangle$ is obtained in complete analogy with the usual case, by applying the DOOT rules:

$$|z\rangle\langle z| = \frac{1}{\nu_{p,q}(|z|^2)} \# \frac{\nu_{p,q}(z \mathcal{A}_+) \nu_{p,q}(z^* \mathcal{A}_-)}{\nu_{p,q}(\mathcal{A}_+ \mathcal{A}_-)} \#. \quad (60)$$

where, according to the DOOT rules, the vacuum projector $|0\rangle\langle 0|$ can be taken outside the symbols $\# \cdot \#$.

The completeness relation of the c-GH-CSs then leads to

$$\begin{aligned}
\int d\mu_{p,q}^{(c)}(z) |z\rangle\langle z| &= \frac{\prod_{j=1}^q \Gamma(b_j)}{\frac{j=1}{p} \# \frac{1}{\nu_{p,q}(\mathcal{A}_+\mathcal{A}_-)} \#} \\
&\times \int_0^\infty d|z|^2 G_{p,q+1}^{q+1,0} \left(|z|^2 \left| \begin{array}{l} /; \quad \{a_i - 1\}_{i=1}^p \\ 0, \{b_j - 1\}_{j=1}^q; \quad / \end{array} \right. \right) \\
&\times \int_0^{2\pi} \frac{d\varphi}{2\pi} \# \nu_{p,q}(z\mathcal{A}_+) \nu_{p,q}(z^*\mathcal{A}_-) \# = 1,
\end{aligned} \tag{61}$$

because the angular integral is

$$\begin{aligned}
&\int_0^{2\pi} \frac{d\varphi}{2\pi} \# \nu_{p,q}(z\mathcal{A}_+) \nu_{p,q}(z^*\mathcal{A}_-) \# \\
&= \int_0^\infty dE \frac{\# (\mathcal{A}_+\mathcal{A}_-)^{E/2} \#}{[\rho_{p,q}(E)]^2} |z|^{2E}.
\end{aligned} \tag{62}$$

In addition, from the completeness relation, the following integral in complex space results, which refers to the ν -function with operator argument:

$$\begin{aligned}
&\int d^2z G_{p,q+1}^{q+1,0} \left(|z|^2 \left| \begin{array}{l} /; \quad \{a_i - 1\}_{i=1}^p \\ 0, \{b_j - 1\}_{j=1}^q; \quad / \end{array} \right. \right) \\
&\times \# \nu_{p,q}(z\mathcal{A}_+) \nu_{p,q}(z^*\mathcal{A}_-) \# \\
&= \frac{\prod_{j=1}^q \Gamma(b_j)}{\frac{j=1}{p} \# \nu_{p,q}(\mathcal{A}_+\mathcal{A}_-) \#} \\
&\prod_{i=1}^p \Gamma(a_i)
\end{aligned} \tag{63}$$

On the other hand, the probability density for the transition from the state $|E\rangle$ to the coherent state $|z\rangle$ is given by

$$P_{E;p,q}(|z|^2) \equiv |\langle z|E\rangle|^2 = \frac{|z|^{2E}}{\nu_{p,q}(|z|^2) \rho_{p,q}(E)}, \tag{64}$$

whose generalized inverse limit $c \rightarrow d$ also leads to a generalized Poisson distribution. In fact, if we apply the inverse limit, that is, the continuous–discrete transition $c \rightarrow d$, we recover precisely the usual Poisson probability density function corresponding to the discrete case.

4 Other interesting properties of the generalized ν -function

To verify the expressions obtained for the continuous spectrum, we now apply the reciprocal limit, that is, the continuous–discrete transition $c \rightarrow d$. As a result, we must recover the corresponding expressions for the discrete (discontinuous) spectrum. For example:

$$\begin{aligned}
\lim_{c \rightarrow d} \nu_{p,q}(|z|^2) &= \lim_{c \rightarrow d} \int_0^\infty \frac{|z|^{2E}}{\rho_{p,q}(E)} dE \\
&= \sum_{n=0}^\infty \frac{\prod_{i=1}^p (a_i)_n}{\prod_{j=1}^q (b_j)_n} \frac{|z|^{2n}}{n!} \\
&\equiv {}_p\mathcal{F}_q(\{a\}_1^p; \{b\}_1^q; |z|^2).
\end{aligned} \tag{65}$$

In particular, for the case $p = 0$ and $q = 0$, we have ${}_0\mathcal{F}_0(; ; |z|^2) = e^{|z|^2}$, and therefore we obtain

$$\begin{aligned}
\lim_{c \rightarrow d} \nu_{0,0}(|z|^2) &\equiv \lim_{c \rightarrow d} \nu(|z|^2) \\
&= \lim_{c \rightarrow d} \int_0^\infty \frac{|z|^{2E}}{\Gamma(E+1)} dE \\
&= \sum_{n=0}^\infty \frac{|z|^{2n}}{n!} = {}_0\mathcal{F}_0(; ; |z|^2) = e^{|z|^2}.
\end{aligned} \tag{66}$$

We can also define a ν operator (that is, a ν function that has an operator as argument):

$$\nu_{p,q}(\mathcal{A}_-) \equiv \int_0^\infty \frac{(\mathcal{A}_-)^E}{\rho_{p,q}(E)} dE, \tag{67a}$$

$$\nu_{p,q}(\mathcal{A}_+) \equiv \int_0^\infty \frac{(\mathcal{A}_+)^E}{\rho_{p,q}(E)} dE. \tag{67b}$$

Their action on c-GH-CSs is easily obtained if we take into account the definition of coherent states in the Barut-Girardello manner [9]:

$$\mathcal{A}_- |z\rangle = z |z\rangle, \tag{68a}$$

$$\langle z| \mathcal{A}_+ = z^* \langle z|, \tag{68b}$$

$$\mathcal{A}_+\mathcal{A}_- |z\rangle = |z|^2 |z\rangle. \tag{68c}$$

and we obtain

$$\begin{aligned}\nu_{p,q}(\mathcal{A}_-)|z\rangle &= \int_0^\infty \frac{1}{\rho_{p,q}(E)} (\mathcal{A}_-)^E |z\rangle dE \\ &= \int_0^\infty \frac{z^E}{\rho_{p,q}(E)} |z\rangle dE = \nu_{p,q}(z)|z\rangle.\end{aligned}\quad (69)$$

$$\langle z|\nu_{p,q}(\mathcal{A}_+) = \nu_{p,q}(z^*)\langle z|. \quad (70)$$

Therefore, the function $\nu_{p,q}(z)$ in the complex variable z is the eigenvalue of the operator-valued function $\nu_{p,q}(\mathcal{A}_-)$ in the coherent state $|z\rangle$.

The mean (expected) value of a DOOT-ordered product in the coherent state $|z\rangle$ is then

$$\langle z|\# \nu_{p,q}(\mathcal{A}_+) \nu_{p,q}(\mathcal{A}_-) \# |z\rangle = \nu_{p,q}(z^*) \nu_{p,q}(z). \quad (71)$$

It is easy to verify that the action of the ν -operator (that is, a ν -function whose argument is an operator) on the c -GH-CSs is

$$\nu_{p,q}(z'^* \mathcal{A}_-) |z'\rangle = \nu_{p,q}(|z'|^2) |z'\rangle, \quad (72a)$$

$$\langle z|\nu_{p,q}(z \mathcal{A}_+) = \nu_{p,q}(|z|^2) \langle z|. \quad (72b)$$

The mean (expected) value in the coherent-state representation $|z\rangle$ is

$$\begin{aligned}\langle z|\# \nu_{p,q}(z \mathcal{A}_+) \nu_{p,q}(z^* \mathcal{A}_-) \# |z\rangle \\ = \sqrt{\nu_{p,q}(|z|^2)} \sqrt{\nu_{p,q}(|z'|^2)} \nu_{p,q}(z^* z').\end{aligned}\quad (73)$$

Let us now continue by calculating several matrix elements in the c -GH-CS representation of the function $\nu_{p,q}(\cdot)$ when it is evaluated on different operator arguments.

$$\langle z|\nu_{p,q}(z'^* \mathcal{A}_-) |z'\rangle = \nu_{p,q}(|z'|^2) \langle z|z'\rangle, \quad (74a)$$

$$\langle z|\nu_{p,q}(z \mathcal{A}_+) |z'\rangle = \nu_{p,q}(|z|^2) \langle z|z'\rangle. \quad (74b)$$

$$\langle z|\nu_{p,q}(e^{-z'^* \mathcal{A}_-}) |z'\rangle = \nu_{p,q}(e^{-|z'|^2}) \langle z|z'\rangle, \quad (75a)$$

$$\langle z|\nu_{p,q}(e^{z \mathcal{A}_+}) |z'\rangle = \nu_{p,q}(e^{|z|^2}) \langle z|z'\rangle. \quad (75b)$$

$$\begin{aligned}\langle z|\# \nu_{p,q}(e^{z \mathcal{A}_+}) \nu_{p,q}(e^{-z'^* \mathcal{A}_-}) \# |z'\rangle \\ = \nu_{p,q}(e^{|z|^2}) \nu_{p,q}(e^{-|z'|^2}) \langle z|z'\rangle,\end{aligned}\quad (76a)$$

$$\begin{aligned}\langle z|\# \nu_{p,q}(e^{z \mathcal{A}_+}) \nu_{p,q}(e^{-z^* \mathcal{A}_-}) \# |z\rangle \\ = \nu_{p,q}(e^{|z|^2}) \nu_{p,q}(e^{-|z|^2}).\end{aligned}\quad (76b)$$

Considering that, within the GH-CS formalism combined with the DOOT rules, the creation and annihilation operators \mathcal{A}_+ and \mathcal{A}_- commute, i.e. $[\mathcal{A}_+, \mathcal{A}_-] = 0$, we may apply the Baker–Campbell–Hausdorff formula

$$\exp(\mathcal{X}) \exp(\mathcal{Y}) = \exp(\mathcal{Z}), \quad (77a)$$

$$\begin{aligned}\mathcal{Z} = \mathcal{X} + \mathcal{Y} + \frac{1}{2}[\mathcal{X}, \mathcal{Y}] \\ + \frac{1}{12}[\mathcal{X}, [\mathcal{X}, \mathcal{Y}]] + \frac{1}{12}[\mathcal{Y}, [\mathcal{Y}, \mathcal{X}]] + \dots.\end{aligned}\quad (77b)$$

Let us calculate the diagonal elements of the function $\nu_{p,q}(\cdot)$ when its argument is the displacement operator:

$$\mathcal{D}(z) \equiv \# e^{z \mathcal{A}_+ - z^* \mathcal{A}_-} \# = \# e^{z \mathcal{A}_+} e^{-z^* \mathcal{A}_-} \#. \quad (78)$$

The final result is (see the deduction in the Appendix)

$$\begin{aligned}\langle z|\nu_{p,q}(\mathcal{D}(z)) |z\rangle = \langle z|\nu_{p,q}(\# e^{z \mathcal{A}_+ - z^* \mathcal{A}_-} \#) |z\rangle \\ = \int_0^\infty \frac{1}{\Gamma(E+1)} dE = \nu_{p,q}(1).\end{aligned}\quad (79)$$

One of the DOOT rules states that, inside the symbols $\# \cdot \#$, the creation and annihilation operators \mathcal{A}_+ and \mathcal{A}_- are treated as ordinary c -numbers. Consequently, they may be removed from under the integral sign [15]. Therefore, in such expressions we may replace these operators by scalar quantities, $\mathcal{A}_+ \rightarrow x$ and $\mathcal{A}_- \rightarrow y$.

Let us now consider several integrals involving the function $\nu_{p,q}(\cdot)$.

Starting from the closure (completeness) relation of the unit operator and performing the above substitutions, we are led to two integrals of fundamental importance in the coherent-state approach.

Integral over the complex plane (from Eq. (63)):

$$\int \frac{d^2z}{\pi} G_{p,q+1}^{q+1,0} \left(|z|^2 \left| \begin{array}{l} /; \quad \{a_i - 1\}_{i=1}^p \\ 0, \{b_j - 1\}_{j=1}^q; \quad / \end{array} \right. \right) \\ \times \nu_{p,q}(xz) \nu_{p,q}(yz^*) \quad (80) \\ = \left(\prod_{j=1}^q \Gamma(b_j) \right) \left(\prod_{i=1}^p \Gamma(a_i) \right)^{-1} \nu_{p,q}(xy).$$

Integral in real space, from Eqs. (49), (50), and (54):

$$\int_0^\infty d(|z|^2) |z|^{2E} \\ \times G_{p,q+1}^{q+1,0} \left(|z|^2 \left| \begin{array}{l} /; \quad \{a_i - 1\}_{i=1}^p \\ 0, \{b_j - 1\}_{j=1}^q; \quad / \end{array} \right. \right) \quad (81) \\ = \left(\prod_{j=1}^q \Gamma(b_j) \right) \left(\prod_{i=1}^p \Gamma(a_i) \right)^{-1} \rho_{p,q}(E).$$

By specifying the indices p and q , the sets of parameters $\{a_i\}_{i=1}^p$ and $\{b_j\}_{j=1}^q$, as well as by performing a suitable change of integration variable, the above integrals allow us to evaluate a variety of other integrals involving the function $\nu_{p,q}(x|z|^2)$, where x is a real or complex number.

As a first example, we obtain

$$\int_0^\infty d(|z|^2) \nu_{p,q} \left(\frac{1}{x} |z|^2 \right) \\ \times G_{p,q+1}^{q+1,0} \left(|z|^2 \left| \begin{array}{l} /; \quad \{a_i - 1\}_{i=1}^p \\ 0, \{b_j - 1\}_{j=1}^q; \quad / \end{array} \right. \right) \quad (82) \\ = \left(\prod_{j=1}^q \Gamma(b_j) \right) \left(\prod_{i=1}^p \Gamma(a_i) \right)^{-1} \frac{1}{\ln x}.$$

Particularly, if we take $x = s$, make the substitution $|z|^2 = st$, and specify $p = 0$, $q = 0$ (so that $\nu_{0,0}(\cdot) = \nu(\cdot)$), we obtain (see Appendix):

$$\int_0^\infty e^{-st} \nu(t) dt = \frac{1}{s \ln s}, \quad s > 0, s \neq 1, \quad (83)$$

which is, in fact, the Laplace transform of the function $\nu(t)$, a formula that appears in Erdélyi's book [1], p. 222. On the other hand, if we take $p = 1$, $a_1 = 1$, $q = 1$ and $b_1 = b + 1$, then in this situation we have $\rho_{1,1}(E) = \Gamma(b + 1 + E)$, and

$$G_{1,2}^{2,0} \left(|z|^2 \left| \begin{array}{l} /; \quad 0 \\ 0, b; \quad / \end{array} \right. \right) = G_{1,0}^{0,1}(|z| | b) \\ = e^{-|z|^2} (|z|)^{2b}. \quad (84)$$

Then, the integral becomes

$$\int_0^\infty d(|z|^2) \nu_{1,1} \left(\frac{1}{x} |z|^2 \right) e^{-|z|^2} (|z|^2)^b \\ = \int_0^\infty dE \frac{x^{-E}}{\rho_{1,1}(E)} \int_0^\infty d(|z|^2) e^{-|z|^2} (|z|^2)^{b+E} \\ = \int_0^\infty dE \frac{x^{-E}}{\Gamma(b+1+E)} \Gamma(b+1) \Gamma(b+1+E) \\ = \Gamma(b+1) \int_0^\infty x^{-E} dE = \frac{\Gamma(b+1)}{\ln x}. \quad (85)$$

Generally, if we choose the function $\nu_{p,q}(e^{-s|z|^2})$, then, after expanding it into its power-series representation, we must appeal to the Laplace transform of the corresponding Meijer G -function (see Appendix):

$$\int_0^\infty d(|z|^2) \nu_{0,0} e^{-s|z|^2} \\ \times G_{p,q+1}^{q+1,0} \left(|z|^2 \left| \begin{array}{l} /; \quad \{a_i - 1\}_{i=1}^p \\ 0, \{b_j - 1\}_{j=1}^q; \quad / \end{array} \right. \right) \quad (86) \\ = \sum_{l=0}^\infty \rho_{p,q}(l) \frac{(-1)^l}{l!} s^l \left(\frac{\partial}{\partial s} \right)^l \nu(e^{-s}).$$

A similar integral can be derived for the two-variable function $\nu(z, \alpha)$ (see Appendix):

$$\int_0^\infty d(|z|^2) \nu \left(\frac{1}{C} |z|^2, \alpha \right) \\ \times G_{p,q+1}^{q+1,0} \left(|z|^2 \left| \begin{array}{l} /; \quad \{a_i - 1\}_{i=1}^p \\ 0, \{b_j - 1\}_{j=1}^q; \quad / \end{array} \right. \right) \quad (87)$$

$$= C^{-\alpha} \frac{\prod_{j=1}^q \Gamma(b_j + \alpha)}{\prod_{i=1}^p \Gamma(a_i + \alpha)} \nu_{p,q+1}(C^{-1}).$$

Particularly, in Eq. (80), for the case $p = 0$ and $q = 0$, we have $G_{0,1}^{1,0}(|z|^2 | 0) = e^{-|z|^2}$ and we obtain

$$\frac{1}{\pi} \int d^2z e^{-|z|^2} \nu(xz) \nu(yz^*) = \nu(xy). \quad (88)$$

At the end of this section, it is necessary to make the following observation: when the generalized function $\nu(x)$ appears under an integral sign, it may also be defined through other structure functions, characterized by different indices and different parameter sets. For example:

$$\begin{aligned} \nu_{r,s}(X) &\equiv \int_0^\infty \frac{X^E}{\rho_{r,s}(E)} dE, \\ &\equiv {}_r\mathcal{F}_s(\{c_i\}_{i=1}^r; \{d_j\}_{j=1}^s; X), \end{aligned} \quad (89a)$$

$$\rho_{r,s}(E) = \Gamma(E+1) \frac{\prod_{j=1}^s (d_j)_E}{\prod_{i=1}^r (c_i)_E}. \quad (89b)$$

The only reason why, throughout this paper, we employed the structure function $\rho_{r,s}(E)$ was to avoid overcomplicating the formulas.

5 Concluding remarks

In this paper we have sought to extend the properties and applications of the ν -function $\nu(\cdot)$, a subject that has been very little (or almost not at all) addressed in the specialized literature. Our analysis started from a first application presented in our previous work [8], where we examined the connection between the coherent-state formalism for continuous spectra and the ν -function $\nu(\cdot)$. There we showed that the ν -function plays the role of the normalization function of the coherent states $|z\rangle$ associated with the continuous spectrum of a quantum system. This role becomes apparent through the formulation and use of the discrete-continuous limit $d \rightarrow c$, by which any quantity or observable $X_d(n, n_{\max})$ characteristic of the discrete spectrum has a well-defined counterpart $X_c(E)$ in the continuous spectrum. In the present paper we have generalized the definition of the function $\nu(z)$, in the sense that in the denominator of its integral definition, instead of the simple gamma function $\Gamma(E+1)$, where E denotes the continuous spectrum of the Hamiltonian, a more general structure function $\rho_{p,q}(E)$ appears, containing products and ratios of gamma functions. This structure function, in its discrete (discontinuous) form, is directly related to the most general coherent states, namely the generalized

hypergeometric coherent states (GH-CSs). In this way, we introduced a new function—the *generalized ν -function* $\nu_{p,q}(z)$ —for which the usual ν -function becomes a particular case: $\nu(z) = \nu_{0,0}(z)$. We have examined a number of structural and operational properties of this generalized function.

In addition, we also dealt with the generalized functions $\nu_{p,q}(\cdot)$ whose argument depends on the creation or annihilation operators that define the GH-CSs. The results involving the functions $\nu_{p,q}(\cdot)$ are fully consistent with the well-known relations of coherent-state theory:

$$f(\mathcal{A}_-) |z\rangle = f(z) |z\rangle, \quad (90a)$$

$$\langle z | f(\mathcal{A}_+) = \langle z | f(z^*). \quad (90b)$$

These relations involving operators are important because, due to the rules of the diagonal operational ordering technique (DOOT), the operators are treated as simple c -numbers, which can be removed from under the DOOT symbol $\# \cdot \#$ [15]. Consequently, the operators can be replaced by scalar quantities, leading to new classical mathematical identities. As applications, we have derived several integrals involving the generalized functions $\nu_{p,q}(\cdot)$ and examined explicit examples. In this way, we opened the possibility of obtaining many further integrals and relations involving the functions $\nu_{p,q}(\cdot)$, by particularizing the indices p and q , the parameter sets $\{a_i\}_{i=1}^p$ and $\{b_j\}_{j=1}^q$, and by applying suitable changes of the integration variables.

Moreover, let us point out that all calculations in this paper were performed using coherent states defined in the Barut-Girardello sense [9]. In principle, the previous results also remain valid for the dual coherent states defined in the sense of Klauder-Perelomov, denoted by $|z\rangle_{\text{KP}}$ [10].

$$\begin{aligned} |z\rangle_{\text{KP}} &= \frac{e^{z\mathcal{A}_+ - z^*\mathcal{A}_-} |0\rangle}{{}_q\mathcal{F}_p(\{b_j\}_{j=1}^q; \{a_i\}_{i=1}^p; |z|^2)} \\ &= \frac{1}{{}_q\mathcal{F}_p(\{b_j\}_{j=1}^q; \{a_i\}_{i=1}^p; |z|^2)} \\ &\quad \times \sum_{n=0}^{\infty} \frac{z^n}{\rho_{q,p}(n)} |n\rangle, \end{aligned} \quad (91a)$$

$$\rho_{q,p}(n) = \Gamma(n+1) \frac{\prod_{i=1}^p (a_i)_n}{\prod_{j=1}^q (b_j)_n}. \quad (91b)$$

By applying the discrete–continuous limit $d \rightarrow c$, the same results are obtained, taking into account the duality between the two types of coherent states, BG-CSs versus KP-CSs [11]. The role of the CSs normalization function for the continuous spectrum represents, to our knowledge, the first application of the ν -function in quantum optics. Conversely, the coherent-state formalism leads to several mathematical applications involving the ν -function, in the sense that it allows one to evaluate integrals containing this function. This establishes a genuine feedback mechanism between quantum mechanics (through the coherent-state formalism) and higher mathematics (through the theory of special functions).

As a general conclusion, we may state that coherent states—both those associated with discrete spectra and those corresponding to continuous energy spectra—constitute a fundamental bridge between quantum and classical (phase-space) representations. The coherent-state formalism has found applications in many diverse fields, including quantum physics (quantum optics, squeezing and photon-added states, measurement theory, quantum Hall effect), quantum information theory and practice (entanglement phenomena, cryptography), solid-state physics (ferromagnetism, superconductivity, collective phenomena), and mathematical physics (theory and applications of special functions).

All these areas of application fully justify the growing interest, in recent years, in the coherent states formalism, both for systems with discrete spectra and for those with continuous energy spectra.

Appendix

1. Derivation of Equation (86)

$$\begin{aligned} & \int_0^\infty d(|z|^2) \nu_{0,0} e^{-s|z|^2} \\ & \quad \times G_{p,q+1}^{q+1,0} \left(|z|^2 \left| \begin{array}{c} /; \\ 0, \{b_j - 1\}_{j=1}^q \end{array} \right. ; \begin{array}{c} \{a_i - 1\}_{i=1}^p \\ / \end{array} \right) \\ & = \int_0^\infty dE \frac{(e^{-s})^E}{\Gamma(E+1)} \sum_{l=0}^\infty \frac{(-sE)^l}{l!} \\ & \quad \times \int_0^\infty d(|z|^2) (|z|^2)^l \\ & \quad \times G_{p,q+1}^{q+1,0} \left(|z|^2 \left| \begin{array}{c} /; \\ 0, \{b_j - 1\}_{j=1}^q \end{array} \right. ; \begin{array}{c} \{a_i - 1\}_{i=1}^p \\ / \end{array} \right) \end{aligned}$$

$$\begin{aligned} & = \left(\prod_{j=1}^q \Gamma(b_j) \right) \left(\prod_{i=1}^p \Gamma(a_i) \right)^{-1} \\ & \quad \times \sum_{l=0}^\infty \frac{(-s)^l}{l!} \left(\prod_{j=1}^q \Gamma(b_j)_l \right) \left(\prod_{i=1}^p \Gamma(a_i)_l \right)^{-1} \\ & \quad \times \int_0^\infty dE \frac{(e^{-s})^E}{\Gamma(E+1)} (-E)^l \\ & = \sum_{l=0}^\infty \frac{(-1)^l}{l!} \left(\prod_{j=1}^q \Gamma(b_j + l) \right) \left(\prod_{i=1}^p \Gamma(a_i + l) \right)^{-1} \\ & \quad \times (-1)^l \left(\frac{\partial}{\partial s} \right)^l \int_0^\infty dE \frac{(e^{-s})^E}{\Gamma(E+1)} (-E)^l \\ & = \sum_{l=0}^\infty \rho_{p,q}(l) \frac{(-1)^l}{l!} \left(\frac{\partial}{\partial s} \right)^l \nu(e^{-s}). \end{aligned} \tag{92}$$

2. Derivation of Equation (79)

$$\begin{aligned} \langle z | \nu_{p,q}(\mathcal{D}(z)) | z \rangle & = \langle z | \nu_{p,q} \left(\# e^{z\mathcal{A}_+ - z^*\mathcal{A}_-} \# \right) | z \rangle \\ & = \langle z | \int_0^\infty dE \# \frac{(e^{z\mathcal{A}_+ - z^*\mathcal{A}_-})^E}{\rho_{p,q}(E)} \# | z \rangle \\ & = \int_0^\infty dE \frac{1}{\rho_{p,q}(E)} \langle z | \# (e^{z\mathcal{A}_+ - z^*\mathcal{A}_-})^E \# | z \rangle \\ & = \int_0^\infty dE \frac{1}{\rho_{p,q}(E)} \langle z | \# (e^{zE\mathcal{A}_+})(e^{-z^*E\mathcal{A}_-}) \# | z \rangle \\ & = \int_0^\infty dE \frac{1}{\rho_{p,q}(E)} \# \left[\left(\sum_{j=0}^\infty \frac{(zE)^j}{j!} \langle z | (\mathcal{A}_+)^j \right) \right. \\ & \quad \times \left. \left(\sum_{l=0}^\infty \frac{(z^*E)^l}{l!} (\mathcal{A}_-)^l | z \rangle \right) \right] \# \\ & = \int_0^\infty dE \frac{1}{\rho_{p,q}(E)} \left[\left(\sum_{j=0}^\infty \frac{(zE)^j}{j!} \langle z | (z^*)^j \right) \right. \\ & \quad \times \left. \left(\sum_{l=0}^\infty \frac{(z^*E)^l}{l!} z^l | z \rangle \right) \right] \\ & = \int_0^\infty dE \frac{1}{\rho_{p,q}(E)} \left(\sum_{j=0}^\infty \frac{(|z|^2 E)^j}{j!} \right) \\ & \quad \times \left(\sum_{l=0}^\infty \frac{(|z|^2 E)^l}{l!} \right) \end{aligned}$$

$$\begin{aligned}
&= \int_0^\infty dE \frac{1}{\rho_{p,q}(E)} \exp(|z|^2) \exp(|z|^2) \\
&= \int_0^\infty dE \frac{1}{\rho_{p,q}(E)} = \nu_{p,q}(1).
\end{aligned}$$

3. Derivation of Equation (82)

$$\begin{aligned}
\text{Int} &\equiv \int_0^\infty d(|z|^2) \nu\left(\frac{1}{C}|z|^2, \alpha\right) \\
&\times G_{p,q+1}^{q+1,0}\left(|z|^2 \left| \begin{array}{l} /; \quad \{a_i - 1\}_{i=1}^p \\ 0, \{b_j - 1\}_{j=1}^q; \quad / \end{array} \right.\right) \\
&= \int_0^\infty dE \frac{C^{-(\alpha+E)}}{\Gamma(\alpha+E+1)} \frac{\prod_{j=1}^q \Gamma(b_j + \alpha + E)}{\prod_{i=1}^p \Gamma(a_i + \alpha + E)} \\
&= \int_0^\infty dE \frac{C^{-(\alpha+E)}}{\Gamma(\alpha+E+1)} \rho_{p,q}(\alpha + E) \\
&\times \int_0^\infty d(|z|^2) \nu_{p,q}\left(\frac{1}{x}|z|^2\right) \\
&\times G_{p,q+1}^{q+1,0}\left(|z|^2 \left| \begin{array}{l} /; \quad \{a_i - 1\}_{i=1}^p \\ 0, \{b_j - 1\}_{j=1}^q; \quad / \end{array} \right.\right) \quad (94) \\
&= \int_0^\infty dE \frac{x^{-E}}{\rho_{p,q}(E)} \int_0^\infty d(|z|^2) (|z|^2)^E \\
&\times G_{p,q+1}^{q+1,0}\left(|z|^2 \left| \begin{array}{l} /; \quad \{a_i - 1\}_{i=1}^p \\ 0, \{b_j - 1\}_{j=1}^q; \quad / \end{array} \right.\right) \\
&= \left(\prod_{j=1}^q \Gamma(b_j)\right) \left(\prod_{i=1}^p \Gamma(a_i)\right)^{-1} \int_0^\infty dE x^{-E} \\
&= \left(\prod_{j=1}^q \Gamma(b_j)\right) \left(\prod_{i=1}^p \Gamma(a_i)\right)^{-1} (-1) \frac{1}{\ln x} x^{-E} \Big|_0^\infty \\
&= \left(\prod_{j=1}^q \Gamma(b_j)\right) \left(\prod_{i=1}^p \Gamma(a_i)\right)^{-1} \frac{1}{\ln x}.
\end{aligned}$$

4. Derivation of Equation (87)

$$\begin{aligned}
\text{Int} &\equiv \int_0^\infty d(|z|^2) \nu\left(\frac{1}{C}|z|^2, \alpha\right) \\
&\times G_{p,q+1}^{q+1,0}\left(|z|^2 \left| \begin{array}{l} /; \quad \{a_i - 1\}_{i=1}^p \\ 0, \{b_j - 1\}_{j=1}^q; \quad / \end{array} \right.\right) \\
&= \int_0^\infty dE C^{-(\alpha+E)} \frac{\prod_{j=1}^q \Gamma(b_j + \alpha + E)}{\prod_{i=1}^p \Gamma(a_i + \alpha + E)} \quad (95) \\
&= \int_0^\infty dE \frac{C^{-(\alpha+E)}}{\Gamma(\alpha+E+1)} \rho_{p,q}(\alpha + E),
\end{aligned}$$

where

$$\begin{aligned}
\rho_{p,q}(\alpha + E) &= \Gamma(\alpha + E + 1) \\
&\times \frac{\prod_{j=1}^q \Gamma(b_j + \alpha) \prod_{j=1}^q (b_j + \alpha)_E}{\prod_{i=1}^p \Gamma(a_i + \alpha) \prod_{i=1}^p (a_i + \alpha)_E}, \quad (96)
\end{aligned}$$

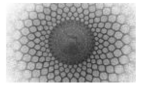
$$\begin{aligned}
\text{Int} &\equiv C^{-\alpha} \left(\prod_{j=1}^q \Gamma(b_j + \alpha)\right) \left(\prod_{i=1}^p \Gamma(a_i + \alpha)\right)^{-1} \\
&\times \int_0^\infty dE (l)_E \frac{\prod_{j=1}^q (b_j + \alpha)_E}{\prod_{i=1}^p (a_i + \alpha)_E} \frac{C^{-E}}{\Gamma(E+1)} \quad (97) \\
&= C^{-\alpha} \frac{\prod_{j=1}^q (b_j + \alpha)}{\prod_{i=1}^p (a_i + \alpha)} \nu_{p,q+1}(C^{-1}).
\end{aligned}$$

Acknowledgment

The author expresses his deep gratitude to the reviewer for pertinent comments and suggestions, which have led to a substantial improvement of the presentation of this article.

References

1. A. Erdélyi, W. Magnus, F. Oberhettinger, F. G. Tricomi, *Higher Transcendental Functions, Vol. 3: The Function $y(x)$ and Related Functions*, McGraw–Hill, New York (1955)
2. I. S. Gradshteyn, I. M. Ryzhik, *Table of Integrals, Series and Products*, 7th ed., Academic Press, Amsterdam (2007)
3. T. Appl, D. H. Schiller, *J. Phys. A: Math. Gen.* **37**, 7 (2004)
4. J. P. Gazeau, J. R. Klauder, *J. Phys. A: Math. Gen.* **32**, 123 (1999)
5. D. Popov, *Electron. J. Theor. Phys.* **3**, 11 (2006)
6. A. M. Mathai, R. K. Saxena, *Generalized Hypergeometric Functions with Applications in Statistics and Physical Sciences*, Lecture Notes in Mathematics, Vol. 348, Springer–Verlag, Berlin (1973)
7. J. R. Klauder, *J. Math. Phys.* **4**, 8 (1963)
8. D. Popov, M. Popov, *Rom. Rep. Phys.* **68**, 4 (2016)
9. A. O. Barut, L. Girardello, *Commun. Math. Phys.* **21**, 41 (1971)
10. A. Perelomov, *Generalized Coherent States and their Applications*, Springer, Berlin (1986)
11. D. Popov, arXiv:2302.04245, (2023)
12. D. Popov, S.-H. Dong, M. Popov, *Ann. Phys.* **362**, 449 (2015)
13. A. Inomata, M. Sadiq, in *Proceedings of the 8th International Conference “Path Integrals. From Quantum Information to Cosmology”* <http://www1.jinr.ru/Proceedings/Burdik-2005/pdf/inomata.pdf>, (2005)
14. M. Thaik, A. Inomata, *J. Phys. A: Math. Theor.* **38**, 1767 (2005).
15. D. Popov, M. Popov, *Phys. Scr.* **90**, 035101 (2015)



Infinitely Many Fast Homoclinic Solutions for Nonlinear Damped Systems Involving the p -Laplacian under Local Conditions

Mohsen Timoumi^{1a}

¹Dpt Mathematics, Faculty of Sciences, 5000 Monastir, Tunisia

Received: 17 September 2025 / Accepted: 28 Novembre 2025 / Published: 28 Novembre 2025

Abstract This paper is concerned with proving that an infinite number of fast homoclinic solutions exist for a specific type of damped vibration system with nonlinearities governed by the p -Laplacian operator. Unlike most existing works, which typically require coercivity, periodicity, or global growth conditions on the potential, we establish our results under weaker, localized assumptions. In particular, the damping and stiffness terms are allowed to be non-coercive, and the potential function satisfies local conditions near the origin. Our approach relies on variational methods and the symmetric mountain pass theorem. Two main existence results are obtained, illustrating the effectiveness of this method in treating strongly nonlinear systems with nonstandard growth and damping terms.

1 Introduction

Second-order differential systems involving the p -Laplacian operator arise naturally in various scientific fields, including non-Newtonian fluid mechanics, nonlinear filtration theory, and nonlinear elasticity [1]. In this context, we study the following nonlinear damped vibration system with a p -Laplacian operator:

$$\begin{aligned} \frac{d}{dt} (|\dot{u}(t)|^{p-2}\dot{u}(t)) + q(t)|\dot{u}(t)|^{p-2}\dot{u}(t) \\ - a(t)|u(t)|^{p-2}u(t) + \nabla W(t, u(t)) = 0, \quad t \in \mathbb{R}. \end{aligned} \quad (1)$$

where $p \geq 2$, $q, a \in C(\mathbb{R}, \mathbb{R})$, and the potential $W : \mathbb{R} \times \mathbb{R}^N \rightarrow \mathbb{R}$ is continuous and differentiable with respect to its second variable.

This system generalizes the classical damped vibration equation, which corresponds to the case $p = 2$. When $p = 2$

and $q \neq 0$, the equation reduces to a linear second-order differential system with variable coefficients, for which the existence and multiplicity of homoclinic orbits have been extensively studied via variational methods and critical point theory. Many works have focused on establishing fast homoclinic solutions under superquadratic or asymptotically quadratic conditions on the potential, particularly in periodic or coercive settings [2–15].

On the other hand, when $p \neq 2$ and $q = 0$, the system becomes conservative and retains the p -Laplacian structure. In this setting, several researchers have also investigated the existence and multiplicity of homoclinic solutions using variational approaches [16–20].

However, in the general case where $p > 1$ and $q \neq 0$, results remain scarce due to the technical challenges introduced by the nonlinear damping term, which breaks the self-adjoint structure and complicates the variational analysis. Existing works in this general framework often impose strong assumptions on the nonlinearity or the potential. For instance, in [21], the authors considered a potential composed of two parts satisfying super- and sub-quadratic Ambrosetti-Rabinowitz-type conditions, and applied both the classical and symmetric mountain pass theorems to obtain fast homoclinic orbits. More recently, [22] used Jeanjean's monotonicity trick along with concentration-compactness principles to establish the existence of infinitely many fast homoclinic solutions without relying on the classical Ambrosetti-Rabinowitz condition. However, such results generally assume that $W(t, x)$ is periodic in time and globally superquadratic in the spatial variable.

In contrast to these works, the present paper investigates the existence of infinitely many fast homoclinic solutions under more relaxed assumptions. Specifically, we allow the coefficient $a(t)$ to be non-coercive, and consider potentials $W(t, x)$ that satisfy only local conditions with respect to both time t and the spatial variable x . Notably, we do not require

^ae-mail: m_timoumi@yahoo.com

periodicity in t or global growth conditions at infinity for the potential. Instead, the potential may exhibit superquadratic growth locally near the origin, which significantly broadens the class of admissible nonlinearities and allows us to treat more general and realistic systems.

Our approach relies on variational methods and, in particular, on the symmetric mountain pass theorem due to Kajikiya [23]. To handle the lack of compactness, we construct suitable truncations of the potential and apply refined estimates to show that the associated energy functional satisfies the Palais-Smale condition. We then prove the existence of an infinite sequence of nontrivial critical points converging to zero in the energy space, which correspond to fast homoclinic solutions of the original system.

We now introduce the precise assumptions:

- (Q_ν) There exists a constant $\nu > 1$ such that

$$Q(t) = \int_0^t q(s) ds \rightarrow +\infty \quad \text{as } |t| \rightarrow \infty,$$

$$\int_{|t| \geq 1} \frac{e^{Q(t)}}{|t| \ln^\nu |t|} dt < \infty.$$

- (A) There exists $a_0 > 0$ such that

$$a(t) \geq a_0, \quad \forall t \in \mathbb{R},$$

- (A_ν) $\text{meas}_Q(\{t \in \mathbb{R} : a(t)/(|t| \ln^\nu |t|) < b\}) < \infty,$
 $\forall b > 0.$

- (W_1) $W(t, 0) = 0$ and $\exists r > 0$ such that $W(t, -x) = W(t, x)$ for all (t, x) with $|x| \leq r$.

- (W_2) $\exists a < b$ and $\alpha > p$ such that

$$\lim_{|x| \rightarrow 0} \frac{W(t, x)}{|x|^\alpha} = +\infty \quad \text{uniformly for } t \in [a, b].$$

- (W_3) $\exists R_0 > 0$ such that

$$\lim_{|x| \rightarrow 0} \frac{|\nabla W(t, x)|}{a(t)|x|^{p-1}} = 0 \quad \text{uniformly for } |t| \geq R_0.$$

- (W_4) $\exists c > 0, \sigma \in (\frac{p}{2}, p), R_1 > 0, \rho \in (0, r)$ with

$$|\nabla W(t, x)| \leq c|x|^{\sigma-1}, \quad \forall |t| \geq R_1, |x| \leq \rho.$$

We now state our main results. The first covers the case where the potential satisfies a local symmetry condition near

zero and has locally uniform superquadratic growth over a bounded time interval.

Theorem 1.1. Suppose assumptions (A) and (W_1) through (W_3) are satisfied. Then the system $(\mathcal{D}\mathcal{V})$ has infinitely many nontrivial fast homoclinic solutions.

Example 1.1. Let $a(t) = |t \cos t| + 1$, and let $p < \gamma < \alpha$ be constants. Define

$$W(t, x) = a(t) |x|^\gamma, \quad |x| \leq 1. \quad (2)$$

One can verify that a satisfies the condition (A) , and $W(t, x)$ satisfies the conditions $(W_1) - (W_3)$.

The second result allows for non-coercive coefficients $a(t)$ under a weighted measure condition, and assumes certain local estimates on the gradient of the potential.

Theorem 1.2. Suppose assumptions (A) , (A_ν) , (W_1) , (W_2) , and (W_4) are satisfied. Then the system $(\mathcal{D}\mathcal{V})$ has infinitely many nontrivial fast homoclinic solutions.

Example 1.2. Let $\sigma \in [\frac{p}{2}, p], \alpha > \gamma > p + 1$ be constants. Let $[a, b] = [\frac{\pi}{6}, \frac{\pi}{3}]$. Define

$$W(t, x) = |x|^\sigma \cos t + |x|^\gamma \sin t. \quad (3)$$

One can verify that $W(t, x)$ satisfies the conditions (W_1) , (W_2) , and (W_4) .

These results represent a significant extension of the current theory, allowing for more general p -Laplacian systems under minimal local conditions. To the best of our knowledge, this is the first result establishing the existence of infinitely many fast homoclinic solutions under such minimal local assumptions in the presence of nonlinear damping and non-coercive stiffness.

2 Preliminaries

Our analysis of fast homoclinic solutions for $(\mathcal{D}\mathcal{V})$ begins with a review of key properties of the weighted Sobolev space E . This space serves as the domain for a variational functional J such that its critical points are exactly the homoclinic solutions of $(\mathcal{D}\mathcal{V})$. For $1 \leq s < \infty$, we define $L_Q^s(\mathbb{R})$ as the Banach space of measurable functions from \mathbb{R} to \mathbb{R}^N with the norm:

$$\|u\|_{L_Q^s} = \left(\int_{\mathbb{R}} e^{Q(t)} |u(t)|^s dt \right)^{\frac{1}{s}}. \quad (4)$$

Additionally, we define $L_Q^\infty(\mathbb{R})$ as the Banach space of functions from \mathbb{R} to \mathbb{R}^N with the norm:

$$\|u\|_{L_Q^\infty} = \text{ess sup} \left\{ e^{\frac{Q(t)}{2}} |u(t)| / t \in \mathbb{R} \right\}. \quad (5)$$

Next, we define the Sobolev space $W_Q^{1,p}(\mathbb{R})$ as:

$$W_Q^{1,p}(\mathbb{R}) = \left\{ u \in L_Q^p(\mathbb{R}) / \dot{u} \in L_Q^p(\mathbb{R}) \right\}, \quad (6)$$

equipped with the usual norm:

$$\|u\|_{W_Q^{1,p}} = \left(\int_{\mathbb{R}} e^{Q(t)} \left[|\dot{u}(t)|^p + |u(t)|^p \right] dt \right)^{\frac{1}{p}}. \quad (7)$$

Under the condition (A), we introduce the Banach space:

$$E = \left\{ u \in W_Q^{1,p}(\mathbb{R}) : \int_{\mathbb{R}} e^{Q(t)} (|\dot{u}(t)|^p + a(t)|u(t)|^p) dt < \infty \right\}. \quad (8)$$

with the norm:

$$\|u\| = \left(\int_{\mathbb{R}} e^{Q(t)} \left[|\dot{u}(t)|^p + a(t)|u(t)|^p \right] dt \right)^{\frac{1}{p}}. \quad (9)$$

It is well known that E is continuously embedded in $L_Q^s(\mathbb{R})$ for all $p \leq s \leq \infty$.

Definition 2.1. We define a solution u of $(\mathcal{D}\mathcal{V})$ to be a fast homoclinic solution provided that u belongs to the space E .

Lemma 2.1. [16] For $u \in W_Q^{1,p}(\mathbb{R})$, the following inequalities hold:

$$\|u\|_{L^\infty}^p \leq \left(\frac{p-1}{2^{p'}} \right) \frac{1}{p'} \int_{\mathbb{R}} (|\dot{u}(s)|^p + |u(s)|^p) ds. \quad (10)$$

and for $u \in E$,

$$\|u\|_{L^\infty}^p \leq \left(\frac{p-1}{2^q a_0} \right)^{\frac{1}{q}} \|u\|^p. \quad (11)$$

$$|u(t)|^p \leq (p-1)^{\frac{1}{p'}} \int_t^\infty \times [a(s)]^{-\frac{1}{p'}} (|\dot{u}(s)|^p + a(s)|u(s)|^p) ds, \quad t \in \mathbb{R}. \quad (12)$$

$$|u(t)|^p \leq (p-1)^{\frac{1}{p'}} \int_{-\infty}^t \times [a(s)]^{-\frac{1}{p'}} (|\dot{u}(s)|^p + a(s)|u(s)|^p) ds, \quad t \in \mathbb{R}. \quad (13)$$

where p' is the exponent conjugate of p : $\frac{1}{p'} + \frac{1}{p} = 1$.

Lemma 2.2. Suppose that $(Q_V), (A_V)$ are satisfied. Then E is compactly embedded in $L_Q^s(\mathbb{R})$ for any $s \in [\frac{p}{2}, \infty[$. Moreover, for all $s \in [\frac{p}{2}, \infty]$, there exists a constant $\eta_s > 0$ such that

$$\|u\|_{L_Q^s} \leq \eta_s \|u\|, \quad \forall u \in E. \quad (14)$$

Proof: Let $\varepsilon > 0$ be arbitrary. Assumption (A_V) guarantees the existence of a radius $r_\varepsilon \geq e$ for which the measure of the set B_ε is less than or equal to ε , where

$$B_\varepsilon = \left\{ t \in \mathbb{R} \setminus [-r_\varepsilon, r_\varepsilon] \mid \frac{a(t)}{|t| \ln^V |t|} < \frac{1}{\varepsilon} \right\}. \quad (15)$$

and

$$\int_{|t| \geq r_\varepsilon} e^{Q(t)} \frac{1}{|t| \ln^V |t|} dt < \varepsilon. \quad (16)$$

Let

$$D_\varepsilon = \mathbb{R} \setminus (B_\varepsilon \cup]-r_\varepsilon, r_\varepsilon[), \quad (17)$$

and

$$a_\varepsilon = \inf_{t \in D_\varepsilon} \frac{a(t)}{|t| \ln^V |t|}. \quad (18)$$

Then $\frac{1}{a_\varepsilon} \leq \varepsilon$. Consider a sequence (u_k) converging weakly to u in the space E . An application of the Banach-Steinhaus theorem yields

$$M = \sup_{k \in \mathbb{N}} \|u_k - u\| < \infty. \quad (19)$$

The continuous embeddings $E \hookrightarrow W_Q^{1,p}(\mathbb{R}) \hookrightarrow L_Q^s(\mathbb{R})$ hold for every $s \in [p, \infty]$. Consequently, we can find a constant $M_s > 0$ satisfying

$$\|u_k - u\|_{L_Q^s} \leq M_s, \quad \forall k \in \mathbb{N}. \quad (20)$$

Since $a(t) \geq a_0$ in $I_\varepsilon =]-r_\varepsilon, r_\varepsilon[$, the operator $E \rightarrow W_Q^{1,p}(I_\varepsilon)$, $u \mapsto u|_{I_\varepsilon}$ defines a linear operator that is continuous. Here, the symbol $W_Q^{1,p}(I_\varepsilon)$ refers to the weighted Sobolev space over the interval I_ε

$$W_Q^{1,p}(I_\varepsilon) = \left\{ u : I_\varepsilon \rightarrow \mathbb{R} / \int_{I_\varepsilon} e^{Q(t)} [|\dot{u}(t)|^p + |u(t)|^p] dt < +\infty \right\}. \quad (21)$$

An application of the Sobolev embedding theorem shows that

$$u_k \rightarrow u \text{ uniformly in } \bar{I}_\varepsilon. \quad (22)$$

Step 1. We first demonstrate the compactness of the embedding of E into $L_Q^p(\mathbb{R})$. To see this, observe that

$$\begin{aligned} & \int_{|t| \geq r_\varepsilon} e^{Q(t)} |u_k(t) - u(t)|^p dt = \\ & \int_{B_\varepsilon} e^{Q(t)} |u_k(t) - u(t)|^p dt \\ & + \int_{D_\varepsilon} e^{Q(t)} |u_k(t) - u(t)|^p dt \\ & \leq \text{meas}_Q(B_\varepsilon) \|u_k - u\|_{L^\infty}^p \\ & + \int_{D_\varepsilon} e^{Q(t)} |t \ln^\nu |t| |u_k(t) - u(t)|^p dt \\ & \leq \varepsilon \left(\frac{M_\infty}{\sqrt{m_0}} \right)^p + \frac{1}{a_\varepsilon} \int_{\mathbb{R}} e^{Q(t)} a(t) |u_k(t) - u(t)|^p dt \\ & \leq \varepsilon \left[\left(\frac{M_\infty}{\sqrt{m_0}} \right)^p + M^p \right]. \end{aligned} \quad (23)$$

where $m_0 = \inf_{t \in \mathbb{R}} e^{Q(t)}$. Combining (2.10) with (2.11) yields $\|u_k - u\|_{L_Q^p} \rightarrow 0$ as $k \rightarrow \infty$.

Step 2. $s \in]p, \infty[$. Next, we assert that the embedding of E into $L_Q^s(\mathbb{R})$ is also compact. This can be shown by noting

$$\begin{aligned} \|u_k - u\|_{L_Q^s}^s &= \int_{\mathbb{R}} e^{Q(t)} |u_k - u|^s dt \\ &\leq \left(\frac{M_\infty}{\sqrt{m_0}} \right)^{s-p} \|u_k - u\|_{L_Q^p}^p. \end{aligned} \quad (24)$$

Building on the result from Step 1, we conclude that $u_k \rightarrow u$ in $L_Q^s(\mathbb{R})$.

Step 3. $s \in [\frac{p}{2}, p[$. We claim that $u_k \rightarrow u$ in $L_Q^s(\mathbb{R})$. Let $\tau = \frac{v}{p-s}$. Then $s > \frac{p}{1+v}$ and $\tau s > 1$. For $v \in L_Q^s(\mathbb{R})$, Hölder's inequality implies

$$\begin{aligned} & \int_{|t| \geq r_\varepsilon} e^{Q(t)} |v(t)|^s dt = \int_{B_\varepsilon} e^{Q(t)} |v(t)|^s dt \\ & + \int_{D_\varepsilon} e^{Q(t)} |v(t)|^s dt \\ & \leq \left(\int_{B_\varepsilon} e^{Q(t)} dt \right)^{\frac{p-1}{p}} \left(\int_{B_\varepsilon} e^{Q(t)} |v(t)|^{ps} dt \right)^{\frac{1}{p}} \\ & + \int_{\substack{t \in D_\varepsilon \\ |t|^{-1/s} \ln^{-\tau} |t| |v(t)| \leq 1}} e^{Q(t)} |v(t)|^s dt \\ & + \int_{\substack{t \in D_\varepsilon \\ |t|^{-1/s} \ln^{-\tau} |t| |v(t)| \geq 1}} e^{Q(t)} |v(t)|^s dt \\ & \leq (\text{meas}_Q(B_\varepsilon))^{\frac{p-1}{p}} \|v\|_{L_Q^{ps}}^s + \int_{|t| \geq r_\varepsilon} \frac{e^{Q(t)}}{|t| \ln^{\tau s} |t|} dt \\ & + \int_{\substack{t \in D_\varepsilon \\ |t|^{-1/s} \ln^{-\tau} |t| |v(t)| \geq 1}} \frac{e^{Q(t)}}{|t| \ln^{\tau s} |t|} \\ & \quad \times (|t|^{1/s} \ln^\tau |t| |v(t)|)^s dt \\ & \leq \varepsilon^{\frac{p-1}{p}} \|v\|_{L_Q^{ps}}^s + \int_{|t| \geq r_\varepsilon} \frac{e^{Q(t)}}{|t| \ln^\nu |t|} dt \\ & + \int_{\substack{t \in D_\varepsilon \\ |t|^{-1/s} \ln^{-\tau} |t| |v(t)| \geq 1}} (|t|^{1/s} \ln^\tau |t| |v(t)|)^p dt \\ & \leq \varepsilon^{\frac{p-1}{p}} \|v\|_{L^{ps}}^s + \varepsilon + \int_{|t| \geq r_\varepsilon} |t|^{\frac{p}{s}-1} \ln^{\tau(p-s)} |t| |v(t)|^p dt \\ & \leq \varepsilon^{\frac{p-1}{p}} \|v\|_{L^{ps}}^s + \varepsilon + \int_{|t| \geq r_\varepsilon} |t| \ln^\nu |t| |v(t)|^p dt \\ & \leq \varepsilon^{\frac{p-1}{p}} \|v\|_{L^{ps}}^s + \varepsilon + \frac{1}{a_\varepsilon} \int_{|t| \geq r_\varepsilon} a(t) |v(t)|^p dt \\ & \leq \varepsilon^{\frac{p-1}{p}} \|v\|_{L^{ps}}^s + \varepsilon + \varepsilon \|v\|^p \\ & \leq \varepsilon^{\frac{p-1}{p}} \left(\|v\|_{L_Q^{ps}}^s + 1 + \|v\|^p \right). \end{aligned} \quad (25)$$

Hence, we have

$$\begin{aligned} & \int_{|t| \geq r_\varepsilon} e^{Q(t)} |u_k(t) - u(t)|^s dt \\ & \leq \varepsilon^{\frac{p-1}{p}} \left[\|u_k - u\|_{L_Q^{ps}}^s + 1 + \|u_k - u\|^p \right]. \end{aligned} \quad (26)$$

Since $ps \geq p$, we deduce that

$$\int_{|t| \geq r_\varepsilon} e^{Q(t)} |u_k(t) - u(t)|^s dt \leq \varepsilon^{\frac{p-1}{p}} \left[M_{ps}^s + 1 + M^p \right]. \quad (27)$$

As above $\int_{I_\varepsilon} e^{Q(t)} |u_k(t) - u(t)|^s dt \rightarrow 0$ as $k \rightarrow \infty$. Hence $u_k \rightarrow u$ in $L^s_Q(\mathbb{R})$.

The proof of Lemma 2.2 is completed. \blacksquare

Our proof applies critical point theory, specifically the symmetric mountain pass theorem due to Kajikiya [5], to establish the main result. Before proceeding, we recall the concept of genus.

Let X be a Banach space and let A be a subset of X . The set A is said to be symmetric if for every element $u \in A$, the element $-u$ is also in A . Let A be a closed symmetric set not containing the origin. Its genus, denoted by $\gamma(A)$, is the smallest integer k for which one can construct an odd continuous mapping from \mathbb{R} to $\mathbb{R}^k \setminus \{0\}$. If no such k exist, we define $\gamma(A) = +\infty$. Additionally, we define $\gamma(\emptyset) = 0$, where \emptyset denotes the empty set. We now introduce the set Γ_k , defined as

$$\Gamma_k = \left\{ A \subset X \mid \begin{array}{l} A \text{ is a closed symmetric subset,} \\ 0 \notin A, \gamma(A) \geq k \end{array} \right\}. \quad (28)$$

Below, we summarize the essential properties of the genus that will be utilized in our argument.

Lemma 2.3. [5, Proposition 7.5.] Let A and B be closed symmetric subsets of a Banach space X that do not contain the origin. The following properties hold:

- (i) If $A \subset B$, then $\gamma(A) \leq \gamma(B)$.
- (ii) The N -dimensional sphere S^N has a genus of $N + 1$ by the Borsuk-Ulam theorem.

Lemma 2.4. [5, Theorem 1] Let E be an infinite-dimensional Banach space and $\Phi \in C^1(X, \mathbb{R})$ be an even functional with $\Phi(0) = 0$. Suppose that Φ satisfies the following conditions:

- (1) Φ is bounded from below and satisfies the (PS) -condition;
- (2) For each $k \in \mathbb{N}$, there exists $A_k \in \Gamma_k$ such that

$$\sup_{u \in A_k} \Phi(u) < 0. \quad (29)$$

The theorem guarantees two types of sequences: (a) a sequence of critical points (u_k) with negative energy converging to zero, and (b) two distinct sequences: one of non-zero critical points with zero energy that tend to zero, and another of critical points with negative energy tending to zero, which itself converges to a non-zero limit.

3 Proof of Theorem 1.1.

Our strategy is to apply critical point theory to a modified version of the potential $W(t, x)$, denoted $\tilde{W}(t, x)$, which coincides with $W(t, x)$ near the origin but is altered for large $|x|$. This modification is defined as follows:

Choose a constant $\varepsilon_0 \in]0, 1[$. By (W_3) , there exists a constant $\delta_0 \in]0, r]$ such that

$$|\nabla W(t, x)| \leq \varepsilon_0 a(t) |x|^{p-1}, \quad \forall |t| \geq R_0 \text{ and } |x| \leq \delta_0. \quad (30)$$

Define a nonincreasing cut-off function $g \in C^1(\mathbb{R}^+, \mathbb{R}^+)$ such that $g(s) = 1$ for $0 \leq s \leq \frac{\delta_0^p}{2^p}$, $g(s) = 0$ for $s \geq \delta_0^p$ and $0 \leq g(s) \leq 1$ for all $s \in \mathbb{R}^+$. Let

$$\tilde{W}(t, x) = g(|x|^p) W(t, x), \quad \forall (t, x) \in \mathbb{R} \times \mathbb{R}^N. \quad (31)$$

This modified potential leads us to consider the following associated system $(\tilde{\mathcal{W}})$:

$$\begin{aligned} \frac{d}{dt} \left(|\dot{u}(t)|^{p-2} \dot{u}(t) \right) + q(t) \dot{u}(t) - a(t) u(t) \\ + \nabla \tilde{W}(t, u(t)) = 0, \quad t \in \mathbb{R}. \end{aligned} \quad (32)$$

and we can now define the action functional J for the modified system $(\tilde{\mathcal{W}})$ by

$$\begin{aligned} J(u) &= \frac{1}{p} \int_{\mathbb{R}} e^{Q(t)} (|\dot{u}(t)|^p + a(t) |u(t)|^p) dt \\ &\quad - \int_{\mathbb{R}} e^{Q(t)} \tilde{W}(t, u(t)) dt \\ &= \frac{1}{p} \|u\|^p - \int_{\mathbb{R}} e^{Q(t)} \tilde{W}(t, u(t)) dt. \end{aligned} \quad (33)$$

It is well-known that $J \in C^1(E, \mathbb{R})$ and for all $u, v \in E$

$$\begin{aligned} J'(u)v &= \int_{\mathbb{R}} e^{Q(t)} \left(|\dot{u}(t)|^{p-2} \dot{u}(t) \cdot \dot{v}(t) \right. \\ &\quad \left. + a(t) |u(t)|^{p-2} u(t) \cdot v(t) \right) dt \\ &\quad - \int_{\mathbb{R}} e^{Q(t)} \nabla \tilde{W}(t, u(t)) \cdot v(t) dt. \end{aligned} \quad (34)$$

Moreover, critical points of J are fast homoclinic solutions of $(\tilde{\mathcal{W}})$.

Lemma 3.1. Assume that (A) , (W_1) , and (W_3) hold. Then $J(0) = 0$ and J is even and bounded from below.

Proof By (W_1) , it is clear that J is even and $J(0) = 0$. From Eq. (30) and the fact that $W(t, 0) = 0$, we obtain

$$W(t, x) \leq \frac{\varepsilon_0}{p} a(t) |x|^p, \quad \forall |t| \geq R_0 \text{ and } |x| \leq \delta_0. \quad (35)$$

By combining Eq. (35) and the properties of g , we get

$$\begin{aligned} J(u) &= \frac{1}{p} \|u\|^p - \int_{\mathbb{R}} e^{Q(t)} g(|u(t)|^p) W(t, u(t)) dt \\ &= \frac{1}{p} \|u\|^p - \int_{\{|t| \geq R_0\}} e^{Q(t)} g(|u(t)|^p) W(t, u(t)) dt \\ &\quad - \int_{\{|t| \leq R_0\}} e^{Q(t)} g(|u(t)|^p) W(t, u(t)) dt \\ &= \frac{1}{p} \|u\|^p - \int_{\{|t| \geq R_0, |u(t)| \leq \delta_0\}} e^{Q(t)} \\ &\quad \times g(|u(t)|^p) W(t, u(t)) dt \\ &\quad - \int_{\{|t| \leq R_0, |u(t)| \leq \delta_0\}} e^{Q(t)} g(|u(t)|^p) W(t, u(t)) dt \\ &\geq \frac{1}{p} \|u\|^p - \frac{\varepsilon_0}{p} \int_{\mathbb{R}} e^{Q(t)} a(t) |u(t)|^p dt - c_1 \\ &\geq \frac{1 - \varepsilon_0}{p} \|u\|^p - c_1. \end{aligned} \quad (36)$$

where $c_1 = \sup_{|t| \leq R_0, |x| \leq \delta_0} e^{Q(t)} g(|x|^p) W(t, x)$. Hence, J is bounded from below and coercive in E .

Lemma 3.2. Under assumptions (A) and (W_3) , the functional J satisfies the Palais-Smale condition.

Proof We will prove that J satisfies the (PS)-condition. Let (u_n) be a (PS)-sequence, that is, there exists a positive constant M_0 such that

$$|J(u_n)| \leq M_0, \quad \forall n \in \mathbb{N}, \quad \text{and} \quad J'(u_n) \longrightarrow 0 \text{ as } n \rightarrow \infty. \quad (37)$$

Combining estimates (3.3) and (3.4), we deduce the boundedness of the sequence (u_n) in the space E , that is,

$$\|u_n\| \leq c_2, \quad \forall n \in \mathbb{N}. \quad (38)$$

The reflexivity of E allows us to find a weakly convergent subsequence, which we continue to denote by (u_n) for convenience:

$$u_n \rightharpoonup u_0 \text{ weakly in } E \text{ as } n \rightarrow \infty. \quad (39)$$

By (W_3) , for any $0 < \varepsilon < \varepsilon_0$, there exists a constant $0 < \delta < \delta_0$ such that

$$|\nabla W(t, x)| \leq \varepsilon a(t) |x|^{p-1}, \quad \forall |t| \geq R_0, |x| \leq \delta, \quad (40)$$

which, with the condition $W(t, 0) = 0$, yields

$$|W(t, x)| \leq \frac{\varepsilon}{p} a(t) |x|^p, \quad \forall |t| \geq R_0, |x| \leq \delta. \quad (41)$$

By (Q_v) , there exists a constant $T_0 \geq R_0$ such that

$$Q(t) \geq \ln \left(\frac{1}{\delta^p} (p-1)^{\frac{1}{p'}} c_2^p \right). \quad (42)$$

Combining Lemma 2.1, (38), and (42), we have

$$\begin{aligned} |u_n(t)|^p &\leq (p-1)^{\frac{1}{p'}} \\ &\times \int_t^\infty e^{-Q(s)} e^{Q(s)} \left[|u_n(s)|^p + a(s) |u_n(s)|^p \right] ds \\ &\leq (p-1)^{\frac{1}{p'}} \frac{\delta^p}{(p-1)^{\frac{1}{p'}} c_2^{p'}} \|u_n\|^{p'} \leq \delta^p, \\ &\quad \forall t \geq T_0, n \in \mathbb{N}. \end{aligned} \quad (43)$$

Similarly, we get

$$Q(t) \geq \ln \left(\frac{1}{\delta^p} (p-1)^{\frac{1}{p'}} c_2^p \right). \quad (44)$$

Inequalities (38) and (39) yield that $\|u_0\| \leq \liminf_{n \rightarrow \infty} \|u_n\| \leq c_2$, thus by similar steps one can get

$$|u_0(t)|^p \leq \delta^p, \quad \forall |t| \geq T_0. \quad (45)$$

It follows from (3.7), (3.10)-(3.12), and the properties of g that

$$\begin{aligned} &\left| \int_{|t| \geq T_0} e^{Q(t)} g(|u_n(t)|^p) \nabla W(t, u_n(t)) \cdot (u_n(t) - u_0(t)) dt \right. \\ &\quad \left. - \int_{|t| \geq T_0} e^{Q(t)} g(|u_0(t)|^p) \nabla W(t, u_0(t)) \cdot (u_n(t) - u_0(t)) dt \right| \\ &\leq \int_{|t| \geq T_0} e^{Q(t)} (|\nabla W(t, u_n(t))| + |\nabla W(t, u_0(t))|) (|u_n(t)| + |u_0(t)|) dt \\ &\leq 2\varepsilon \int_{|t| \geq T_0} e^{Q(t)} a(t) (|u_n(t)|^{p-1} + |u_0(t)|^{p-1}) \times (|u_n(t)| + |u_0(t)|) dt \\ &\leq 4\varepsilon \int_{|t| \geq T_0} e^{Q(t)} a(t) (|u_n(t)|^p + |u_0(t)|^p) dt \\ &\leq 4\varepsilon (\|u_n\|^p + \|u_0\|^p) \leq 8\varepsilon c_2^p. \end{aligned} \quad (46)$$

Conditions (41), (43)-(45), and the properties of g yield

$$\begin{aligned}
& \left| p \int_{|t| \geq T_0} e^{Q(t)} g'(|u_n(t)|^p) |u_n(t)|^{p-2} u_n(t) \right. \\
& \quad \times W(t, u_n(t)) \cdot (u_n(t) - u_0(t)) dt \\
& \quad - p \int_{|t| \geq T_0} e^{Q(t)} g'(|u_0(t)|^p) |u_0(t)|^{p-2} u_0(t) \\
& \quad \times W(t, u_0(t)) \cdot (u_n(t) - u_0(t)) dt \left. \right| \\
& \leq 2p \delta_0^p \int_{|t| \geq T_0} e^{Q(t)} |g'(|u_n(t)|^p)| |W(t, u_n(t))| dt \\
& \quad + 2p \delta_0^p \int_{|t| \geq T_0} e^{Q(t)} |g'(|u_0(t)|^p)| |W(t, u_0(t))| dt \\
& \leq 2p \delta_0^p c_3 \int_{\mathbb{R}} e^{Q(t)} \frac{\varepsilon}{p} a(t) (|u_n(t)|^p + |u_0(t)|^p) dt \\
& \leq 4 \delta_0^p c_3 c_2^p \varepsilon.
\end{aligned} \tag{47}$$

where $c_3 = \max_{t \in [\frac{\delta_0^p}{2^p}, \delta_0^p]} |g'(t)|$. From Lemma 2.2 and (3.5), we obtain

$$|u_n(t)| \leq \|u_n\|_{L^\infty} \leq \eta_\infty \|u_n\| \leq \eta_\infty c_2 = c_4, \quad \forall t \in \mathbb{R}, \forall n \in \mathbb{N}. \tag{48}$$

and

$$|u_0(t)| \leq \|u_0\|_{L^\infty} \leq \eta_\infty \|u_0\| \leq \eta_\infty c_2 = c_4, \quad \forall t \in \mathbb{R}. \tag{49}$$

Combining (48) and (49), we get for a positive constant c_5

$$\begin{aligned}
|\nabla W(t, u_n(t))| &\leq c_5, \\
|\nabla W(t, u_0(t))| &\leq c_5, \quad \forall t \in [-T_0, T_0], \forall n \in \mathbb{N}.
\end{aligned} \tag{50}$$

and

$$\begin{aligned}
|W(t, u_n(t))| &\leq c_5, \\
|W(t, u_0(t))| &\leq c_5, \quad \forall t \in [-T_0, T_0], \forall n \in \mathbb{N}.
\end{aligned} \tag{51}$$

Since E is continuously embedded in $W_Q^{1,p}([-T_0, T_0], \mathbb{R}^N)$, Sobolev's embedding theorem implies that

$$u_n \rightarrow u_0 \quad \text{uniformly on } [-T_0, T_0]. \tag{52}$$

Then, by (50), (52), and the properties of g , we have

$$\begin{aligned}
& \left| \int_{|t| \leq T_0} e^{Q(t)} g(|u_n(t)|^p) \right. \\
& \quad \times \nabla W(t, u_n(t)) \cdot (u_n(t) - u_0(t)) dt \\
& \quad - \int_{|t| \leq T_0} e^{Q(t)} g(|u_0(t)|^p) \\
& \quad \times \nabla W(t, u_0(t)) \cdot (u_n(t) - u_0(t)) dt \left. \right| \\
& \leq \int_{|t| \leq T_0} e^{Q(t)} (|\nabla W(t, u_n(t))| \\
& \quad + |\nabla W(t, u_0(t))|) |u_n(t) - u_0(t)| dt \\
& \leq 2c_5 \int_{|t| \leq T_0} e^{Q(t)} |u_n(t) - u_0(t)| dt \rightarrow 0 \\
& \quad \text{as } n \rightarrow \infty.
\end{aligned} \tag{53}$$

so there exists $N_1 \in \mathbb{N}$ such that

$$\begin{aligned}
& \left| \int_{|t| \leq T_0} e^{Q(t)} g(|u_n(t)|^p) \right. \\
& \quad \times \nabla W(t, u_n(t)) \cdot (u_n(t) - u_0(t)) dt \\
& \quad - \int_{|t| \leq T_0} e^{Q(t)} g(|u_0(t)|^p) \\
& \quad \times \nabla W(t, u_0(t)) \cdot (u_n(t) - u_0(t)) dt \left. \right| \leq \varepsilon, \quad \forall n \geq N_1.
\end{aligned} \tag{54}$$

In addition, from (51), (52), and the properties of g , one gets

$$\begin{aligned}
& \left| p \int_{|t| \leq T_0} e^{Q(t)} g'(|u_n(t)|^p) |u_n(t)|^{p-2} u_n(t) \right. \\
& \quad \times W(t, u_n(t)) \cdot (u_n(t) - u_0(t)) dt \\
& \quad - p \int_{|t| \leq T_0} e^{Q(t)} g'(|u_0(t)|^p) |u_0(t)|^{p-2} u_0(t) \\
& \quad \times W(t, u_0(t)) \cdot (u_n(t) - u_0(t)) dt \left. \right| \leq 2p c_5 \delta_0^{p-1} \\
& \quad \times \sup_{s \in [\frac{\delta_0^p}{2^p}, \delta_0^p]} |g'(s)| \int_{|t| \leq T_0} e^{Q(t)} |u_n(t) - u_0(t)| dt \\
& \rightarrow 0 \quad \text{as } n \rightarrow \infty.
\end{aligned} \tag{55}$$

Hence, there exists $N_2 \in \mathbb{N}$ such that

$$\begin{aligned}
& \left| p \int_{|t| \leq T_0} e^{Q(t)} g'(|u_n(t)|^p) |u_n(t)|^{p-2} u_n(t) \right. \\
& \quad \times W(t, u_n(t)) \cdot (u_n(t) - u_0(t)) dt \\
& \quad - p \int_{|t| \leq T_0} e^{Q(t)} g'(|u_0(t)|^p) |u_0(t)|^{p-2} u_0(t) \\
& \quad \times W(t, u_0(t)) \cdot (u_n(t) - u_0(t)) dt \left. \right| \\
& \leq \varepsilon, \quad \forall n \geq N_2.
\end{aligned} \tag{56}$$

Combining (46), (47), (54), and (56), we obtain

$$\begin{aligned}
& \|u_n - u_0\|^p - (J'(u_n) - J'(u_0))(u_n - u_0) \\
&= \int_{\mathbb{R}} e^{Q(t)} g(|u_n(t)|^p) \\
&\quad \times \nabla W(t, u_n(t)) \cdot (u_n(t) - u_0(t)) dt \\
&\quad - \int_{\mathbb{R}} e^{Q(t)} g(|u_0(t)|^p) \\
&\quad \times \nabla W(t, u_0(t)) \cdot (u_n(t) - u_0(t)) dt \\
&\quad + p \int_{\mathbb{R}} e^{Q(t)} g'(|u_n(t)|^p) |u_n(t)|^{p-2} u_n(t) \\
&\quad \times W(t, u_n(t)) \cdot (u_n(t) - u_0(t)) dt \\
&\quad - p \int_{\mathbb{R}} e^{Q(t)} g'(|u_0(t)|^p) |u_0(t)|^{p-2} u_0(t) \\
&\quad \times W(t, u_0(t)) \cdot (u_n(t) - u_0(t)) dt \\
&\leq (8c_2^p + 4p\delta_0^p c_3 c_2^p + 2)\varepsilon, \quad \forall n \geq \max(N_1, N_2).
\end{aligned} \tag{57}$$

This with (3.5) and (3.6) shows that $u_n \rightarrow u_0$ in E . Hence J satisfies the (PS)-condition.

Lemma 3.3. Assume that (A) and (W₂) hold, then for all $k \in \mathbb{N}$, there exists an $A_k \in \Gamma_k$ such that $\sup_{u \in A_k} J(u) < 0$.

Proof For any fixed $k \in \mathbb{N}$, we divide the interval $I = [a, b]$ into k equal closed subintervals, denoted by I_i for $i = 1, \dots, k$. For each i , let $K_i \subset I_i$ be a subset such that K_i has the same center as I_i and has a length of $\frac{b-a}{2k}$. Now, choose k functions $\varphi_i \in C^1(\mathbb{R}, \mathbb{R}^N)$ for $i = 1, \dots, k$ such that

$$\begin{aligned}
& \text{supp}(\varphi_i) \subset I_i, \quad \text{supp}(\varphi_i) \cap \text{supp}(\varphi_j) = \emptyset, \quad \forall i \neq j, \\
& |\varphi_i(t)| \leq 1, \quad |\varphi_i'(t)| \leq M, \quad \forall t \in \mathbb{R}, \\
& |\varphi_i(t)| = 1, \quad \forall t \in K_i.
\end{aligned} \tag{58}$$

where M is a constant independent of i . Let

$$\begin{aligned}
V_k &= \left\{ (t_1, \dots, t_k) \in \mathbb{R}^k \mid \max_{1 \leq i \leq k} |t_i| = 1 \right\}, \\
X_k &= \left\{ \sum_{i=1}^k t_i \varphi_i \mid (t_1, \dots, t_k) \in V_k \right\}.
\end{aligned} \tag{59}$$

It is evident that $\text{supp}(u) \subset I$ for any $u = \sum_{i=1}^k t_i \varphi_i$. The paper [8] implies that X_k is a closed subset of E with $\gamma(X_k) = k$. By the properties of φ_i , for fixed $k \in \mathbb{N}$, there exists a constant $\beta_k > 0$ such that

$$\|u\| \leq \beta_k, \quad \forall u \in X_k. \tag{60}$$

From (W₂), there exist two positive constants η and R such that

$$W(t, x) \geq R|x|^\alpha, \quad \forall t \in [a, b], |x| \leq \eta. \tag{61}$$

For every $u = \sum_{i=1}^k t_i \varphi_i \in X_k$, let $s_k \in]0, \min(\eta, \frac{\delta_0}{2\eta_\infty \beta_k})[$. Then, by (3.22), we have

$$\begin{aligned}
|s_k u(t)|^p &\leq s_k^p \|u\|_{L^\infty}^p \leq s_k^p \eta_\infty^p \|u\|^p \\
&\leq \frac{\delta_0^p}{2^p \eta_\infty^p \beta_k^p} \eta_\infty^p \beta_k^p = \frac{\delta_0^p}{2^p}.
\end{aligned} \tag{62}$$

which implies that $g(|s_k u(t)|^p) = 1$. Moreover, by the properties of φ_i , we obtain

$$\begin{aligned}
|s_k t_i \varphi_i(t)| &= s_k |t_i| |\varphi_i(t)| \\
&\leq s_k \leq \eta, \quad \forall i = 1, \dots, k.
\end{aligned} \tag{63}$$

The definitions of V_k and φ_i imply that there exists a $j \in \{1, \dots, k\}$ such that $|t_j| = 1$ and $|\psi_j(t)| = 1$ for any $t \in K_j$. Now, from (3.22) – (3.24), we get

$$\begin{aligned}
J(s_k u) &= \frac{1}{p} \|s_k u\|^p - \int_{\mathbb{R}} e^{Q(t)} W(t, s_k u(t)) dt \\
&= \frac{s_k^p}{p} \|u\|^p - \int_a^b e^{Q(t)} W(t, s_k u(t)) dt \\
&\leq \frac{s_k^p}{p} \beta_k^p - \sum_{i=1}^k \int_{I_i} e^{Q(t)} W(t, s_k t_i \varphi_i(t)) dt \\
&\leq \frac{s_k^p}{p} \beta_k^p - \int_{K_j} e^{Q(t)} W(t, s_k t_j \psi_j(t)) dt \\
&\leq \frac{s_k^p}{p} \beta_k^p - R \int_{K_j} e^{Q(t)} |s_k t_j \psi_j(t)|^\alpha dt \\
&\leq \frac{s_k^p}{p} \beta_k^p - m_0 R s_k^\alpha \text{meas}(K_j) \\
&= \frac{s_k^p}{p} \beta_k^p - \frac{b-a}{2k} m_0 R s_k^\alpha, \quad \forall u \in X_k.
\end{aligned} \tag{64}$$

Note that R can be any sufficiently large number, so choose $R \geq \frac{2k\beta_k^p}{m_0(b-a)} s_k^{p-\alpha}$. From (3.25), we have

$$J(s_k u_k) \leq \frac{s_k^p}{p} \beta_k^p - s_k^p \beta_k^p = -\frac{1}{q} s_k^p \beta_k^p < 0, \quad \forall u \in X_k. \quad (65)$$

For each $k \in \mathbb{N}$, let $A_k = s_k X_k$. Then, we have $\gamma(A_k) = \gamma(s_k X_k) = k$, so $A_k \in \Gamma_k$ and $\sup_{u \in A_k} J(u) < 0$. The proof is complete.

Lemmas 3.1 – 3.3 establish that J satisfies all the hypotheses of Lemma 2.4, implying the existence of a sequence of nontrivial critical points $(u_n) \subset E$ of the functional J , where $u_n \rightarrow 0$ in E as $n \rightarrow \infty$. Therefore, (u_n) forms a sequence of fast homoclinic solutions for the system $(\mathcal{D}\mathcal{V})$. From Lemma 2.2, it follows that $\sup_{t \in \mathbb{R}} |u_n(t)| \rightarrow 0$ as $n \rightarrow \infty$. Consequently, there exists a positive constant n_0 such that for all $n \geq n_0$, we have $\sup_{t \in \mathbb{R}} |u_n(t)| \leq \delta_0$, where δ_0 is as defined previously. This implies that for all $n \geq n_0$, u_n is a fast homoclinic solution to the system $(\mathcal{D}\mathcal{V})$. The proof of Theorem 1.1 is thus complete.

4 Proof of Theorem 1.2.

Let the cut-off function $h \in C^1(\mathbb{R}^+, \mathbb{R}^+)$ be defined such that $h(t) = 1$ for $t \in [0, \frac{\rho}{2}]$, $h(t) = 0$ for $t \geq \rho$, and $-\rho \leq h'(t) < 0$ for $\frac{\rho}{2} < t < \rho$. We define the modified function

$$\widehat{W}(t, x) = h(|x|) W(t, x) + c(1 - h(|x|)) |x|^\sigma, \quad (66)$$

$$\forall (t, x) \in \mathbb{R} \times \mathbb{R}^N.$$

where c is defined in (W_4) . Next, we introduce the following modified system $(\widehat{\mathcal{D}\mathcal{V}})$

$$\frac{d}{dt} \left(|\dot{u}(t)|^{p-2} \dot{u}(t) \right) + q(t) \dot{u}(t) - L(t) u(t) + \nabla \widehat{W}(t, u(t)) = 0, \quad t \in \mathbb{R}. \quad (67)$$

We then define the variational functional \widehat{J} associated with the modified system as

$$\begin{aligned} \widehat{J}(u) &= \frac{1}{p} \int_{\mathbb{R}} e^{Q(t)} \left(|\dot{u}(t)|^p + a(t) |u(t)|^p \right) dt \\ &\quad - \int_{\mathbb{R}} e^{Q(t)} \widehat{W}(t, u(t)) dt \\ &= \frac{1}{p} \|u\|^p - \int_{\mathbb{R}} e^{Q(t)} \widehat{W}(t, u(t)) dt. \end{aligned} \quad (68)$$

It is well established that $\widehat{J} \in C^1(E, \mathbb{R})$, and for any $u, v \in E$, the derivative of \widehat{J} is given by

$$\begin{aligned} \widehat{J}'(u)v &= \int_{\mathbb{R}} e^{Q(t)} \left(|\dot{u}(t)|^{p-2} \dot{u}(t) \cdot \dot{v}(t) \right. \\ &\quad \left. + a(t) |u(t)|^{p-2} u(t) \cdot v(t) \right) dt \\ &\quad - \int_{\mathbb{R}} e^{Q(t)} \nabla \widehat{W}(t, u(t)) \cdot v(t) dt. \end{aligned} \quad (69)$$

Furthermore, the critical points of \widehat{J} correspond to fast homoclinic solutions of $(\widehat{\mathcal{D}\mathcal{V}})$.

Lemma 4.1. Assume that the conditions (A) , (A_v) , (W_1) , and (W_4) are satisfied. Then, the functional \widehat{J} is bounded from below and fulfills the (PS) -condition.

Proof From (W_4) and the fact that $W(t, 0) = 0$, it follows that

$$|W(t, x)| \leq \frac{c}{\sigma} |x|^\sigma \leq c |x|^\sigma, \quad \forall |t| \geq R_1 \text{ and } |x| \leq \rho. \quad (70)$$

which, together with the properties of h , gives

$$|\widehat{W}(t, x)| \leq c |x|^\sigma, \quad \forall |t| \geq R_1 \text{ and } |x| \leq \rho. \quad (71)$$

For $\frac{\rho}{2} \leq |x| < \rho$, we have

$$\begin{aligned} |\nabla \widehat{W}(t, x)| &= \left| h(|x|) \nabla W(t, x) + h'(|x|) \frac{x}{|x|} W(t, x) \right. \\ &\quad \left. + c \sigma (1 - h(|x|)) |x|^{\sigma-2} x \right. \\ &\quad \left. - c h'(|x|) |x|^{\sigma-1} x \right| \\ &\leq d |x|^{\sigma-1}. \end{aligned} \quad (72)$$

where $d = c \left(1 + \frac{\rho^2}{\sigma} + \sigma + \rho^2 \right)$. For $|x| > \rho$, we get

$$|\nabla \widehat{W}(t, x)| = c \sigma |x|^{\sigma-1}. \quad (73)$$

For $|x| < \frac{\rho}{2}$, it follows that

$$|\nabla \widehat{W}(t, x)| = |\nabla W(t, x)| \leq c |x|^{\sigma-1}. \quad (74)$$

Thus, we conclude that

$$|\nabla \widehat{W}(t, x)| \leq d |x|^{\sigma-1}, \quad \forall |t| \geq R_1, x \in \mathbb{R}^N. \quad (75)$$

Hence, we can write the functional \widehat{J} as

$$\begin{aligned}
\widehat{J}(u) &= \frac{1}{p} \|u\|^p - \int_{\mathbb{R}} e^{Q(t)} \widehat{W}(t, u(t)) dt \\
&= \frac{1}{p} \|u\|^p - \int_{\{|t| \geq R_1\}} e^{Q(t)} \widehat{W}(t, u(t)) dt \\
&\quad - \int_{\{|t| \leq R_1\}} e^{Q(t)} \widehat{W}(t, u(t)) dt \\
&= \frac{1}{p} \|u\|^p - \int_{\{|t| \geq R_1, |u(t)| \leq \rho\}} e^{Q(t)} \widehat{W}(t, u(t)) dt \\
&\quad - \int_{\{|t| \leq R_1, |u(t)| \leq \rho\}} e^{Q(t)} \widehat{W}(t, u(t)) dt \quad (76) \\
&\geq \frac{1}{p} \|u\|^p - c \int_{\{|t| \geq R_1\}} e^{Q(t)} |u(t)|^\sigma dt - c_6 \\
&\geq \frac{1}{p} \|u\|^p - c \int_{\mathbb{R}} e^{Q(t)} |u(t)|^\sigma dt - c_6 \\
&= \frac{1}{p} \|u\|^p - c \|u\|_{L_Q^\sigma}^\sigma - c_6 \\
&\geq \frac{1}{p} \|u\|^p - c \eta_\sigma^\sigma \|u\|^\sigma - c_6.
\end{aligned}$$

where $c_6 = 2R_1 \sup_{\{|t| \leq R_1, |x| \leq \rho\}} e^{Q(t)} |\nabla \widehat{W}(t, x)|$. Since $\sigma < p$, we conclude that \widehat{J} is bounded from below and coercive in E . Next, let $(u_n) \subset E$ be a (PS)-sequence of \widehat{J} , i.e., there exists a positive constant c_7 such that

$$|\widehat{J}(u_n)| \leq c_7, \quad \widehat{J}'(u_n) \rightarrow 0 \text{ as } n \rightarrow \infty. \quad (77)$$

From (76) and (77), we deduce that there exists a positive constant c_8 such that

$$\|u_n\| \leq c_8, \quad \forall n \in \mathbb{N}. \quad (78)$$

Since E is reflexive, (78) implies that (u_n) has a subsequence (denoted by (u_n)) such that

$$u_n \rightharpoonup u_n \text{ weakly in } E \text{ as } n \rightarrow \infty. \quad (79)$$

Using similar arguments as in Lemma 3.2, we can show that there exists a constant $T_1 \geq R_1$ such that

$$|u_n(t)| \leq \rho \quad \text{and} \quad |u_0(t)| \leq \rho, \quad \forall |t| \geq T_1, \forall n \in \mathbb{N}. \quad (80)$$

Moreover, we have

$$u_n \rightarrow u_0 \quad \text{uniformly on } [-T_1, T_1]. \quad (81)$$

$$\begin{aligned}
&\|u_n - u_0\|^p - (\widehat{J}'(u_n) - \widehat{J}'(u_0))(u_n - u_0) \\
&= \int_{\mathbb{R}} e^{Q(t)} [\nabla \widehat{W}(t, u_n(t)) - \nabla \widehat{W}(t, u_0(t))] \\
&\quad \times (u_n(t) - u_0(t)) dt \\
&= \int_{\{|t| \geq T_1\}} e^{Q(t)} [\nabla \widehat{W}(t, u_n(t)) - \nabla \widehat{W}(t, u_0(t))] \\
&\quad \times (u_n(t) - u_0(t)) dt \\
&\quad + \int_{\{|t| \leq T_1\}} e^{Q(t)} [\nabla \widehat{W}(t, u_n(t)) - \nabla \widehat{W}(t, u_0(t))] \\
&\quad \times (u_n(t) - u_0(t)) dt \\
&\leq d \int_{\{|t| \geq T_1\}} e^{Q(t)} (|u_n(t)|^{\sigma-1} + |u_0(t)|^{\sigma-1}) \\
&\quad \times |u_n(t) - u_0(t)| dt \\
&\quad + c_9 \int_{\{|t| \leq T_1\}} e^{Q(t)} |u_n(t) - u_0(t)| dt \\
&\leq d \left[\left(\int_{\{|t| \geq T_1\}} e^{Q(t)} |u_n(t)|^{\frac{(\sigma-1)p}{p-2}} dt \right)^{\frac{p-2}{p}} \right. \\
&\quad \left. + \left(\int_{\{|t| \geq T_1\}} e^{Q(t)} |u_0(t)|^{\frac{(\sigma-1)p}{p-2}} dt \right)^{\frac{p-2}{p}} \right] \\
&\quad \times \left(\int_{\{|t| \geq T_1\}} e^{Q(t)} |u_n(t) - u_0(t)|^{\frac{p}{2}} dt \right)^{\frac{2}{p}} \\
&\quad + c_9 \int_{\{|t| \leq T_1\}} e^{Q(t)} |u_n(t) - u_0(t)| dt \\
&\leq d \left(\|u_n\|_{L_Q^{\frac{(\sigma-1)p}{p-2}}}^{\sigma-1} + \|u_0\|_{L_Q^{\frac{(\sigma-1)p}{p-2}}}^{\sigma-1} \right) \|u_n - u_0\|_{L_Q^{\frac{p}{2}}} \\
&\quad + c_9 \int_{\{|t| \leq T_1\}} e^{Q(t)} |u_n(t) - u_0(t)| dt \\
&\leq 2d \eta_{\frac{(\sigma-1)p}{p-2}}^{\sigma-1} c_8^{\sigma-1} \|u_n - u_0\|_{L_Q^{\frac{p}{2}}} \\
&\quad + c_9 \int_{\{|t| \leq T_1\}} e^{Q(t)} |u_n(t) - u_0(t)| dt \\
&\quad \rightarrow 0 \quad \text{as } n \rightarrow \infty.
\end{aligned} \quad (82)$$

Hence, $u_n \rightarrow u_0$ in E as $n \rightarrow \infty$, that is \widehat{J} satisfies the (PS)-condition.

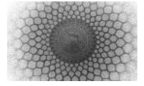
By (W_1) , the fact that $W(t, 0) = 0$ and the properties of h , it follows that \widehat{J} is even and $\widehat{J}(0) = 0$. Combining this with Lemma 3.2 and Lemma 4.1, we conclude that \widehat{J} satisfies all the conditions of Lemma 2.4. Therefore, \widehat{J} has a sequence (u_n) of nontrivial critical points that converges to 0 as $n \rightarrow \infty$ in E . As a result, (u_n) is a sequence of fast homoclinic solutions for $(\widehat{\mathcal{D}}\mathcal{V})$. By Lemma 2.2, we deduce

that $\sup_{t \in \mathbb{R}} |u_n(t)| \rightarrow 0$ as $n \rightarrow \infty$. Thus, there exists a positive constant n_0 such that for all $n \geq n_0$, $\sup_{t \in \mathbb{R}} |u_n(t)| \leq \rho$, where ρ is as defined earlier. Hence, for all $n \geq n_0$, u_n is a fast homoclinic solution of $(\mathcal{D}\mathcal{V})$. This completes the proof of Theorem 1.2.

Acknowledgment. The author sincerely thanks the anonymous referees and the Executive Editor for their careful reading of the manuscript and for their valuable comments and helpful suggestions, which have greatly improved the quality of this paper.

References

1. M.A. Herrero, J.L. Vazquez, *Comm. Part. Differ. Equ.* **7**, (1982)
2. R.P. Agarwal, P. Chen, X. Tang, *Appl. Math. Comp.* **219**, (2013)
3. P. Chen, X.H. Tang, *Math. Nachr.* **286**, (2013)
4. F. Khelifi, M. Timoumi, *Indigat. Math.* **28**, (2017)
5. M. Timoumi, *J. Nonlinear Funct. Anal.* **2016**, (2016)
6. M. Timoumi, *Comm. Opt. Theory* **2017**, (2017)
7. M. Timoumi, *Diff. Eq. Dynam. Sys.* (2024)
8. M. Timoumi, *J. Elli. Parab. Eq.* **6**, (2020)
9. M. Timoumi, *J. Nonlinear Funct. Anal.* **2020**, (2020)
10. M. Timoumi, *Sahand Comm. Math. Analysis* **21**, (2024)
11. M. Timoumi, *J. Nonlinear Var. Anal.* **5**, (2021)
12. M. Timoumi, W. Selmi, *Commun. Korean Math. Soc.* **37**, (2022)
13. M. Timoumi, *Z. Anal. Anwend.* **43**, (2024)
14. M. Timoumi, *Mediterr.J. Math.* **2018**, (2018)
15. X. Wu, W. Zhang, *Nonlinear Anal.* **74**, (2011)
16. X. Lin, X.H. Tang, *Taiwanese J. of Math.* **17**, (2013)
17. X. Lv, S. Lu, *Appl. Math. and Comp.* **218**, (2012)
18. L. Wan, *Bound. Value Pr.* **2020**, (2020)
19. X. Zhang, *Electr. J. Diff. Eq.* **2013**, (2013)
20. Z. Zhang, R. Yuan, *Qual. Theory Dyn. Syst.* **16**, (2017)
21. P. Chen, Xh. Tang, Yy. Zhang, *Acta Math. Appl. Sin. Engl. Ser.* **38**, (2022)
22. M. Timoumi, *Le Matematiche* **LXXIX**, (2024)
23. R. Kajikiya, *J. Functional Anal.* **225**, (2005)
24. P. Liu, F. Guo, *Acta Math. Sinica, English Ser.* **38**, (2022)



The existence of solutions for two types of nonlinear equations on locally finite graphs

Zidong Qiu^{1,a}

¹Department of Mathematics and Physics, Zibo normal college, Shandong, 255188, China

Received: 25 September 2025 / Accepted: 28 November 2028 / Published: 28 November 2025

Abstract In this paper, we focus on connected locally finite graphs $G = (V, E)$. First we assume that there are two constants μ_0 and ω_0 , which make the measure function and symmetric weight function satisfy $\mu(x) \geq \mu_0 \forall x \in V$, $\omega_{xy} \geq \omega_0, \forall xy \in E$. Based on this assumption, we obtain two interesting embedding theorems on finite graphs: $W_0^{1,2}(B_k) \hookrightarrow L^p(B_k)$, $W^{1,2}(B_k) \hookrightarrow L^p(B_k)$. Although their inclusion relations are obvious on finite graphs, here we mainly give the control relations under the same control coefficient. Secondly, Δ is the Laplace operator on a general graph. Due to Lin and Yang (2022), using calculus of variations from local to global, we establish the existence of solutions to the exponential power type nonlinear Schrödinger equation, says $-\Delta u + hu = f u e^{\frac{u^2}{2}} + g, x \in V$, and the existence of solutions for fractional nonlinear mean field equations, says $-\Delta u + hu = \frac{g e^u}{\int_V g e^u d\mu} + \frac{f}{u+m}, x \in V$. When f, g and h satisfy some conditions, we prove the existence of non explicit solutions for the above two kinds of equations in a specific space.

1 Introduction

The nonlinear Schrödinger equation and the mean field equation are two crucial and widely studied models in mathematical physics. The classical nonlinear Schrödinger equation describes a series of profound phenomena in continuous Euclidean space, from the transmission of light waves in nonlinear optical fibers to the dynamics of macroscopic quantum wave functions in Bose Einstein condensates[1, 2]. Its mathematical theory and physical applications have been developed to a very mature level. At the same time, the mean field equation, such as the Liouville equation derived from mean field theory in statistical physics or geometric analysis[3], plays a central

role in understanding the collective behavior of multi-body systems, vortex point distribution, and problems in conformal geometry.

In recent years, significant progress has been made in the study of partial differential equations on graphs. We can refer to article[4–16] and the references in it for details. As a discrete extension of Euclidean spaces and Riemannian manifolds, the Laplacian operator and its related equations on the graphs have attracted widespread attention. Grigor'yan, Lin, and Yang[17–19] successfully solved the existence problem of solutions for several types of elliptical equations on graphs by using variational methods, including classic problems such as the Kazdan-Warner equation, Yamabe equation, and Schrödinger equation. Subsequently, as for certain nonlinear Schrödinger equation on locally finite graphs, Zhang and Zhao[20] have obtained non trivial solutions. Fabio Punzo and Marcello Svagna[21] explored the uniqueness problem of solutions to the Schrödinger equation on an infinite graph, with a focus on the case where potential energy tends to zero at infinity. Yang and Zhao[22] first applied the quality constrained variational method system to NLS problems on graphs. In terms of research methods, Sun and Wang[23] innovatively applied the Brouwer degree theory to prove the existence of solutions to the Kazdan- Warner equation on connected finite graphs from another perspective. Liu[24] conducted similar research on the mean field equation. In addition, Huang Wang and Yang[25] studied the mean field equation on finite graphs and its relationship with the relativistic Abel Chern Simons model.

The graph-based NLSE finds applications across multiple physical domains:

In the field quantum networks, Modeling Bose-Einstein condensates in optical lattice potentials, where the discrete nonpolynomial NLSE describes self-attractive BECs in combined trap geometries. On-site collapse phenomena

^ae-mail: xiaodong19961002@vip.qq.com

and soliton stability follow Vakhitov-Kolokolov criteria[26]; In the field of plasma physics, Network-structured plasma systems support novel wave patterns describable by graph NLSE, with applications to fusion device modeling[27]; For 2D Turbulence, Neri's mean field equation describes vortex statistics under stochastic circulation assumptions, with mass quantization phenomena for blow-up sequences[28]; As for social/epidemiological dynamics, Network-structured population models use mean field approaches for phase transition analysis[29, 30].

In the latest research progress, Lin and Yang[12] developed a variational method from local to global on local finite graphs, Qiu and Liu[31] studied the Schrödinger equation with fe^u as the nonlinear term. Based on their research ideas, the current research focus has shifted to exploring the exponential power type fe^{u^2} nonlinear Schrödinger equation and fractional term $\frac{f}{u+m}$ nonlinear mean field equation. Simultaneously we provide two embedding theorems on finite graphs. These works laid an important foundation for the theory of partial differential equations in discrete spaces.

We first declare some annotations and concepts about graphs. Let V is a set of vertices, $E = \{xy|x, y \in V, x \sim y\}$ where $x \sim y$ represents the connection between x and y . Take $G = (V, E)$ is a graph, in this paper, we discuss connected locally finite graphs with symmetric weights and positive finite measures, we always assume that G satisfies the following conditions (a) – (d).

(a) (Locally finite) For any $x \in V$, there exist only finite vertices $y \in V$ such that $xy \in E$.

(b) (Connected) For any $x, y \in V$, there exist finite edges connecting x and y .

(c) (Symmetric weight) For any $x, y \in V$, let $\omega : V \times V \rightarrow \mathbb{R}$ be a positive symmetric weight, i.e. $\omega_{xy} > 0$ and $\omega_{xy} = \omega_{yx}$.

(d) (Positive finite measure) $\mu : V \rightarrow \mathbb{R}^+$ with $x \mapsto \mu(x)$ is a measure function.

Take $C(V)$ as the space composed of all real valued functions on the graph. Regarding any function $u \in C(V)$ on the graph, its Laplacian operator is defined as follows

$$\Delta u(x) = \frac{1}{\mu(x)} \sum_{y \sim x} \omega_{xy}(u(y) - u(x)). \quad (1)$$

In addition, we immediately provide the definition of the gradient modulus of u

$$|\nabla u|(x) = \left(\frac{1}{2\mu(x)} \sum_{y \sim x} \omega_{xy}(u(y) - u(x))^2 \right)^{\frac{1}{2}}. \quad (2)$$

We define the integral of function $u \in C(V)$ as

$$\int_V f d\mu = \sum_{x \in V} \mu(x) f(x). \quad (3)$$

For $\forall p \in [1, +\infty)$, the Lebesgue space $L^p(V) \triangleq \{u | \int_V |u|^p d\mu < +\infty\}$, and the norm on it is

$$\|u\|_{L^p(V)} = \left(\sum_{x \in V} |u(x)|^p \mu(x) \right)^{\frac{1}{p}}, \quad (4)$$

when $p = +\infty$,

$$\|u\|_{\infty} = \sup_{x \in V} |u(x)|. \quad (5)$$

For any $x, y \in V$, since graph G is connected, there exists a shortest path γ connecting x and y . The distance between x and y is defined by $\rho(x, y)$, which means the number of edges belonging to the shortest path γ . That is, if $xy \in E$, then $\rho(x, y) = 1$, if $xy \in E$, without loss of generality, we may choose a shortest path $\gamma = \{x_1, x_2, \dots, x_{k+1}\}$ connecting x and y , then $\rho(x, y) = k$. Take a certain point $O \in V$, for O , establish a distance function as follows

$$\rho(x) = \rho(x, O). \quad (6)$$

The opening ball with O as the center and radius k is denoted by

$$B_k = \{x \in V : \rho(x) < k\}, \quad (7)$$

and the boundary of B_k is written as

$$\partial B_k = \{x \in V : \rho(x) = k\}. \quad (8)$$

For any fixed k , Grigor'yan et al. [18] defined the Sobolev space $W_0^{1,2}(B_k)$ and its norm by

$$W_0^{1,2}(B_k) = \left\{ u : B_k \cup \partial B_k \rightarrow \mathbb{R} \mid u|_{\partial B_k} = 0, \int_{B_k} |\nabla u|^2 d\mu < +\infty \right\}, \quad (9)$$

and

$$\|u\|_{W_0^{1,2}(B_k)} = \left(\int_{B_k} |\nabla u|^2 d\mu \right)^{\frac{1}{2}}. \quad (10)$$

Next we provide another important Sobolev space $W^{1,2}(V)$ and its norm, which are defined by

$$W^{1,2}(V) = \left\{ u : V \rightarrow \mathbb{R} \mid \int_V (|\nabla u|^2 + u^2) d\mu < +\infty \right\} \quad (11)$$

and

$$\|u\|_{W^{1,2}(V)} = \left(\int_V (|\nabla u|^2 + u^2) d\mu \right)^{\frac{1}{2}}. \quad (12)$$

The above two spaces are both Hilbert spaces.

Let $h(x) \geq h_0 > 0$ for all $x \in V$, we define a space of functions

$$\mathcal{H} = \left\{ u \in W_0^{1,2}(V) : \int_V (|\nabla u|^2 + hu^2) d\mu < \infty \right\}, \quad (13)$$

with a norm

$$\|u\|_{\mathcal{H}} = \left(\int_V (|\nabla u|^2 + hu^2) d\mu \right)^{\frac{1}{2}}. \quad (14)$$

It is clear that \mathcal{H} is a Hilbert space with the inner product

$$\langle u, v \rangle_{\mathcal{H}} = \int_V (\nabla u \cdot \nabla v + huv) d\mu, \quad \forall u, v \in \mathcal{H}. \quad (15)$$

where $\nabla u \cdot \nabla v$ is defined as

$$\nabla u \cdot \nabla v = \frac{1}{2\mu(x)} \sum_{y \sim x} \omega(x,y) (u(y) - u(x))(v(y) - v(x)). \quad (16)$$

When $\omega_{xy} > \omega_0 \forall xy \in E$, Lin and Yang[32] proposed a more general embedding theorem.

In this paper, we will consider the following exponential power type the following nonlinear Schrödinger equation on locally finite graph, says

$$\begin{cases} -\Delta u + hu = fue^{u^2} + g, \text{ in } V, \\ u \in \mathcal{H}, \end{cases} \quad (17)$$

and the following fractional term nonlinear mean field equation on locally finite graph, says

$$\begin{cases} -\Delta u + hu = \frac{ge^u}{\int_V ge^u d\mu} + \frac{f}{u+m}, \text{ in } V, \\ u \in \mathcal{H} \cap L^\infty(V), \end{cases} \quad (18)$$

where Δ is the Laplacian operator given as in (1), and \mathcal{H} is defined as in (14).

2 Notations and main results

Theorem 1 (Embedding theorem I) Let $G=(V, E)$ be a graph satisfying conditions (a)–(d). B_k is the opening ball with O as the center and a radius of k , Among them, $\forall O \in V, \forall k \in \mathbb{Z}^+, \rho(x)$ is the distance function with respect to O on B_k . At the same time, it satisfies the following properties:

(1) $\omega_{xy} \geq \omega_0 > 0$; (2) $h(x) \geq h_0 > 0$; (3) $p > 0$ is a constant Then, for $\forall u \in W_0^{1,2}(B_k)$, we have $\|u\|_{L^p(B_k)} \leq C\|u\|_{W_0^{1,2}(B_k)}$.

Theorem 2 (Embedding theorem II) Let $G=(V, E)$ be a graph satisfying conditions (a)–(d). B_k is the opening ball with o as the center and a radius of k , Among them, $\forall O \in V, \forall k \in \mathbb{Z}^+$, If it meets the two conditions of its subordinates:

(1) $\mu(x) \geq \mu_0 > 0$ established for any $x \in V$; (2) $0 < q \leq \infty$

Then for $\forall u \in W^{1,2}(B_k)$, we have $\|u\|_{L^q(B_k)} \leq C\|u\|_{W^{1,2}(B_k)}$. Among them, C is related to B_k, μ_0, q .

Theorem 3 (Conclusion on the Existence of Solutions)

$$\begin{cases} -\Delta u + hu = fue^{u^2} + g, \text{ in } V, \\ u \in \mathcal{H}. \end{cases} \quad (19)$$

If the equation satisfies the following conditions:

(1) $h(x) \geq h_0 > 0$;

$$(2) -h_0 < -M < f < 0;$$

$$(3) f \in L^1(V); (4) g \in L^2(V).$$

We have that the equation (17) has a solution in \mathcal{H} .

we present an embedding theorem 4 that will be used, which has already been proven in [31].

Theorem 4 (Embedding theorem [31]) *Let $G=(V, E)$ be a graph satisfying conditions (a)–(d). For any $u \in W_0^{1,2}(B_k)$ and any $1 \leq q \leq \infty$, there exists a positive constant C depending only on q, h_0 and B_k such that*

$$\|u\|_{L^q(V)} \leq C\|u\|_{W_0^{1,2}(B_k)}. \quad (20)$$

Theorem 5 (Conclusion on the Existence of Solutions) *If the equation (18) satisfies the following six conditions*

- (1). G is a connected locally finite graph
- (2). $\mu(x) \geq \mu_0 > 0$
- (3). $h(x) \geq a_0 > 0$
- (4). $g \geq 0, g \in L^1(V)$ and $\forall O \in V, \forall l > 1, g \neq 0$ in B_l
- (5). $f \in L^q(V), q \in [1, 2],$ and $f \geq 1$
- (6). $m \in \mathbb{R}, 0 < |m| < 1$

then the equation (18) has a solution.

3 Proof of Theorem 1-3

Let's first prove Theorem 1

Proof For $\forall O \in V$, We establish a distance function for point O , denoted as $\rho(x)$. $\forall k \in \mathbb{Z}^+$, We take the opening ball with O as the center and k as the radius, it is recorded as $B_k = \{x \in V, \rho(x, O) < k\}$. We will discuss on the arbitrary opening ball B_k . $\forall x \in B_k, \rho(x, O)$ represents the distance from a point in B_k to a fixed point O , The shortest path is labeled according to the direction from that point to the fixed point, and we have $\gamma = \{x_1, x_2, x_3, \dots, x_{m+1}\}$, Among them, $x = x_1, O = x_{m+1}, x_i$ is the point adjacent to x_{i+1} , and $\rho(x, O) = m$. According to the definition of integral on finite graph, we can naturally know that $\rho(x) \in L^p(B_k)$. In the following proof, we will show that $\|\rho\|_{L^p(B_k)}$ constitutes the control coefficient.

In [31], Qiu and Liu have proven that $\|u\|_{W_0^{1,2}(B_k)} = (\int_{B_k} (|\nabla u|^2 + hu^2)d\mu)^{\frac{1}{2}}$ is the equivalent norm of the

original norm (10). We will use the newly defined norm to discuss the following proof.

$\forall u \in W_0^{1,2}(B_k)$, due to the property of opening the ball with O as the center and radius k , the node of the shortest path is still taken in B_k , we take the node interpolation on the shortest path for processing. $|u(x)| = |u(x_1)| = |u(x_1) - u(x_2) + u(x_2) - \dots - u(x_{m+1}) + u(x_{m+1})| \leq |u(x_1) - u(x_2)| + |u(x_2) - u(x_3)| + \dots + |u(x_m) - u(x_{m+1})| + |u(O)|$.

Firstly, let's establish the relationship between $|u(x)|$ and $\|u\|_{W_0^{1,2}(B_k)}$ below.

$$\begin{aligned} \|u\|_{W_0^{1,2}(B_k)}^2 &= \int_{B_k} (|\nabla u|^2 + hu^2)d\mu \\ &= \int_{B_k} |\nabla u|^2 d\mu + \int_{B_k} hu^2 d\mu \\ &= \sum_{x \in B_k} \mu(x) \cdot \frac{1}{2\mu(x)} \sum_{y \sim x} \omega_{xy}(u(y) - u(x))^2 + \sum_{x \in B_k} \mu(x)h(x)u^2(x) \\ &\geq \sum_{x \in B_k} \mu(x)h(x)u^2(x) \\ &\geq h_0 \sum_{x \in B_k} \mu(x)u^2(x) \\ &\geq h_0\mu(O)u^2(O). \end{aligned} \quad (21)$$

According to the expansion above, we have $|u(O)| \leq \frac{1}{\sqrt{h_0\mu(O)}}\|u\|_{W_0^{1,2}(B_k)}$. Regarding

$$\sum_{i=1}^m |u(x_i) - u(x_{i+1})| \leq m \max_{1 \leq i \leq m} |u(x_i) - u(x_{i+1})|. \quad (22)$$

Since $\omega_{xy} \geq \omega_0 > 0$ holds true for $\forall xy \in E$, so we naturally have that $\frac{\omega_{xy}}{\omega_0} \geq 1, \sqrt{\frac{\omega_{xy}}{\omega_0}} \geq 1$, therefore, which leads to $|u(x_i) - u(x_{i+1})| \leq \sqrt{\frac{\omega_{x_i x_{i+1}}}{\omega_0}} |u(x_i) - u(x_{i+1})|$, And we can obtain that

$$\begin{aligned} &\max_{1 \leq i \leq m} |u(x_i) - u(x_{i+1})| \\ &\leq \max_{1 \leq i \leq m} \sqrt{\frac{\omega_{x_i x_{i+1}}}{\omega_0}} |u(x_i) - u(x_{i+1})| \\ &= \frac{1}{\sqrt{\omega_0}} \max_{1 \leq i \leq m} \sqrt{\omega_{x_i x_{i+1}}} |u(x_i) - u(x_{i+1})|, \end{aligned} \quad (23)$$

Inserting (23) into (22), we have that the original formula $\leq \frac{m}{\sqrt{\omega_0}} \max_{1 \leq i \leq m} \sqrt{\omega_{x_i x_{i+1}}} |u(x_i) - u(x_{i+1})|$, where $m = \rho(x)$.

Next, we will establish the relationship between $\max_{1 \leq i \leq m} \sqrt{\omega_{x_i x_{i+1}}} |u(x_i) - u(x_{i+1})|$ and $W_0^{1,2}(B_k)$ norms to discover the connection between them.

Let's assume that $\max_{1 \leq i \leq m} \sqrt{\omega_{x_i x_{i+1}}} |u(x_i) - u(x_{i+1})| = \sqrt{\omega_{x_m x_{m+1}}} |u(x_m) - u(x_{m+1})|$, due to

$$\|u\|_{W_0^{1,2}(B_k)} = \left(\int_{B_k} (|\nabla u|^2 + h u^2) d\mu \right)^{1/2}. \quad (24)$$

we have

$$\begin{aligned} \|u\|_{W_0^{1,2}(B_k)}^2 &= \int_{B_k} (|\nabla u|^2 + h u^2) d\mu \\ &\geq \int_{B_k} |\nabla u|^2 d\mu \\ &= \sum_{x \in B_k} \mu(x) \cdot \frac{1}{2\mu(x)} \\ &\quad \times \sum_{y \sim x} \omega_{xy} (u(y) - u(x))^2 \\ &= \frac{1}{2} \sum_{x \in B_k, y \sim x} \omega_{xy} (u(y) - u(x))^2 \\ &\geq \frac{1}{2} \omega_{x_m x_{m+1}} (u(x_m) - u(x_{m+1}))^2 \end{aligned} \quad (25)$$

Then, we get $\|u\|_{W_0^{1,2}(B_k)}^2 \geq \frac{1}{2} \omega_{x_m x_{m+1}} (u(x_m) - u(x_{m+1}))^2$, $\sqrt{2} \|u\|_{W_0^{1,2}(B_k)} \geq \sqrt{\omega_{x_m x_{m+1}}} |u(x_m) - u(x_{m+1})|$. Which leads to $\sum_{i=1}^m |u(x_i) - u(x_{i+1})| \leq \frac{m\sqrt{2}}{\sqrt{\omega_0}} \|u\|_{W_0^{1,2}(B_k)}$. So far, we have

$$\begin{aligned} |u(x)| &\leq \frac{m\sqrt{2}}{\sqrt{\omega_0}} \|u\|_{W_0^{1,2}(B_k)} + \frac{1}{\sqrt{h_0 \mu(O)}} \|u\|_{W_0^{1,2}(B_k)} \\ &= \left(\frac{m\sqrt{2}}{\sqrt{\omega_0}} + \frac{1}{\sqrt{h_0 \mu(O)}} \right) \|u\|_{W_0^{1,2}(B_k)}, \end{aligned} \quad (26)$$

which is established for $\forall x \in B_k$.

Finally, let's establish the relationship between $W_0^{1,2}(B_k)$ norm and $L^p(B_k)$ norm below.

We have known that $\rho(x, O) \in L^p(B_k)$. From the connectivity, we have obviously obtained that $\forall y \in B_k, x \neq y$

we have $\rho(x, y) \geq 1$. Below we investigate $\|u\|_{L^p(B_k)}$.

$$\begin{aligned} \|u\|_{L^p(B_k)} &= \left(\int_{B_k} |u(x)|^p d\mu \right)^{\frac{1}{p}} \leq \\ &= \left(\int_{B_k} \left(\frac{\rho(x)\sqrt{2}}{\sqrt{\omega_0}} + \frac{1}{\sqrt{h_0 \mu(O)}} \right)^p \|u\|_{W_0^{1,2}(B_k)}^p d\mu \right)^{\frac{1}{p}} \\ &= \|u\|_{W_0^{1,2}(B_k)} \left(\int_{B_k} \left(\frac{\rho(x)\sqrt{2}}{\sqrt{\omega_0}} + \frac{1}{\sqrt{h_0 \mu(O)}} \right)^p d\mu \right)^{\frac{1}{p}} \\ &\leq \|u\|_{W_0^{1,2}(B_k)} \left(\int_{B_k} \left(\frac{\rho(x)\sqrt{2}}{\sqrt{\omega_0}} \right)^p d\mu \right)^{\frac{1}{p}} \\ &\quad + \left(\int_{B_k} \left(\frac{1}{\sqrt{h_0 \mu(O)}} \right)^p d\mu \right)^{\frac{1}{p}} \\ &= \|u\|_{W_0^{1,2}(B_k)} \left(\frac{\sqrt{2}}{\sqrt{\omega_0}} \|\rho\|_{L^p(B_k)} + \frac{1}{\sqrt{h_0 \mu(O)}} \left(\int_{B_k} 1 d\mu \right)^{\frac{1}{p}} \right). \end{aligned} \quad (27)$$

Where $\|1\|_{L^p(B_k)}^p = \sum_{x \in B_k} \mu(x)$. In view of $\rho(x) \geq 1$, one has $|\rho(x)|^p \geq 1$, $\mu(x) |\rho(x)|^p \geq \mu(x)$, $\sum_{x \in B_k \setminus \{O\}} \mu(x) |\rho(x)|^p \geq \sum_{x \in B_k \setminus \{O\}} \mu(x)$. And thus, we obtain the following comparison expression, which says

$$\begin{aligned} \|1\|_{L^p(B_k)} &\leq \left(\sum_{x \in B_k \setminus \{O\}} \mu(x) |\rho(x)|^p + \mu(O) \right)^{\frac{1}{p}} \\ &\leq 2^{\frac{1}{p}} \cdot \max \left\{ \left(\sum_{x \in B_k} \mu(x) |p|^p \right)^{\frac{1}{p}}, \mu(O)^{\frac{1}{p}} \right\} \\ &\leq 2^{\frac{1}{p}} (\|\rho\|_{L^p(B_k)} + \mu(O)^{\frac{1}{p}}). \end{aligned} \quad (28)$$

Based on the above discussion, one has

$$\begin{aligned} \|u\|_{L^p(B_k)} &\leq \|u\|_{W_0^{1,2}(B_k)} \left(\frac{\sqrt{2}}{\sqrt{\omega_0}} \|\rho\|_{L^p(B_k)} + \frac{2^{\frac{1}{p}}}{\sqrt{h_0 \mu(O)}} (\|\rho\|_{L^p(B_k)} + \mu(O)^{\frac{1}{p}}) \right) \\ &= \|u\|_{W_0^{1,2}(B_k)} \left(\frac{\sqrt{2}}{\sqrt{\omega_0}} + \frac{2^{\frac{1}{p}}}{\sqrt{h_0 \mu(O)}} \|\rho\|_{L^p(B_k)} + \frac{2^{\frac{1}{p}}}{\sqrt{h_0 \mu(O)}} \mu(O)^{\frac{1}{p}} \right), \end{aligned} \quad (29)$$

where the coefficient only depends on $\omega_0, p, \mu(O), h_0, B_k$. By now, we have completed the proof of Theorem 1.

In the following narrate, we will provide the proof of Theorem 2.

Proof The $W^{1,2}(B_k)$ norm of u is denoted as (12), and we investigate $\|u\|_{W^{1,2}(B_k)}^2$. When $0 < p < \infty$,

$$\begin{aligned} \|u\|_{W^{1,2}(B_k)}^2 &= \int_{B_k} |\nabla u|^2 + u^2 d\mu \\ &= \int_{B_k} |\nabla u|^2 d\mu + \int_{B_k} u^2 d\mu \\ &= \sum_{x \in B_k} \mu(x) \cdot \frac{1}{2\mu(x)} \sum_{y \sim x} \omega_{xy}(u(y) \\ &\quad - u(x))^2 + \sum_{x \in B_k} \mu(x) u^2(x) \quad (30) \\ &\geq \sum_{x \in B_k} \mu(x) u^2(x) \\ &\geq \mu_0 \sum_{x \in B_k} u^2(x) \\ &\geq \mu_0 u^2(x). \end{aligned}$$

The above unequal relationship holds for $\forall x \in B_k$. Which will immediately lead to $|u(x)| \leq \sqrt{\frac{1}{\mu_0}} \|u\|_{W^{1,2}(B_k)}$.

When $p = \infty$, $\sup\{|u|, x \in B_k\} \leq \sqrt{\frac{1}{\mu_0}} \|u\|_{W^{1,2}(B_k)}$,

Thus, we obtain that $\|u\|_{L^\infty(B_k)} \leq \sqrt{\frac{1}{\mu_0}} \|u\|_{W^{1,2}(B_k)}$. Next, we will investigate L^p norm of u .

$$\begin{aligned} \|u(x)\|_{L^p(B_k)}^p &= \sum_{x \in B_k} \mu(x) |u(x)|^p \\ &\leq \sum_{x \in B_k} \mu(x) \frac{1}{\sqrt{\mu_0^p}} \|u\|_{W^{1,2}(B_k)}^p \\ &= \frac{1}{\sqrt{\mu_0^p}} \|u\|_{W^{1,2}(B_k)}^p \sum_{x \in B_k} \mu(x) \quad (31) \\ &= \frac{1}{\sqrt{\mu_0^p}} \|u\|_{W^{1,2}(B_k)}^p \text{Vol}(B_k). \end{aligned}$$

According to the derivation above, we get $\|u(x)\|_{L^p(B_k)} \leq \text{Vol}(B_k)^{\frac{1}{p}} \frac{1}{\sqrt{\mu_0}} \|u\|_{W^{1,2}(B_k)}$. And then, we have completed the proof of Theorem 2.

Finally, we will prove the existence conditions of the solution and provide a proof of Theorem 3.

Proof We fix $O \in V$, taking the distance function $\rho(x)$. We take the opening ball $B_k = \{x \in V : \rho(x) < k\}$ with O as the center and radius k . Discussing equations at the opening ball.

$$-\Delta u + hu - fue^{u^2} - g = 0. \quad (32)$$

Its variational energy functional is

$$\begin{aligned} J_k(u) &= \frac{1}{2} \int_{B_k} (|\nabla u|^2 + hu^2) d\mu \\ &\quad - \frac{1}{2} \int_{B_k} fe^{u^2} d\mu - \int_{B_k} gud\mu. \end{aligned} \quad (33)$$

Now let's find a lower bound for it. In view of $e^{u^2} \geq u^2 + 1$ and $-h_0 < -M < f < 0$, we have $fe^{u^2} \leq fu^2 + f$,

$$|fe^{u^2}| \leq |fu^2 + f| \leq |fu^2| + |f| < Mu^2 + |f|. \quad (34)$$

Combining the above equation (34), we naturally obtain that

$$\begin{aligned} \frac{1}{2} \int_{B_k} fe^{u^2} d\mu &\leq \frac{1}{2} \int_{B_k} |fe^{u^2}| d\mu \\ &< \frac{1}{2} \int_{B_k} Mu^2 + |f| d\mu \quad (35) \\ &\leq \frac{M}{2} \int_{B_k} u^2 d\mu + \frac{1}{2} \int_V |f| d\mu, \end{aligned}$$

wherein, $f \in L^1(V)$. Due to $h(x) \geq h_0 > 0$, one has $\frac{h(x)}{h_0} \geq 1$ and $\frac{h(x)}{h_0} u^2(x) \geq u^2(x)$. In addition $\frac{|\nabla u|^2}{h_0} > 0$, so we have

$$\frac{h}{h_0} u^2 + \frac{|\nabla u|^2}{h_0} \geq u^2, \quad (36)$$

$$\int_{B_k} u^2 d\mu \leq \frac{1}{h_0} \int_{B_k} hu^2 + |\nabla u|^2 d\mu.$$

It following from aforementioned (35) (36), one immediately has

$$\begin{aligned} \int_{B_k} fe^{u^2} d\mu &< \frac{M}{2h_0} \int_{B_k} (hu^2 + |\nabla u|^2) d\mu \\ &\quad + \frac{1}{2} \int_V |f| d\mu. \end{aligned} \quad (37)$$

Next, we will handle the term $\int_{B_k} gud\mu$.

$$\begin{aligned}
\int_{B_k} g u \, d\mu &\leq \int_{B_k} |g u| \, d\mu \\
&\leq \|g\|_{L^2(B_k)} \|u\|_{L^2(B_k)} \\
&\leq \|g\|_{L^2(V)} \left(\int_{B_k} u^2 \, d\mu \right)^{1/2}.
\end{aligned} \tag{38}$$

Because $h \geq h_0 > 0$, one has $\frac{h}{h_0} \geq 1$, $\frac{h}{h_0} u^2 \geq u^2$. Besides, $\frac{|\nabla u|^2}{h_0} > 0$, which implies $\int_{B_k} u^2 \, d\mu \leq \frac{1}{h_0} \int_{B_k} |\nabla u|^2 + h u^2 \, d\mu$, and $\|u\|_{L^2(B_k)} \leq \frac{1}{\sqrt{h_0}} \|u\|_{W_0^{1,2}(B_k)}$. And then, we have $\int_{B_k} g u \, d\mu \leq \|g\|_{L^2(V)} \cdot \frac{1}{\sqrt{h_0}} \|u\|_{W_0^{1,2}(B_k)}$.

Using the Young's inequality, it can be obtained that $\int_{B_k} g u \, d\mu \leq \frac{\varepsilon}{h_0} \|g\|_{L^2(V)}^2 + \frac{1}{4\varepsilon} \|u\|_{W_0^{1,2}(B_k)}^2$, taking $\varepsilon = \frac{h_0}{h_0 - M}$, then we get $\frac{1}{2} - \frac{M}{2h_0} - \frac{1}{4\varepsilon} > 0$. So far, we have obtained that

$$\begin{aligned}
J_k(u) &= \frac{1}{2} \int_{B_k} (|\nabla u|^2 + h u^2) \, d\mu \\
&\quad - \frac{1}{2} \int_{B_k} f e^{u^2} \, d\mu - \int_{B_k} g u \, d\mu \\
&> \frac{1}{2} \int_{B_k} |\nabla u|^2 + h u^2 \, d\mu \\
&\quad - \frac{M}{2h_0} \int_{B_k} |\nabla u|^2 + h u^2 \, d\mu \\
&\quad - \frac{1}{2} \int_V |f| \, d\mu \\
&\quad - \frac{1}{h_0 - M} \|g\|_{L^2(V)}^2 - \frac{h_0 - M}{4h_0} \|u\|_{W_0^{1,2}(B_k)}^2,
\end{aligned} \tag{39}$$

where $\frac{1}{2} - \frac{M}{2h_0} - \frac{1}{4\varepsilon} > 0$, so we have $J_k(u) \geq -\frac{1}{2} \|f\|_{L^1(V)} - \frac{1}{h_0 - M} \|g\|_{L^2(V)}^2$, which holds true for $\forall u \in W_0^{1,2}(B_k)$.

On opening balls with different radii, variational functionals have the same lower bound, and if there is a lower bound, there is an infimum. We mark $\Lambda_k = \inf_{u \in W_0^{1,2}(B_k)} J_k(u)$. Because

$$\begin{aligned}
J_k(0) &= \frac{1}{2} \int_{B_k} |\nabla 0|^2 + 0^2 \, d\mu \\
&\quad - \int_{B_k} f e^0 \, d\mu - \int_{B_k} g \cdot 0 \, d\mu \\
&= - \int_{B_k} f \, d\mu \\
&= \int_{B_k} |f| \, d\mu \\
&\leq \int_V |f| \, d\mu = \|f\|_{L^1(V)},
\end{aligned} \tag{40}$$

and $0 \in W_0^{1,2}(B_k)$, we can see from the definition of the infimum that $\Lambda_k \leq J_k(0) \leq \|f\|_{L^1(V)}$. Thus, one has

$$-\frac{1}{h_0 - M} \|g\|_{L^2(V)}^2 - \frac{1}{2} \|f\|_{L^1(V)} \leq \Lambda_k \leq \|f\|_{L^1(V)}. \tag{41}$$

Below we will explain that the infimum can be reached. From the above, it can be seen that (41) holds for $\forall k \in \mathbb{Z}^+$. So $\{\Lambda_k\}$ is a bounded sequence. Because of the nature of the infimum, on the opening ball with a fixed radius $k \in \mathbb{Z}^+$, for $n = 1$, $\Lambda_k + 1$ is not lower bound, $\exists u_1^{(k)}$, s.t. $J_k(u_1^{(k)}) < \Lambda_k + 1$; $n = 2$, $\Lambda_k + \frac{1}{2}$ is not lower bound, similarly $\exists u_2^{(k)}$, s.t. $J_k(u_2^{(k)}) < \Lambda_k + \frac{1}{2}$; ... , and so on, we get $u_n^{(k)}$, s.t. $J_k(u_n^{(k)}) < \Lambda_k + \frac{1}{n}$. Thus, we have $\Lambda_k \leq J_k(u_n^{(k)}) < \Lambda_k + \frac{1}{n}$. Let $n \rightarrow \infty$, so we get $\lim_{n \rightarrow \infty} J_k(u_n^{(k)}) = \Lambda_k$.

Given $\varepsilon_0 > 0$, $\exists N$, when $n > N$, we have $|J_k(u_n^{(k)}) - \Lambda_k| < \varepsilon_0$, i.e. $J_k(u_n^{(k)}) < \varepsilon_0 + \Lambda_k$. Because $\Lambda_k \leq \|f\|_{L^1(V)}$, we have $J_k(u_n^{(k)}) \leq \|f\|_{L^1(V)} + \varepsilon_0$. In addition,

$$\begin{aligned}
&\left(\frac{1}{2} - \frac{M}{2h_0} - \frac{h_0 - M}{4h_0} \right) \|u_n^{(k)}\|_{W_0^{1,2}(B_k)}^2 \\
&\quad - \frac{1}{2} \|f\|_{L^1(V)} - \frac{1}{h_0 - M} \|g\|_{L^2(V)}^2 \\
&\leq \|f\|_{L^1(V)} + \varepsilon_0.
\end{aligned} \tag{42}$$

so we get

$$\begin{aligned}
&\|u_n^{(k)}\|_{W_0^{1,2}(B_k)}^2 \\
&\leq \left(\frac{3}{2} \|f\|_{L^1(V)} + \varepsilon_0 + \frac{1}{h_0 - M} \|g\|_{L^2(V)}^2 \right) \\
&\quad \times \frac{1}{\left(\frac{1}{2} - \frac{M}{2h_0} - \frac{h_0 - M}{4h_0} \right)}.
\end{aligned} \tag{43}$$

which holds true for $n > N$. When $n \leq N$, there is a maximum value for finite terms, we mark

$$\max\{\|u_n^{(k)}\|_{W_0^{1,2}(B_k)} : n = 1, 2, \dots, N\} \triangleq M^*. \tag{44}$$

Let

$$\begin{aligned}
M^{**} &= \\
&\max \left\{ M^*, \left[\left(2 \|f\|_{L^1(V)} + \varepsilon_0 + \frac{1}{h_0 - M} \|g\|_{L^2(V)}^2 \right) \right. \right. \\
&\quad \left. \left. \times \frac{1}{\left(\frac{1}{2} - \frac{M}{h_0} - \frac{h_0 - M}{4h_0} \right)} \right]^{1/2} \right\}.
\end{aligned} \tag{45}$$

thus, for $\forall n \in \mathbb{N}^*$, we have $0 \leq \|u_n^{(k)}\|_{W_0^{1,2}(B_k)} \leq M^{**}$ and that $\{u_n^{(k)}\}$ is a bounded point sequence in $W_0^{1,2}(B_k)$ as functions defined on B_k . In consideration of $W_0^{1,2}(B_k)$ is self compacting set, there exists a $u_k \in W_0^{1,2}(B_k)$ s.t $u_n^{(k)} \rightarrow u_k$ under the $\|\cdot\|_{W_0^{1,2}(B_k)}$, where $\{u_n^{(k)}\}$ is a subsequence of the origin sequence.

Next, we will explain that convergence according to the norm must converge point by point. $\forall \varepsilon > 0, \exists N$, when $n > N$, we have $\|u_n^{(k)} - u_k\|_{W_0^{1,2}(B_k)} < \varepsilon$. Unfold it, we'll get that

$$\int_{B_k} \left(|\nabla(u_n^{(k)} - u_k)|^2 + h(u_n^{(k)} - u_k)^2 \right) d\mu < \varepsilon. \quad (46)$$

The first item is non negative, so we have $\int_{B_k} h(u_n^{(k)} - u_k)^2 d\mu < \varepsilon$. In view of $h(x) \geq h_0$, it implies

$$h_0 \int_{B_k} (u_n^{(k)} - u_k)^2 d\mu \leq \int_{B_k} h(u_n^{(k)} - u_k)^2 d\mu < \varepsilon. \quad (47)$$

Expand the above equation (47), one has

$$\begin{aligned} & h_0 \min_{x \in B_k} \mu(x) (u_n^{(k)}(x) - u_k(x))^2 \\ & \leq h_0 \min_{x \in B_k} \mu(x) \sum_{x \in B_k} (u_n^{(k)}(x) - u_k(x))^2 \\ & \leq h_0 \sum_{x \in B_k} \mu(x) (u_n^{(k)}(x) - u_k(x))^2 < \varepsilon. \end{aligned} \quad (48)$$

where the rightmost item is $h_0 \int_{B_k} (u_n^{(k)} - u_k)^2 d\mu$, and the above equation is correct for $\forall x \in B_k$. Thus, we get $|u_n^{(k)}(x) - u_k(x)| < \varepsilon \cdot \frac{1}{h_0 \min_{x \in B_k} \mu(x)}$ and $u_n^{(k)}$ converges

uniformly to u_k . And then, we obtain point by point convergence, i.e. $\lim_{n \rightarrow \infty} u_n^{(k)}(x) = u_k(x)$.

At this point, we have

$$\begin{aligned} \lim_{n \rightarrow \infty} J_k(u_n^{(k)}) &= J_k\left(\lim_{n \rightarrow \infty} u_n^{(k)}\right) \\ &= J_k(u_k) = \Lambda_k, \quad u_k \in W_0^{1,2}(B_k). \end{aligned} \quad (49)$$

Which indicates that the infimum can be reached.

The critical point function u_k satisfies Euler-Lagrange equation: $\frac{d}{dt} J_k(u_k + t\phi)|_{t=0} = 0$, so we have

$$\begin{cases} -\Delta u_k + h u_k = f u_k e^{u_k^2} + g & \text{in } B_k, \\ u_k = 0 & \text{on } \partial B_k. \end{cases} \quad (50)$$

So far, we have obtained the solution of the equation locally.

Next, we will perform extension processing. Due to (39) holds true for $\forall u \in W_0^{1,2}(B_k)$, we get

$$\begin{aligned} \|f\|_{L^1(V)} &\geq \Lambda_k = J_k(u_k) \\ &\geq \left(\frac{1}{2} - \frac{M}{2h_0} - \frac{h_0 - M}{4h_0} \right) \|u_k\|_{W_0^{1,2}(B_k)}^2 \\ &\quad - \frac{1}{2} \|f\|_{L^1(V)} - \frac{1}{h_0 - M} \|g\|_{L^2(V)}^2. \end{aligned} \quad (51)$$

and then

$$\begin{aligned} & \|u_k\|_{W_0^{1,2}(B_k)}^2 \\ & \leq \sqrt{\left(\frac{3}{2} \|f\|_{L^1(V)} + \frac{1}{h_0 - M} \|g\|_{L^2(V)}^2 \right) \left(\frac{h_0}{h_0 - M} \right)} \\ & \approx k. \end{aligned} \quad (52)$$

We say that critical point function columns have a common upper bound. Next, we will explain that the infinite norm of the critical point function column on a bounded set is still bounded.

$\forall K \subset V$ is a bounded set, so there exists a sufficiently large radius $k \in \mathbb{Z}^+$, s.t $B_k \supset K$. We consider the infinite norm of the critical point function u_k on B_k over K . In view of

$$\begin{aligned} \|u_k\|_{W_0^{1,2}(B_k)}^2 &= \int_{B_k} \left(|\nabla u_k|^2 + h u_k^2 \right) d\mu \\ &\geq \int_{B_k} h u_k^2 d\mu \\ &\geq \int_K h u_k^2 d\mu = \sum_{x \in K} h(x) \mu(x) u_k^2(x) \\ &\geq h_0 \min_{x \in K} \mu(x) \sum_{x \in K} u_k^2(x). \end{aligned} \quad (53)$$

we have $u_k^2(x) \leq \frac{1}{h_0 \min_{x \in K} \mu(x)} \|u_k\|_{W_0^{1,2}(B_k)}^2$, and

$$\begin{aligned} |u_k(x)| &\leq \sqrt{\frac{1}{h_0 \min_{x \in K} \mu(x)}} \|u_k\|_{W_0^{1,2}(B_k)} \\ &\leq \sqrt{\frac{1}{h_0 \min_{x \in K} \mu(x)}} \\ &\quad \times \sqrt{\left(\frac{3}{2} \|f\|_{L^1(V)} + \frac{1}{h_0 - M} \|g\|_{L^2(V)}^2 \right)} \\ &\quad \times \sqrt{\frac{h_0}{h_0 - M}}, \end{aligned} \quad (54)$$

which holds true for $\forall x \in K$. Thus, we have $\|u_k\|_{L^\infty(K)} \leq C$, in which $C \sim h_0, M, K, \|g\|_{L^2(V)}, \|f\|_{L^1(V)}$. $\{u_k\}$ is defined on $B_k \cup \partial B_k$, extending it to the entire graph:

$$u_k = \begin{cases} u_k(x) & x \in B_k, \\ 0 & x \notin B_k. \end{cases} \quad (55)$$

Especially, taking $x_1 \in V$ is a bounded set. $\exists k \in \mathbb{Z}^+$, s.t $x_1 \in B_k$, and then we can easily get

$$|u_k(x_1)| \leq \sqrt{\frac{1}{h_0 \mu(x_1)}} \times \sqrt{\left(\frac{3}{2} \|f\|_{L^1(V)} + \frac{1}{h_0 - M} \|g\|_{L^2(V)}^2\right)} \times \sqrt{\frac{h_0}{h_0 - M}}. \quad (56)$$

$\forall K > k$, we still have $x_1 \in B_K$, $|u_K(x_1)| \leq \sqrt{\frac{1}{h_0 \mu(x_1)}} \left(\frac{3}{2} \|f\|_{L^1(V)} + \frac{1}{h_0 - M} \|g\|_{L^2(V)}^2\right) \frac{h_0}{h_0 - M}$. The first $k - 1$ critical point functions have finite values at x_1 , so $\{u_k(x_1)\}$ is a bounded point sequence, it has convergent subsequences. We take the opening ball where the convergent subsequence is located and discuss $x_2 \in V$, similarly, take the convergent subsequence, and so on. We ultimately obtained $\exists u^* \in V$ s.t u_k converges locally uniformly to u^* , i.e. $\forall l \in \mathbb{Z}^+, \lim_{n \rightarrow \infty} u_k(x) = u^*(x)$, which holds true for $\forall x \in B_l$. Finally, we will declare that the limit of locally uniformly convergent sequences falls within \mathcal{H} . Obviously, the critical point function sequence after extension satisfies $\{u_k\} \subset \mathcal{H}$. Below we prove $u^* \in \mathcal{H}$, just need to explain that one of the functions in u^* and \mathcal{H} is equal.

$$\begin{aligned} \|u_k\|_{\mathcal{H}}^2 &= \int_V |\nabla u_k|^2 + h u_k^2 d\mu \\ &= \int_{B_k \cup \partial B_k} |\nabla u_k|^2 d\mu + \int_{B_k} h u_k^2 d\mu \\ &= \frac{1}{2} \sum_{x \in B_k \cup \partial B_k} \sum_{y \sim x} \omega_{xy} (u_k(y) - u_k(x))^2 \\ &\quad + \sum_{x \in B_k} h(x) \mu(x) u_k^2(x) \\ &= \frac{1}{2} \sum_{x \in B_k} \sum_{y \sim x} \omega_{xy} (u_k(y) - u_k(x))^2 \\ &\quad + \frac{1}{2} \sum_{x \in \partial B_k} \sum_{y \sim x} \omega_{xy} (u_k(y) - u_k(x))^2 \\ &\quad + \sum_{x \in B_k} h(x) \mu(x) u_k^2(x) \\ &\leq \sum_{x \in B_k} \sum_{y \sim x} \omega_{xy} (u_k(y) - u_k(x))^2 \\ &\quad + 2 \sum_{x \in B_k} h(x) \mu(x) u_k^2(x) \\ &= 2 \|u_k\|_{W_0^{1,2}(B_k)}^2 \leq 2C. \end{aligned} \quad (57)$$

Thus, we can see that $\{u_k\}$ is a bounded sequence in \mathcal{H} . Because \mathcal{H} is a Hilbert space, $\exists \tilde{u} \in \mathcal{H}$ s.t $\{u_k\}$ subsequence $u_k \xrightarrow{weak} \tilde{u}$. i.e. $\forall \Phi \in C_c(V)$, we have $\int_V u_k \Phi d\mu \rightarrow \int_V \tilde{u} \Phi d\mu$. Especially, we take

$$\Phi(x) = \begin{cases} 1 & x = x_1 \\ 0 & x \neq x_1 \end{cases}, \Phi(x) \in C_c(V), \quad (58)$$

then $\int_V u_k \Phi d\mu = \sum_{x \in V} \mu(x) u_k(x) \Phi(x) = \mu(x_1) u_k(x_1)$, $\int_V \tilde{u} \Phi d\mu = \sum_{x \in V} \mu(x) \tilde{u}(x) \Phi(x) = \mu(x_1) \tilde{u}(x_1)$, and $\mu(x_1) u_k(x_1) \rightarrow \mu(x_1) \tilde{u}(x_1)$, as $k \rightarrow \infty$. Due to the multiplication property of limits, we deduce that $u_k(x_1) \rightarrow \tilde{u}(x_1)$, as $k \rightarrow \infty$. And x_1 is arbitrary, so $u_k(x) \rightarrow \tilde{u}(x)$ holds true for $\forall x \in V$. We have known that $u_k(x) \rightarrow u^*(x)$, $\forall x \in V$, combining the uniqueness of the existence of limits, we get that $u^*(x) = \tilde{u}(x) \in \mathcal{H}$. Thus, u^* is a function in \mathcal{H} . We have already known that the critical point function satisfies the distribution equation:

$$\begin{aligned} &\int_{B_k} -\Delta u_k \Phi d\mu + \int_{B_k} h u_k \Phi d\mu \\ &= \int_{B_k} f u_k e^{u_k} \Phi d\mu \\ &\quad + \int_{B_k} g \Phi d\mu, \quad \forall \Phi \in C_c(B_k). \end{aligned} \quad (59)$$

For $\forall x_1 \in V, \exists k \in \mathbb{Z}^+$, s.t $x_1 \in B_k$. The critical point function u_k on B_k still satisfies the above equation. Taking

$$\Phi(x) = \begin{cases} 1 & x = x_1, \\ 0 & x \neq x_1. \end{cases} \quad (60)$$

and then we have

$$\begin{aligned} &\mu(x_1) (-\Delta u_k(x_1)) + \mu(x_1) h(x_1) u_k(x_1) \\ &= \mu(x_1) f(x_1) u_k(x_1) e^{u_k(x_1)} \\ &\quad + \mu(x_1) g(x_1). \end{aligned} \quad (61)$$

i.e.

$$\begin{aligned} &-\Delta u_k(x_1) + h(x_1) u_k(x_1) \\ &= f(x_1) u_k(x_1) e^{u_k(x_1)} + g(x_1). \end{aligned} \quad (62)$$

When $K > k$, we take the corresponding characteristic function, and there is still a value of u_k at x_1 that satisfies the above equation. Let $k \rightarrow \infty$, we get

$$\begin{aligned}
-\Delta u^*(x_1) + h(x_1) u^*(x_1) \\
= f(x_1) u^*(x_1) e^{u^*(x_1)} + g(x_1).
\end{aligned} \tag{63}$$

i.e. u^* satisfies the equation at x_1 . From the arbitrariness of x_1 , u^* is the solution of the equation (17), and $u^* \in \mathcal{H}$. Proof completed.

4 Proof of Theorem 5

Proof Before starting our discussion, let's do some preparation work first. Fixing one point $O \in V$ on the graph, $\forall x \in V$, there is a distance function $\rho(x) = \rho(x, O)$. Taking $B_k = \{x \in V : \rho(x, O) < k\}$ as the opening ball on the graph, and we might as well restrict our discussion to $k > 1$. Actually, only the situation where k is sufficiently large needs to be considered. $W_0^{1,2}(B_k)$ is a Sobolev space, which satisfies $u = 0$ on ∂B_k . We take the norm on it as $\|u\|_{W_0^{1,2}(B_k)} = (\int_{B_k} |\nabla u|^2 + hu^2 d\mu)^{\frac{1}{2}}$, where $h(x) \geq a_0 > 0$ and $\mu(x) \geq \mu_0 > 0$ hold true for $\forall x \in V$. We define variational functionals: $W_0^{1,2}(B_k) \rightarrow \mathbb{R}$ as follows

$$\begin{aligned}
J_k(u) &= \frac{1}{2} \int_{B_k} (|\nabla u|^2 + hu^2) d\mu \\
&\quad - \int_{B_k} f \ln |u + m| d\mu - \log \int_{B_k} ge^u d\mu
\end{aligned} \tag{64}$$

Since $\ln |u + m| < 1 + |u + m| \leq 1 + |u| + |m|$, there are $f \ln |u + m| < f + |fu| + |fm|$ naturally. And then, we have

$$\begin{aligned}
&\int_{B_k} f \ln |u + m| d\mu \\
&< \int_{B_k} |f| d\mu + \int_{B_k} |fu| d\mu \\
&\quad + |m| \int_{B_k} |f| d\mu \\
&= (1 + |m|) \int_{B_k} |f| d\mu + \int_{B_k} |fu| d\mu
\end{aligned} \tag{65}$$

Due to $f \geq 1$ and $q \in [1, 2]$, $\forall x \in V$ we can get $f(x)^q \geq f(x)$, which leads to

$$\begin{aligned}
\int_{B_k} |f| d\mu &\leq \int_{B_k} |f|^q d\mu \\
&\leq \int_V |f|^q d\mu = \|f\|_{L^q(V)}^q.
\end{aligned} \tag{66}$$

Now we discuss $\int_{B_k} |fu| d\mu$. It follows from Hölder inequality that $\|fu\|_{L^1(B_k)} \leq \|f\|_{L^q(B_k)} \cdot \|u\|_{L^p(B_k)}$, wherein $\frac{1}{p} + \frac{1}{q} = 1$, $p = 1 + \frac{1}{q-1}$, $q \in [1, 2]$. Using Theorem 4, we can see that $\|u\|_{L^p(B_k)} \leq C \|u\|_{W_0^{1,2}(B_k)}$, $C \sim q$, h_0, μ_0 . And thus, one has

$$\begin{aligned}
\|fu\|_{L^1(B_k)} &\leq C \|f\|_{L^q(B_k)} \|u\|_{W_0^{1,2}(B_k)} \\
&\leq C \|f\|_{L^q(V)} \|u\|_{W_0^{1,2}(B_k)}.
\end{aligned} \tag{67}$$

By using the Young's inequality to the above equation, it can be obtained that

$$\|fu\|_{L^1(B_k)} \leq \frac{1}{4\varepsilon} \|u\|_{W_0^{1,2}(B_k)}^2 + \varepsilon C^2 \|f\|_{L^q(V)}^2. \tag{68}$$

which holds true for $\forall \varepsilon > 0$. Taking $\varepsilon = 1$, then we have

$$\begin{aligned}
&-\int_{B_k} f \ln |u + m| d\mu \\
&\geq -(1 + |m|) \cdot \|f\|_{L^q(V)}^q \\
&\quad - \frac{1}{4} \|u\|_{W_0^{1,2}(B_k)}^2 - C^2 \|f\|_{L^q(V)}^2.
\end{aligned} \tag{69}$$

What's more,

$$\begin{aligned}
\|v\|_{W_0^{1,2}(B_k)}^2 &= \int_{B_k} |\nabla v|^2 + hv^2 d\mu \geq \int_{B_k} hv^2 d\mu \\
&= \sum_{x \in B_k} h(x) \mu(x) v(x)^2 \\
&\geq a_0 \mu_0 \sum_{x \in B_k} v(x)^2 \\
&\geq a_0 \mu_0 v(x)^2,
\end{aligned} \tag{70}$$

so we have $|v(x)| \leq \frac{1}{\sqrt{a_0 \mu_0}} \|v\|_{W_0^{1,2}(B_k)}$, and it holds for $\forall x \in B_k$. Furthermore, one has $(\frac{v(x)}{\|v\|_{W_0^{1,2}(B_k)}})^2 \leq \frac{1}{a_0 \mu_0}$, which established for $\forall v(x) \in W_0^{1,2}(B_k)$. Because $u = \frac{u}{\|u\|_{W_0^{1,2}(B_k)}} \cdot \|u\|_{W_0^{1,2}(B_k)}$, it follows from Young's inequality that

$$\begin{aligned}
u &= \frac{u}{\|u\|_{W_0^{1,2}(B_k)}} \cdot \|u\|_{W_0^{1,2}(B_k)} \\
&\leq \frac{u^2}{4\varepsilon \|u\|_{W_0^{1,2}(B_k)}^2} + \varepsilon \|u\|_{W_0^{1,2}(B_k)}^2 \\
&\leq \frac{1}{4\varepsilon \mu_0 a_0} + \varepsilon \|u\|_{W_0^{1,2}(B_k)}^2.
\end{aligned} \tag{71}$$

Thus, we have $e^u \leq e^{\frac{1}{4\varepsilon\mu_0 a_0} + \varepsilon\|u\|_{W_0^{1,2}(B_k)}^2}$. In view of $g \geq 0$ and $g \neq 0$, one has $ge^u \leq ge^{\frac{1}{4\varepsilon\mu_0 a_0} + \varepsilon\|u\|_{W_0^{1,2}(B_k)}^2}$. Together with $g \in L^1(V)$, we get

$$\begin{aligned} \int_{B_k} ge^u d\mu &\leq e^{\frac{1}{4\varepsilon\mu_0 a_0} + \varepsilon\|u\|_{W_0^{1,2}(B_k)}^2} \cdot \int_{B_k} g d\mu \\ &\leq e^{\frac{1}{4\varepsilon\mu_0 a_0} + \varepsilon\|u\|_{W_0^{1,2}(B_k)}^2} \cdot \int_V g d\mu \\ &= e^{\frac{1}{4\varepsilon\mu_0 a_0} + \varepsilon\|u\|_{W_0^{1,2}(B_k)}^2} \cdot \|g\|_{L^1(V)}. \end{aligned} \quad (72)$$

This will directly lead to

$$\begin{aligned} \log \int_{B_k} ge^u d\mu &\leq \log(e^{\frac{1}{4\varepsilon\mu_0 a_0} + \varepsilon\|u\|_{W_0^{1,2}(B_k)}^2} \cdot \|g\|_{L^1(V)}) \\ &= \frac{1}{4\varepsilon\mu_0 a_0} + \varepsilon\|u\|_{W_0^{1,2}(B_k)}^2 \\ &\quad + \log\|g\|_{L^1(V)} \end{aligned} \quad (73)$$

Combining with formula (64)(69)(73), we can obtain that

$$\begin{aligned} J_k(u) &\geq \left(\frac{1}{2} - \frac{1}{4} - \varepsilon\right)\|u\|_{W_0^{1,2}(B_k)}^2 \\ &\quad - (1 + |m|)\|f\|_{L^q(V)}^q - C^2\|f\|_{L^q(V)}^2 \\ &\quad - \log\|g\|_{L^1(V)} - \frac{1}{4\varepsilon\mu_0 a_0}. \end{aligned} \quad (74)$$

Taking $\varepsilon = \frac{1}{8}$, one has

$$\begin{aligned} J_k(u) &\geq \frac{1}{8}\|u\|_{W_0^{1,2}(B_k)}^2 - (1 + |m|)\|f\|_{L^q(V)}^q \\ &\quad - C^2\|f\|_{L^q(V)}^2 - \log\|g\|_{L^1(V)} - \frac{2}{\mu_0 a_0}. \end{aligned} \quad (75)$$

$$\begin{aligned} J_k(u) &\geq -(1 + |m|)\|f\|_{L^q(V)}^q \\ &\quad - C^2\|f\|_{L^q(V)}^2 - \log\|g\|_{L^1(V)} - \frac{2}{\mu_0 a_0}, \end{aligned} \quad (76)$$

which holds for $\forall u \in W_0^{1,2}(B_k)$. Hence, $J_k(u)$ has a lower bound in $W_0^{1,2}(B_k)$, and where there is a lower bound, there must be a infimum. Then, we mark $\Lambda_k = \inf_{u \in W_0^{1,2}(B_k)} J_k(u)$ and take the minimized subsequence $(\tilde{u}_j) \subset W_0^{1,2}(B_k)$ s.t $J_k(\tilde{u}_j) \rightarrow \Lambda_k$ as $j \rightarrow \infty$. For $n = 1$, $\Lambda_k + 1$ is not a lower bound, then $\exists \tilde{u}_1 \in W_0^{1,2}(B_k)$ s.t $J_k(\tilde{u}_1) < \Lambda_k + 1$; what's more, for $n = 2$, $\Lambda_k + \frac{1}{2}$ is

also not a lower bound, similarly, $\exists \tilde{u}_2 \in W_0^{1,2}(B_k)$ s.t $J_k(\tilde{u}_2) < \Lambda_k + \frac{1}{2}$; Repeat the above operation, we ultimately get $\Lambda_k \leq J_k(\tilde{u}_j) < \Lambda_k + \frac{1}{j}$. Let $j \rightarrow \infty$, one has $J_k(\tilde{u}_j) \rightarrow \Lambda_k$. In view of (22), we have

$$J_k(0) = - \int_{B_k} f \ln |m| d\mu - \log \int_{B_k} g d\mu \quad (77)$$

In consideration of $f \geq 1$ and $0 < |m| < 1$, so one has $\ln |m| < 0$ and $f^q \geq f$. Which directly leads to

$$\int_{B_k} f d\mu \leq \int_{B_k} f^q d\mu \leq \|f\|_{L^q(V)}^q \quad (78)$$

and

$$- \ln |m| \int_{B_k} f d\mu \leq - \ln |m| \cdot \|f\|_{L^q(V)}^q \quad (79)$$

For the second item in (77), due to $g(x) \geq 0$ and $g \neq 0$, $\exists x_0 \in B_k$ such that $g(x_0) > 0$.

$$\int_{B_k} g d\mu = \sum_{x \in B_k} g(x)\mu(x) \geq g(x_0)\mu(x_0) > 0, \quad (80)$$

and then, we have

$$- \log \int_{B_k} g d\mu < - \log(g(x_0)\mu(x_0)). \quad (81)$$

Inserting (79), (81) into (77), one has

$$J_k(0) \leq - \ln |m| \cdot \|f\|_{L^q(V)}^q - \log(g(x_0)\mu(x_0)), \quad (82)$$

and one thing needs to be pointed out, since we only discuss the case where the radius of the opening ball is sufficiently large, when the radius $l > k$, $x_0 \in B_k \subset B_l$ can still be taken as a non-zero point, and thus x_0 is considered independent of the radius k . Because

$$\begin{aligned} J_k(u) &\geq \frac{1}{8}\|u\|_{W_0^{1,2}(B_k)}^2 - C^2\|f\|_{L^q(V)}^2 \\ &\quad - (1 + |m|)\|f\|_{L^q(V)}^q - \log\|g\|_{L^1(V)} - \frac{2}{\mu_0 a_0}. \end{aligned} \quad (83)$$

holds for $\forall u \in W_0^{1,2}(B_k)$, especially, we have $J_k(\tilde{u}_j) \geq \frac{1}{8}\|\tilde{u}_j\|_{W_0^{1,2}(B_k)}^2 - C$, where

$$C = C^2 \|f\|_{L^q(V)}^2 + (1 + |m|) \|f\|_{L^q(V)}^q + \log(\|g\|_{L^1(V)}) + \frac{2}{\mu_0 a_0}. \quad (84)$$

Due to $J_k(\tilde{u}_j) \rightarrow \Lambda_k$ as $j \rightarrow \infty$ and the boundedness of convergent sequences, taking $\varepsilon = M > 0$, $\exists J$, when $j > J$, one has $|J_k(\tilde{u}_j) - \Lambda_k| < M$, i.e. $J_k(\tilde{u}_j) < \Lambda_k + M$. And combined with

$$\Lambda_k \leq J_k(0) \leq -\ln |m| \cdot \|f\|_{L^q(V)}^q - \log(g(x_0)\mu(x_0)), \quad (85)$$

it implies that

$$\begin{aligned} \frac{1}{8} \|\tilde{u}_j\|_{W_0^{1,2}(B_k)}^2 - C &\leq J_k(\tilde{u}_j) < \Lambda_k + M \\ &\leq -\ln |m| \cdot \|f\|_{L^q(V)}^q - \log(g(x_0)\mu(x_0)) + M. \end{aligned} \quad (86)$$

and

$$\begin{aligned} \|\tilde{u}_j\|_{W_0^{1,2}(B_k)}^2 &\leq 2\sqrt{2} \\ &\cdot (-\ln |m| \cdot \|f\|_{L^q(V)}^q - \log(g(x_0)\mu(x_0)) + M + C)^{\frac{1}{2}} \quad (87) \\ &\triangleq C. \end{aligned}$$

where $C \not\sim k$. The above indicates that all terms of the minimization sequence (\tilde{u}_j) before the J term are bounded according to the norm $\|\cdot\|_{W_0^{1,2}(B_k)}$. We take the $j > J$ terms and still mark the sequence as (\tilde{u}_j) , its corresponding functional value sequence $(j_k(\tilde{u}_j))$ is a subsequence of the original sequence, and $(j_k(\tilde{u}_j))$ converges to Λ_k similarly. For the new sequence (\tilde{u}_j) , noting that $\|\tilde{u}_j\|_{W_0^{1,2}(B_k)}$ are bounded and $W_0^{1,2}(B_k)$ is pre-compact,

so $\exists u_k \in W_0^{1,2}(B_k)$, such that $\tilde{u}_j \xrightarrow{\|\cdot\|_{W_0^{1,2}(B_k)}} u_k$, where (\tilde{u}_j) is a subsequence.

In the following statement, we will deduce that sequences that converge according to the norm must converge uniformly.

We have known that $\forall \varepsilon > 0$, $\exists J$, when $j > J$, one has $\|\tilde{u}_j - u_k\|_{W_0^{1,2}(B_k)} < \varepsilon$. Expand the above equation, we naturally obtain that

$$\begin{aligned} \mu_0 a_0 \sum_{x \in B_k} (\tilde{u}_j(x) - u_k(x))^2 &\leq \sum_{x \in B_k} h(x)\mu(x)(\tilde{u}_j(x) - u_k(x))^2 \\ &= \int_{B_k} h(\tilde{u}_j - u_k)^2 d\mu \\ &\leq \int_{B_k} |\nabla(\tilde{u}_j - u_k)|^2 + h(\tilde{u}_j - u_k)^2 d\mu < \varepsilon^2. \end{aligned} \quad (88)$$

which deduces that $\forall x \in B_k$, $\mu_0 a_0 (\tilde{u}_j(x) - u_k(x))^2 < \varepsilon^2$, i.e. $|\tilde{u}_j(x) - u_k(x)| < \frac{1}{\sqrt{\mu_0 a_0}} \varepsilon$. Combining the above statements, we can easily get $\tilde{u}_j \rightrightarrows u_k$ in B_k , hence, (\tilde{u}_j) uniformly converges to u_k . Specially, one has pointwise convergence $\lim_{j \rightarrow \infty} \tilde{u}_j = u_k$. Let $j \rightarrow \infty$, we get

$$\Lambda_k = \lim_{j \rightarrow \infty} J_k(\tilde{u}_j) = J_k(\lim_{j \rightarrow \infty} \tilde{u}_j) = J_k(u_k). \quad (89)$$

Thus, u_k is the reachable point of the infimum. What's more, u_k satisfies the Euler-Lagrange equation.

$$\begin{cases} -\Delta u_k + h u_k = \frac{1}{\gamma_k} g e^{u_k} - \frac{f}{u_k + m}, & \text{in } B_k, \\ u_k \in W_0^{1,2}(B_k), \quad \gamma_k = \int_{B_k} g e^u d\mu. \end{cases} \quad (90)$$

Up to now, we have obtained the local solution u_k of the equation (18).

Combining (83) and (85), we can easily obtain that

$$\|u_k\|_{W_0^{1,2}(B_k)} \leq C, \quad C \approx k. \quad (91)$$

For any bounded set $K \subset V$, there is always a sufficiently large $k \in \mathbb{Z}^+$, s.t. $K \subset B_k$. Using Th 4 and (91), we imply that

$$\|u_k\|_{L^\infty(K)} \leq \frac{1}{\sqrt{a_0 \mu_0}} \|u_k\|_{W_0^{1,2}(B_k)} \leq C \approx k. \quad (92)$$

Given that u_k is a function defined on $B_k \cup \partial B_k$, let's extend it to the entire V below. Let

$$u_k = \begin{cases} u_k(x) & x \in B_k, \\ 0 & x \notin B_k. \end{cases} \quad (93)$$

Next, we will take the convergent subsequence point by point. For a set composed of individual points $x_1 \in V$, $\exists k \in \mathbb{Z}^+$, as can be seen from the above, $|u_k(x_1)| \leq C$ and for any $l > k$, which holds $|u_l(x_1)| \leq C$. Due to the existence of convergent sub columns in bounded point columns, it deduce that $u_k(x_1)$ is a convergent sub column, converging to $u^*(x_1)$; For $x_2 \in V$, we consider the kick-off corresponding to $\{u_k(x_1)\}$. $\exists k \in \mathbb{Z}^+$ s.t. $x_2 \in B_k$ and $|u_k(x_2)| \leq C$, which holds for any $l > k$. By the same token, $\{u_k(x_2)\}$ is a convergent sub column, meanwhile, maintain the astringency of $\{u_k(x_1)\}$. Repeat the above operation, we get $u_k(x) \rightarrow u^*(x)$, $\forall x \in V$. Hence, u_k locally converges uniformly to u^* . Combining (91) and Th 4, we can deduce

$$\|u_k\|_{L^\infty(B_k)} \leq \frac{1}{\sqrt{\mu_0 a_0}} \|u_k\|_{W_0^{1,2}(B_k)} \leq C. \quad (94)$$

And then, $|u_k(x)| \leq C$ holds true for any $x \in B_k$. Considering $-C \leq u_k(x) \leq C$ and $g \geq 0$, thus we obtain $ge^{-c} \leq ge^{u_k} \leq ge^c$. Integrate its two sides on B_k , one has $e^{-c} \|g\|_{L^1(B_k)} \leq \gamma_k \leq e^c \|g\|_{L^1(B_k)}$, where $\gamma_k = \int_{B_k} ge^{u_k} d\mu$. It follows from

$$e^{-c} \leq \frac{\gamma_k}{\|g\|_{L^1(B_k)}} \leq e^c, \quad (95)$$

and $\{\frac{\gamma_k}{\|g\|_{L^1(B_k)}}\}$ is a bounded sequence, we can get a convergence subsequence, we still mark it as $\{\frac{\gamma_k}{\|g\|_{L^1(B_k)}}\}$. Because $\lim_{k \rightarrow \infty} \|g\|_{L^1(B_k)} = \|g\|_{L^1(V)}$, $\{\frac{\gamma_k}{\|g\|_{L^1(B_k)}}\}$ is convergent, according to the four operations of the limit, we can know that γ_k is convergent. We mark $\lim_{k \rightarrow \infty} \gamma_k = \gamma^*$. Take the limit for (95), one has

$$\lim_{k \rightarrow \infty} e^{-c} \leq \lim_{k \rightarrow \infty} \frac{\gamma_k}{\|g\|_{L^1(B_k)}} \leq \lim_{k \rightarrow \infty} e^c, \quad (96)$$

i.e.

$$e^c \leq \frac{\gamma^*}{\|g\|_{L^1(V)}} \leq e^c, \quad (97)$$

$$e^{-c} \|g\|_{L^1(V)} \leq \gamma^* \leq e^c \|g\|_{L^1(V)},$$

$\forall x_1 \in V, \exists k \in \mathbb{Z}^+$, s.t. after the extension of the critical function u_k on B_k , it still satisfies the equation at x_1 . i.e.

$$-\Lambda u_k(x_1) + h u_k(x_1) = \frac{ge^{u_k(x_1)}}{\int_{B_k} ge^{u_k} d\mu} + \frac{f}{u_k(x_1) + m}. \quad (98)$$

When the radius $l > k$, the corresponding critical point function still satisfies the above equation at x_1 with respect to the corresponding integral. Let $k \rightarrow \infty$, we have

$$-\Lambda u^*(x_1) + h u^*(x_1) = \frac{ge^{u^*(x_1)}}{\gamma^*} + \frac{f}{u^*(x_1) + m}. \quad (99)$$

Based on the arbitrariness of x_1 , one obtains

$$-\Lambda u^* + h u^* = \frac{ge^{u^*}}{\gamma^*} + \frac{f}{u^* + m} \quad \text{in } V. \quad (100)$$

So far, we have got a limit function u^* that is close to the solution to the equation. Now, we will declare that $\gamma^* = \int_V ge^{u^*} d\mu$. On the one hand, for $\forall l > 1$ fixed, there holds the following formula

$$\begin{aligned} \int_{B_l} ge^{u^*} d\mu &= \lim_{k \rightarrow \infty} \int_{B_l} ge^{u_k} d\mu \\ &\leq \lim_{k \rightarrow \infty} \int_{B_k} ge^{u_k} d\mu = \gamma^*. \end{aligned} \quad (101)$$

Let $l \rightarrow \infty$ to the above formula, one has

$$\int_V ge^{u^*} d\mu \leq \gamma^*. \quad (102)$$

On the other hand, due to $\|u_k\|_{L^\infty(B_k)} \leq C$ and $g \in L^1(V)$, for $\forall \eta > 0$, there exists sufficiently large $l_0 > 1$, s.t. when $l > l_0$, we have $\int_{B_k} ge^{u_k} d\mu \leq \eta + \int_{B_l} ge^{u_k} d\mu$. Actually, $\|u_k\|_{L^\infty(B_k)} \leq C$, we temporarily fix k , one has $|u_k(x)| \leq C$, which holds true for $\forall x \in B_k$. And then, $-C \leq u_k(x) \leq C$, combining with $g \geq 0$, we have $ge^{u_k} \leq ge^C$. Integrate the two ends of the equation on $B_k \setminus B_l$, we get

$$\int_{B_k \setminus B_l} ge^{u_k} d\mu \leq e^C \int_{B_k \setminus B_l} g d\mu \leq e^C \int_{V \setminus B_l} g d\mu. \quad (103)$$

Due to $\int_{V \setminus B_l} g d\mu \rightarrow 0$ when l is sufficiently large, $\int_{B_k \setminus B_l} ge^{u_k} d\mu \leq o_l(1)$. Add $\int_{B_l} ge^{u_k} d\mu$ to both ends simultaneously, one has

$$\int_{B_k} ge^{u_k} d\mu \leq o_l(1) + \int_{B_l} ge^{u_k} d\mu. \quad (104)$$

$\forall \eta > 0, \exists l_0 > 1$, when $l > l_0$, we have $o_l(1) < \eta$, which leads to

$$\int_{B_k} ge^{u_k} d\mu \leq \eta + \int_{B_l} ge^{u_k} d\mu. \quad (105)$$

As for the equation above, we let $k \rightarrow \infty, l \rightarrow \infty, \eta \rightarrow 0^+$, and obtain $\gamma^* \leq \int_V ge^{u^*} d\mu$. Combining with

$\int_V ge^{u^*} d\mu \leq \gamma^*$, and then, we get $\gamma^* = \int_V ge^{u^*} d\mu$. Thus, u^* is a function on the graph and satisfies the equation at every point.

$$\begin{cases} -\Delta u^* + hu^* = \frac{1}{\gamma^* ge^{u^*}} + \frac{f}{u^*+m}, & \text{in } V, \\ \gamma^* = \int_V ge^{u^*} d\mu. \end{cases} \quad (106)$$

Finally, let's declare $u^* \in \mathcal{H} \cap L^\infty(V)$ and first explain $u^* \in \mathcal{H}$. We investigate $\|u_k\|_{\mathcal{H}}^2$,

$$\begin{aligned} \|u_k\|_{\mathcal{H}}^2 &= \int_V (|\nabla u_k|^2 + hu_k^2) d\mu \\ &= \frac{1}{2} \sum_{x \in V} \sum_{y \sim x} \omega_{xy} (u_k(y) - u_k(x))^2 \\ &\quad + \sum_{x \in V} \mu(x) h(x) u_k^2(x) \\ &= \frac{1}{2} \sum_{x \in B_k, y \sim x} \omega_{xy} (u_k(y) - u_k(x))^2 \\ &\quad + \frac{1}{2} \sum_{x \in \partial B_k, y \sim x} \omega_{xy} (u_k(y) - u_k(x))^2 \\ &\quad + \sum_{x \in B_k} \mu(x) h(x) u_k^2(x) \quad (107) \\ &\leq \sum_{x \in B_k, y \sim x} \omega_{xy} (u_k(y) - u_k(x))^2 \\ &\quad + 2 \sum_{x \in B_k} \mu(x) h(x) u_k^2(x) \\ &= 2 \left(\sum_{x \in B_k} \mu(x) \cdot \frac{1}{2\mu(x)} \sum_{y \sim x} \omega_{xy} (u_k(y) - u_k(x))^2 \right. \\ &\quad \left. + \sum_{x \in B_k} \mu(x) h(x) u_k^2(x) \right) \\ &= 2\|u\|_{W_0^{1,2}(B_k)}^2 \\ &\leq C \approx k. \end{aligned}$$

so (u_k) is a bounded sequence in \mathcal{H} . Because \mathcal{H} is a Hilbert space, any bounded point sequence has weakly convergent subsequences, we still label the convergent subsequence as (u_k) , and $u_k \xrightarrow{weak} \tilde{u}$, $u \in \mathcal{H}$. i.e. for $\forall \Phi \in Cc(V)$, we have $\int_V u_k \Phi d\mu \rightarrow \int_V \tilde{u} \Phi d\mu$. Especially, $\forall x_1 \in V$, we take the characteristic function of x_1

$$\Phi(x) = \begin{cases} 1 & x = x_1, \\ 0 & x \neq x_1. \end{cases} \quad (108)$$

Then, $u_k(x_1)\mu(x_1) \rightarrow \tilde{u}(x_1)\mu(x_1)$ as $k \rightarrow \infty$. Next, based on the multiplication property of the limit, we have $u_k(x_1) \rightarrow \tilde{u}(x_1)$. Combining the arbitrariness of x_1 , one

has $u_k(x) \rightarrow \tilde{u}(x)$ in V . Also, because the subsequence of u_k maintains the convergence of the original sequence, we have $u_k(x) \rightarrow u^*(x)$ in V . Due to the uniqueness of the existence of limits, we know that $u^*(x) = \tilde{u}(x) \in \mathcal{H}$. In the following step, we declare that $u^* \in L^\infty(V)$. We only need to examine $\|u^*\|_{\mathcal{H}}^2$.

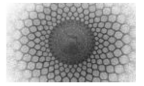
$$\begin{aligned} a_0\mu_0 u^*(x)^2 &\leq a_0\mu_0 \sum_{x \in V} u^*(x)^2 \\ &\leq \sum_{x \in V} h(x) \mu(x) u^*(x)^2 = \int_V h u^{*2} d\mu \quad (109) \\ &\leq \int_V (|\nabla u^*|^2 + h u^{*2}) d\mu. \end{aligned}$$

And then, $|u^*(x)| \leq \frac{1}{\sqrt{a_0\mu_0}} \cdot \|u^*\|_{\mathcal{H}}$, which holds true for $\forall x \in V$. Thus, $\|u^*\|_{L^\infty(V)} = \sup_{x \in V} |u^*(x)| \leq \frac{\|u^*\|_{\mathcal{H}}}{\sqrt{a_0\mu_0}} < +\infty$, which is a finite number. Moreover, $u^* \in \mathcal{H} \cap L^\infty(V)$ and u^* is the solution to the equation. As so far, the conclusion has been proven.

References

1. Zhiyun Gao, Shuni Song, Kun Zhang, Xiaojie Guo, *Optik*, **147**, (2017)
2. Mason A.Porter, P.G. Kevrekidis, Boris A.Malomed, D.J. Frantzeskakis, *Physica D: Nonli. Phen.* **229**, (2007)
3. Ching-Li Chai, Chang-Shou Lin, Chin-Lung Wang, *Cambridge J. Math.* **3**, (2015)
4. S. Akduman, A. Pankov, *Nonlinear Anal.* **184** (2019)
5. D. Bianchi, A. Setti, R. Wojciechowski, **5**, (2022)
6. do Ó J M, Medeiros E, Severo U, *J. Diff. Eq.* **246**, (2009)
7. H. Ge, W. jiang, Kazdan-Warner, *J. Korean Math. Soc.* **55**, (2018)
8. X. Han, M. Shao, *Acta Math. Sin. (Engl. Ser.)* **37**, (2021)
9. A. Huang, Y. Lin, S. Yau, *Commun. Math. Phys.* **377**, (2020)
10. S. Hou, J. Sun, *Calc. Var. Part. Diff. Eq.* **61**, (2022).
11. Y. Lin, Y. Xie, *Bull. Korean Math. Soc.* **59**, (2022)
12. S. Liu, Y. Yang, *Calc. Var. Partial Diff. Eq.* **59**,
13. Y. Liu, *J. Korean Math. Soc.* **59**, (2022)
14. Y. Wu, *Rev. R. Acad. Cienc. Exactas Fís. Nat. Ser. A Mat. RACSAM* **115** (2021)
15. X. Zhang, A. Lin, *Proc. Amer. Math. Soc.* **147** (2019)
16. X. Zhu, *J. Part. Diff. Eq.* **35** (2022)
17. A. Grigor'yan, Y. Lin, Y. Yang, *J. Diff. Eq.* **261** (2016)

18. A. Grigor'yan, Y. Lin, Y. Yang, *Calc. Var. Partial Differ. Equ.* **55** (2016)
19. A. Grigor'yan, Y. Lin, Y. Yang, *Sci. China Math.* **60** (2017)
20. N. Zhang, L. Zhao, *Sci. China Math.* **61** (2018)
21. F. Punzo, M. Svagna, *Partial Diff.l Eq.* **62** (2023)
22. Y. Yang, L. Zhao, *J. Math. Anal. Appl.* **536**, (2024)
23. L. Sun, L. Wang, *Adv. Math.* **404**, (2022),
24. Y. Liu, *Bull. Korean Math. Soc.* **59**, (2022)
25. H.-Y. Huang, J. Wang, W. Yang, *J. Funct. Anal.* **281**, (2021)
26. R. Adami, C. Cacciapuoti, D. Finco, D. Noja, *Rev. Math. Phys.* **23**, (2011)
27. M. Akramov, F. Khashimova, D. Matrasulov, *Phys. Lett. A* **457**, (2023)
28. T. Ricciardi, G. Zecca, *J. Diff. Eq.* **260**, (2016)
29. Y. Lin, Y. Yang, *Calc. Var. Partial Differ. Equ.* **60**, (2021).
30. L. Yang, *Acta Math. Sin.* **39**, (2023)
31. Z. Qiu, Y. Liu, *Arch. Math.* **120**, (2023)
32. Y. Lin, Y. Yang, *Rev. Mat. Complut.* **35**, (2022)



Elliptic coordinates: applications from geodesy

Borzoo Nazari^a, Zeinab Nazari Doliskani^b

¹College of Engineering, University of Tehran, North Kargar St., Tehran, Iran

²Ministry of Education, General Directorate of Education of Kermanshah, Iran

Received: 08 November 2025 / Accepted: 29 November 2025 / Published: 29 November 2025

Abstract In the matter of exact solutions of Einstein's field equations, coordinates play a very decisive role. Sometimes it is very difficult to understand the physical concept of a phenomenon or physical quantity in one coordinate system, while by changing the coordinate system, a simpler understanding of that quantity is obtained. In geodesy, which deals with the simulation and modeling of the gravitational field, it is common to use elliptical coordinates. In this article, we attempt to explain some computational fundamentals in elliptical coordinates and discuss its possible application to gravity.

1 Introduction

The purpose of developing elliptic coordinates in geodesy is to obtain a more accurate model of the Earth, which is not a perfect sphere. In contrast, relativists usually employ spherical coordinates, since the modeling of the Earth is not central to their concerns and spherical symmetry provides a good approximation for most astrophysical bodies under study. Nevertheless, it seems important to emphasize that elliptic coordinates can be useful for examining axisymmetric solutions in general relativity. By employing such coordinates, one may derive more elegant and potentially simpler solution methods for Einstein's field equations.

In this article, we review basic concepts of elliptic coordinates and discuss known solutions of the Laplace equation under the assumption of an ellipsoidal mass distribution acting as the gravitational source.

^ae-mail: borzoo.nazari@ut.ac.ir

^be-mail: nazari.z@gmail.com

2 Two-Dimensional Elliptic Coordinates

We begin by introducing two-dimensional elliptic coordinates, and in the following section the approach will be extended to three dimensions. Every point in the plane can be described using two coordinates. In polar coordinates (r, θ) , for example, specifying an angle determines a direction, and specifying a radius determines where the direction intersects a centered circle—thereby fixing the point. The same idea can be applied to elliptic coordinates: we specify a line (direction) by a known angle, and then instead of a circle, we use an ellipse to determine the position of the point by the intersection of the line and the ellipse. Therefore, we fix the first coordinate, i.e. θ , and find the second coordinate using the ellipse formula as follows:

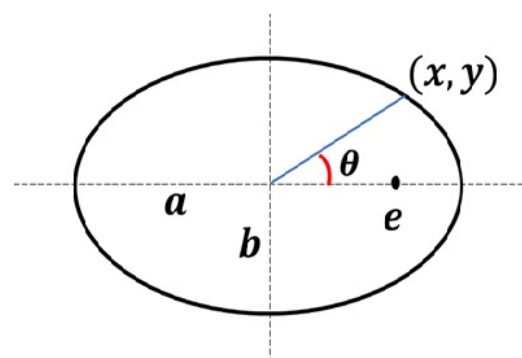


Fig. 1: ellipsoidal coordinates in two dimensions

$$y = x \tan(\theta), \quad (1)$$

$$\frac{x^2}{a^2} + \frac{y^2}{b^2} = 1, \quad (2)$$

we find out that

$$\begin{aligned} x &= a \left[1 + \frac{1}{1-e^2} \tan^2(\theta) \right]^{-1/2}, \\ y &= a \tan(\theta) \left[1 + \frac{1}{1-e^2} \tan^2(\theta) \right]^{-1/2}, \end{aligned} \quad (3)$$

where $e = \frac{c}{a}$ is the eccentricity of the ellipse and $c^2 = a^2 - b^2$. Therefore, the elliptic coordinates are determined by two parameters (a, θ) , assuming that the eccentricity is fixed and known in advance. Up to this point, the variable θ has played the role of the angle in polar coordinates. We now proceed to a different approach and introduce a new coordinate, which seems to have no direct relation to polar coordinates. Considering the equation of the ellipse, one can see that for a given angle λ , we may write:

$$\begin{aligned} x &= a \cos(\lambda), \\ y &= b \sin(\lambda), \end{aligned} \quad (4)$$

which, taking into account the eccentricity, is expressed as follows:

$$\begin{aligned} x &= a \cos(\lambda), \\ y &= a \sqrt{1-e^2} \sin(\lambda). \end{aligned} \quad (5)$$

To obtain a geometric and physical interpretation of the angle λ , one may compare relations (3) and (5) and determine its connection with the polar angle θ . Before doing so, we apply a convention commonly used in geodesy texts to relations (3) and (5). In geodesy literature, instead of treating the eccentricity as constant, the quantity c in the relation $c^2 = a^2 - b^2$ is usually taken to be constant and is denoted by E , and instead of b , the symbol u is used. Under this convention, relations (3) and (5) are rewritten in the following form:

$$\begin{aligned} x &= a \left[1 + \frac{u^2 + E^2}{u^2} \tan^2(\theta) \right]^{-1/2}, \\ y &= a \tan(\theta) \left[1 + \frac{u^2 + E^2}{u^2} \tan^2(\theta) \right]^{-1/2}, \end{aligned} \quad (6)$$

$$\begin{aligned} x &= \sqrt{u^2 + E^2} \cos(\lambda), \\ y &= u \sin(\lambda). \end{aligned} \quad (7)$$

It is easy to see that the change of variable

$$\tan(\lambda) = \frac{a}{u} \tan(\theta), \quad (8)$$

transforms relations (6) and (7) into each other. To better understand the meaning of the angles θ and λ , we consider the following figure:

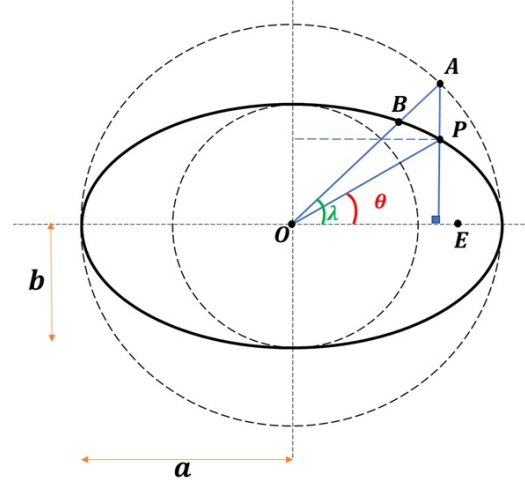


Fig. 2: relationship between the angles θ and λ

In Figure 2, the inscribed and circumscribed circles with radii a and b , respectively, are drawn as dashed curves. The point A is the vertical projection of the point P onto the circumscribed circle. Therefore, the angle λ is the polar angle corresponding to the point A . Based on these assumptions, the validity of relation (8) can be shown easily.

3 Laplacian Operator in the Two-Dimensional Coordinate System $(u, \lambda)_E$

The subscript E indicates that the parameter E is constant in this coordinate system. By applying the transformations (7) to the two-dimensional Laplacian operator

$$\nabla^2 = \partial_x^2 + \partial_y^2, \quad (9)$$

and after some algebraic manipulation, we obtain

$$\begin{aligned} (\partial_x^2 + \partial_y^2)V &= \\ \frac{1}{u^2 + E^2 \sin^2 \lambda} &\left[(u^2 + E^2) \frac{\partial^2 V}{\partial u^2} + \frac{\partial^2 V}{\partial \lambda^2} + u \frac{\partial V}{\partial u} \right]. \end{aligned} \quad (10)$$

To solve the two-dimensional Laplace equation in this elliptic coordinate system, we assume separation of variables:

$$V(u, \lambda) = \Lambda(\lambda)U(u). \quad (11)$$

Introducing the substitution

$$z = u + \sqrt{u^2 + E^2}, \quad (12)$$

the U -equation yields the solution

$$U(u) = A_0 \left(u + \sqrt{u^2 + E^2} \right)^n + B_0 \left(u + \sqrt{u^2 + E^2} \right)^{-n}, \quad (13)$$

where n is a natural number. The angular part becomes

$$\Lambda(\lambda) = A_1 \cos(n\lambda) + B_1 \sin(n\lambda). \quad (14)$$

Finally, note that if $E = 0$, then

$$u = r, \lambda = \theta, \quad (15)$$

and the usual solutions in polar coordinates are recovered.

4 Three-Dimensional Ellipsoidal Coordinate System

The procedure here follows the same approach as in the two-dimensional case. This time, instead of fixing one polar angle θ , we fix two angles θ and ϕ and consider the ellipsoid

$$\frac{x^2 + y^2}{a^2} + \frac{z^2}{c^2} = 1. \quad (16)$$

The first two semi-axes are taken equal to a , which not only simplifies the mathematics but also corresponds to axisymmetric physical bodies. The above surface is an ellipse in the z - y plane rotated about the z -axis.

A point on the ellipsoid in Cartesian coordinates (x, y, z) can be described using spherical coordinates (ρ, θ, ϕ) :

$$\begin{aligned} x &= \rho \sin \theta \cos \phi, & y &= \rho \sin \theta \sin \phi, \\ z &= \rho \cos \theta. \end{aligned} \quad (17)$$

Substituting these into (16) gives

$$\rho = c \sqrt{\frac{c^2 + E^2}{c^2 + E^2 \cos^2 \theta}}. \quad (18)$$

We also note that

$$a^2 = c^2 + E^2, \quad (19)$$

which is the standard relation between the semi-axes.

To introduce a new angular coordinate analogous to the two-dimensional case, we define

$$\cos \beta = \frac{c}{\sqrt{c^2 + E^2 \cos^2 \theta}} \sin \theta. \quad (20)$$

This gives the coordinate transformation known as the Jacobi ellipsoidal coordinates of the first type:

$$\begin{aligned} x &= \sqrt{c^2 + E^2} \cos \beta \cos \phi, \\ y &= \sqrt{c^2 + E^2} \cos \beta \sin \phi, \\ z &= c \sin \beta. \end{aligned} \quad (21)$$

Substituting $c \rightarrow u$ yields the final form of the 3-dimensional ellipsoidal coordinate system.

5 Laplace Equation in Ellipsoidal Coordinates

Using the coordinates (21) and after some algebraic manipulation, the Laplace operator becomes

$$\begin{aligned} \nabla^2 V &= \frac{1}{u^2 + E^2 \sin^2 \beta} \\ &\times \left[\frac{\partial}{\partial u} \left((u^2 + E^2) \frac{\partial V}{\partial u} \right) + \frac{1}{\cos \beta} \frac{\partial}{\partial \beta} \left(\cos \beta \frac{\partial V}{\partial \beta} \right) \right. \\ &\left. + \frac{u^2 + E^2 \sin^2 \beta}{(u^2 + E^2) \cos^2 \beta} \frac{\partial^2 V}{\partial \lambda^2} \right] = 0. \end{aligned} \quad (22)$$

To solve this equation for a static gravitational potential, we assume separation of variables:

$$V(u, \beta, \lambda) = \Lambda(\lambda) B(\beta) H(u). \quad (23)$$

This yields three ordinary differential equations:

$$\frac{d^2 \Lambda}{d\lambda^2} + c_0 \Lambda = 0, \quad (24)$$

$$\frac{d^2 B}{d\beta^2} - \tan \beta \frac{dB}{d\beta} + \left(-\frac{c_0}{\cos^2 \beta} + c_1 \right) B = 0, \quad (25)$$

$$(u^2 + E^2) \frac{d^2 H}{du^2} + 2u \frac{dH}{du} + \left(\frac{c_0 E^2}{u^2 + E^2} - c_1 \right) H = 0. \quad (26)$$

Applying boundary conditions on the potential (such as vanishing at infinity) and using relations (24)-(26), we obtain the potential outside the ellipsoid as

$$V(u, \beta, \lambda) = \sum_{n=0}^{\infty} \sum_{m=-n}^n a_{mn} Q_n^{|m|} \left(\frac{iu}{E} \right) \bar{Y}_{nm}(\lambda, \beta). \quad (27)$$

The coefficients a_{mn} are determined by the boundary conditions. $Q_n^{|m|}(iu/E)$ are the generalized Legendre functions, and $\bar{Y}_{nm}(\lambda, \beta)$ are the normalized spherical harmonics. To determine the coefficients a_{mn} , we may, for example, apply Dirichlet boundary conditions on the ellipsoidal boundary defined by $u = b$. By carrying out this procedure and using the addition theorems of spherical harmonics, we obtain the following relation:

$$a_{mn} = \frac{1}{S} \iint_E w(\beta') \bar{Y}_{nm}(\lambda', \beta') V(b, \lambda', \beta') dS. \quad (28)$$

The surface area of the ellipsoid is

$$S = 4\pi a^2 \left(\frac{1}{2} + \frac{b^2}{4aE} \ln \left(\frac{a+E}{a-E} \right) \right), \quad (29)$$

and the associated weight function is given by

$$w(\beta') = \frac{a}{\sqrt{b^2 + E^2 \sin^2 \beta'}} \left(\frac{1}{2} + \frac{b^2}{4aE} \ln \left(\frac{a+E}{a-E} \right) \right). \quad (30)$$

The generalized Legendre functions satisfy

$$\begin{aligned} Q_n^m \left(\frac{u}{E} \right) &= i^{n+1} Q_n^m \left(\frac{iu}{E} \right) \\ &= (-1)^m \frac{(n+m)!}{(2n+1)!!} \left(\frac{E}{u} \right)^{n+1} \\ &= {}_2F_1 \left(\frac{n-m+1}{2}, \frac{n+m+1}{2}, \frac{2n+3}{2}, \frac{E^2}{u^2} \right) \end{aligned} \quad (31)$$

where ${}_2F_1$ is the Gaussian hypergeometric function.

6 Review of Relativistic Results

Using the coordinate relations given in (21), the metric components of the gravitational field outside an ellipsoidal body can be rewritten in elliptic coordinates, and the unknown functions may then be determined by solving Einstein's field equations. As an example, we may take the g_{00} component of the metric of a complete ellipsoidal mass distribution in the form

$$g_{00} = 1 + \frac{1}{c^2} f(\lambda, u). \quad (32)$$

For the remaining metric components, a general form may be assumed based on the Schwarzschild metric and axial symmetry with respect to β , and the Einstein field equations can be solved accordingly. At this stage, the Newtonian limit in elliptic coordinates may be used to determine the function $f(\lambda, u)$. As mentioned earlier, this analysis is currently being developed by the authors.

7 Conclusion

In this work, we introduced the elliptic coordinate system and derived several well-known differential operators in this framework. Our motivation for employing elliptic coordinates lies in the considerable simplification they provide when solving Einstein's field equations. The authors have continued developing these solutions and have obtained a simplified derivation of the Kerr solution, which is now being prepared for publication. Since axisymmetric solutions play a central role in general relativity and astrophysics, it is natural to use axisymmetric coordinate systems such as the one defined by (21).

Acknowledgments

The first author expresses gratitude to the University of Tehran for supporting this work. Zeinab Nazari Doliskani thanks the Ministry of Education for supporting educational research. A substantial portion of this work was previously presented at the Mathematical Physics Conference held at Qom University of Technology. Borzoo Nazari sincerely thanks the organizers of that conference for their efforts and for selecting this work for publication in the present journal.

Appendix A: A Brief Overview of Generalized Legendre Functions

Equation (25) represents the angular part of the solution to Laplace's equation, and its solutions are well known and

treated in standard texts in mathematical physics. The generalized (or associated) Legendre functions arise as solutions to the associated Legendre differential equation

$$(1-x^2)\frac{d^2y}{dx^2} - 2x\frac{dy}{dx} + \left(\ell(\ell+1) - \frac{m^2}{1-x^2}\right)y = 0, \quad (\text{A.1})$$

where $\ell = 0, 1, 2, \dots$ is the degree and $m = 0, 1, 2, \dots, \ell$ is the order. This equation appears naturally when solving Laplace's equation in spherical coordinates and plays a central role in problems with axial symmetry [1, 6].

Appendix A.1: Legendre Polynomials and Their Generalizations

For $m = 0$, Eq. (A.1) reduces to the Legendre polynomials $P_\ell(x)$. For $m \neq 0$, the solutions generalize to the associated Legendre functions

$$P_\ell^m(x) = (1-x^2)^{m/2} \frac{d^m}{dx^m} P_\ell(x). \quad (\text{A.2})$$

These functions represent the angular dependence of fields in systems with axial (but not full spherical) symmetry.

Appendix A.2: Legendre Functions of the Second Kind

The second linearly independent solution of (A.1) is the Legendre function of the second kind, denoted $Q_\ell^m(x)$ [2]. In gravitational problems, Q_ℓ^m commonly appears in exterior (decaying) potentials, particularly when the coordinates introduce complex arguments, such as

$$Q_\ell^m\left(\frac{iu}{E}\right), \quad (\text{A.3})$$

which naturally arises in ellipsoidal coordinate geometries.

Appendix A.3: Connection to Spherical Harmonics

The generalized Legendre functions form the angular part of spherical harmonics:

$$Y_\ell^m(\theta, \phi) = N_{\ell m} P_\ell^m(\cos \theta) e^{im\phi}, \quad (\text{A.4})$$

where $N_{\ell m}$ is a normalization factor. Thus, spherical harmonics describe the angular dependence of three-dimensional solutions to Laplace's and Helmholtz's equations, while Q_ℓ^m governs the radial dependence in certain exterior potentials.

Appendix B: Normalized Spherical Harmonics

When solving Laplace's equation in spherical coordinates, the angular dependence of the solution is described by the *normalized spherical harmonics*, denoted by $Y_\ell^m(\theta, \phi)$. These functions form a complete orthonormal basis on the unit sphere and are indexed by the integers $\ell = 0, 1, 2, \dots$, $m = -\ell, \dots, \ell$.

The normalized spherical harmonics are defined in terms of the associated Legendre functions $P_\ell^m(x)$:

$$Y_\ell^m(\theta, \phi) = N_{\ell m} P_\ell^{|m|}(\cos \theta) e^{im\phi}, \quad (\text{B.5})$$

where the normalization constant is

$$N_{\ell m} = \sqrt{\frac{2\ell+1}{4\pi} \frac{(\ell-m)!}{(\ell+m)!}}. \quad (\text{B.6})$$

The normalization is chosen so that the spherical harmonics satisfy the orthonormality condition

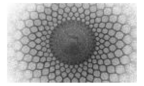
$$\int_0^{2\pi} \int_0^\pi Y_\ell^m(\theta, \phi) Y_{\ell'}^{m'*}(\theta, \phi) \sin \theta d\theta d\phi = \delta_{\ell\ell'} \delta_{mm'}. \quad (\text{B.7})$$

Spherical harmonics play a central role in quantum mechanics as the angular eigenfunctions of the orbital angular momentum operator, and in classical gravitational and electromagnetic potentials where axial or spherical symmetry is present [1, 6, 7].

References

1. J. D. Jackson, *Classical Electrodynamics, third edition*, John Wiley and Sons, (1999)
2. I. S. Gradshteyn, I. M. Ryzhik, D. Zwillinger, V. Moll, *Table of integrals, series and products, 8th edition*, Academic Press, Elsevier Inc. (2014)
3. Borzoo Nazari, 8th Iranian Conference on Mathematical Physics, (2022)
4. Borzoo Nazari, Khayyam 7th annual conference, (2024)

5. Clarence R. Wylie , Louis C. Barrett , *Advanced Engineering Mathematics, 6th edition*, McGraw-Hill College, (1995)
6. George B. Arfken, Hans J. Weber, Frank E. Harris, *Mathematical Methods for Physicists: A Comprehensive Guide, 7th edition*, Academic Press (2012)
7. A. Messiah, *Quantum Mechanics*, North-Holland, Amsterdam, (1961)



A splitting operator-based finite difference method for the solution of 2D Fokker-Planck equations

Neena A S^{1,a}, Dominic P Clemence-Mkhope^{2,b}, Ashish Awasthi^{1,c}

¹ Department of Mathematics, National Institute of Technology Calicut, Calicut-673601, Kerala, India.

² Department of Mathematics and Statistics, NC A & T State University, Greensboro, NC 27411, USA

Received: 05 November 2025 / Accepted: 29 November 2025 / Published: 29 November 2025

Abstract A simple and reliable numerical approach is constructed to solve the linear and nonlinear two-dimensional Fokker-Planck equations (FPEs). Initially, the Fokker-Planck equation is reformulated by decomposing it into one-dimensional components in the x and y directions. Then, local one-dimensional sub-equations are numerically solved by the explicit and implicit finite difference methods. The convergence of the proposed schemes is proved through truncation error and von Neumann stability analyses. The effectiveness and precision of the developed numerical methods are demonstrated using test problems, and the obtained outcomes are compared against the corresponding exact solutions for validation.

1 Introduction

The Fokker-Planck equation (FPE), originally formulated by Fokker (1914) and later by Planck (1917), serves as a mathematical model for describing Brownian particle motion. Over the years, FPEs have found widespread applications in diverse areas such as solid-state physics, quantum optics, chemical physics, theoretical biology, and circuit theory [1]. Various numerical strategies have been developed for their solution, including finite volume schemes [2, 3], Galerkin-type approaches [4–6], finite difference methods [7], and particle-based techniques [8]. To overcome the instabilities of the standard finite difference methods, nonstandard finite difference schemes are used to solve the one-dimensional FPEs in [9]. The most fundamental of these methods, the finite difference technique, has also been used to solve higher-dimensional FPE (2D) [10]. Some semi-analytical techniques have also been used to solve FPEs, of

which the Adomian decomposition method [11] is a well-known example.

From a theoretical physics perspective, the Fokker-Planck equation occupies a central role as the forward Kolmogorov representation of stochastic dynamics and as the macroscopic limit of Langevin and Liouville equations. It combines the conservation of probability and the relaxation toward equilibrium distributions controlled by underlying potential landscapes, and bridges the gap between tiny random processes and macroscopic transport events. In addition to being a numerical simplification, the operator splitting technique used in this study decomposes the Fokker-Planck operator into commuting drift and diffusion generators, each with unique mathematical and physical features. This decomposition parallels the Lie-Trotter and Strang formulations widely used in quantum and statistical mechanics to separate reversible and irreversible dynamics. Therefore, the current research advances our understanding of Fokker-Planck evolution from a mathematical-physics perspective.

Higher-dimensional FPEs naturally arise in systems involving multiple interacting variables, such as in population dynamics, neural networks, and chemical reactions involving multiple species. However, the increased complexity due to high dimensionality imposes significant computational challenges, often referred to as the "curse of dimensionality" [12]. To address this, researchers have developed more efficient algorithms, including operator splitting methods [13], sparse grid techniques [14], and dimensionality reduction strategies [15]. For instance, splitting methods have been employed to decouple the multidimensional FPE into simpler sub-problems, making the numerical integration more tractable. Moreover, tensor-based methods [16] and sparse spectral approaches [17] have also been proposed to reduce computational costs while maintaining accuracy in higher-dimensional settings. These advancements extend the appli-

^ae-mail: asneena@gmail.com

^be-mail: clemence@ncat.edu

^cCorresponding author e-mail: aawasthi@nitc.ac.in

cability of numerical FPE solvers to realistic, multi-variable systems in physics, biology, and engineering.

In recent years, many researchers have provided numerical solutions for one-dimensional FPEs through sophisticated methods, such as structure-preserving schemes [18–20], deep KD-tree algorithm [21], stable Petrov-Galerkin discretization [22], a method based on KRnet (ADDA-KR) [23], an extension of the generalized Hermite pseudospectral method [24], and a physically guided deep learning-based method [25]. In addition to solving one-dimensional FPEs, there are existing sophisticated numerical methods for solving higher-dimensional forms [26], such as one based on wavelet theory in [27] and Chang–Cooper two-level algorithms [28]. However, only a handful of high-order finite difference schemes are available in the literature [29–32].

This paper presents a finite difference numerical method for two-dimensional FPEs using the splitting technique, for which not many studies are found in the literature. The present study was motivated by the application of the splitting operator for Burger’s equation in [33]. The goal of the proposed method is to solve the higher-dimensional FPEs with simple and accurate algorithms. The splitting technique is a locally one-dimensional method for higher dimensional partial differential equations, which resolves the difficulties faced by numerical methods directly applied to higher-dimensional PDEs [34]. In this sense, this work is an extension of the simplest numerical methods in [35] to higher dimensional FPEs. The main benefits of the splitting operator method are that it is swift and straightforward to use, requiring fewer significant numerical computations to solve higher-dimensional PDEs.

The evolution of the concentration function $w(x, t)$, with respect to the spatial coordinate x and temporal variable t , is modeled by the general linear FPE, which is written in the form,

$$\frac{\partial w}{\partial t} = \left[-\frac{\partial}{\partial x} A(x) + \frac{\partial^2}{\partial x^2} B(x) \right] w(x, t), \quad (1)$$

with the initial state

$$w(x, 0) = f(x), \quad x \in \mathbb{R}, \quad (2)$$

where $B(x) > 0$ denotes the diffusion coefficient and $A(x)$ represents the drift coefficient. Its extension to two variables x_1, x_2 is given by

$$\frac{\partial w}{\partial t} = \left[-\sum_{i=1}^2 \frac{\partial}{\partial x_i} A_i(\mathbf{x}) + \sum_{i,j=1}^2 \frac{\partial^2}{\partial x_i \partial x_j} B_{i,j}(\mathbf{x}) \right] w, \quad (3)$$

with the initial state,

$$w(\mathbf{x}, 0) = g(\mathbf{x}), \quad \mathbf{x} = (x_1, x_2) \in \mathbb{R}^2. \quad (4)$$

The non-linear FPE in two variables x_1, x_2 is represented as,

$$\begin{aligned} \frac{\partial w}{\partial t} = & -\sum_{i=1}^2 \frac{\partial}{\partial x_i} (A_i(\mathbf{x}, t, w) w) \\ & + \sum_{i,j=1}^2 \frac{\partial^2}{\partial x_i \partial x_j} (B_{ij}(\mathbf{x}, t, w) w). \end{aligned} \quad (5)$$

The rest of the paper is organized as follows. Section 2 contains the model of the problem and the formulation of the numerical method. Section 3 discusses the convergence and stability of the proposed schemes. Section 4 provides numerical examples to show the efficiency of the schemes. Section 5 presents a brief discussion and conclusion.

2 Formulation of the computational techniques

2.1 Splitting operator technique

Consider, in expanded form, the linear FPE (3) in the domain $\Omega = [0, T] \times [a, b] \times [c, d]$,

$$\begin{aligned} \frac{\partial w}{\partial t} = & -A_1 \frac{\partial w}{\partial x} - w \frac{\partial A_1}{\partial x} - A_2 \frac{\partial w}{\partial y} - w \frac{\partial A_2}{\partial y} \\ & + B_{11} \frac{\partial^2 w}{\partial x^2} + 2 \frac{\partial B_{11}}{\partial x} \frac{\partial w}{\partial x} + w \frac{\partial^2 B_{11}}{\partial x^2} \\ & + B_{22} \frac{\partial^2 w}{\partial y^2} + 2 \frac{\partial B_{22}}{\partial y} \frac{\partial w}{\partial y} + w \frac{\partial^2 B_{22}}{\partial y^2}. \end{aligned} \quad (6)$$

with the initial state,

$$w(\mathbf{x}, 0) = g(\mathbf{x}), \quad \mathbf{x} = (x, y). \quad (7)$$

The development of the scheme is as follows: First Eqn.(6) is split into two equations as

$$\begin{aligned} \frac{1}{2} \frac{\partial w}{\partial t} = & -A_1 \frac{\partial w}{\partial x} - w \frac{\partial A_1}{\partial x} + B_{11} \frac{\partial^2 w}{\partial x^2} \\ & + 2 \frac{\partial B_{11}}{\partial x} \frac{\partial w}{\partial x} + w \frac{\partial^2 B_{11}}{\partial x^2}, \end{aligned} \quad (8a)$$

$$\begin{aligned} \frac{1}{2} \frac{\partial w}{\partial t} = & -A_2 \frac{\partial w}{\partial y} - w \frac{\partial A_2}{\partial y} + B_{22} \frac{\partial^2 w}{\partial y^2} \\ & + 2 \frac{\partial B_{22}}{\partial y} \frac{\partial w}{\partial y} + w \frac{\partial^2 B_{22}}{\partial y^2}. \end{aligned} \quad (8b)$$

As counterparts of Eqn. (6), the formulations in (8a) and (8b) correspond to the x - and y -directions, respectively. The resulting system is given in Eqns. (8) is then approximated numerically via the finite difference method, using both explicit and implicit discretizations, while avoiding any form of linearization. The process begins by computing the solution at the $(n + \frac{1}{2})^{\text{th}}$ level along the x -direction, employing the values from the n^{th} level while treating y as constant; these intermediate solutions correspond to points on the horizontal axis. Thereafter, the $(n + 1)^{\text{th}}$ level solution is obtained along the y -direction from the $(n + \frac{1}{2})^{\text{th}}$ level results, with x held constant; these solutions lie on the vertical axis. It follows that the computed approximation at the $(n + 1)^{\text{th}}$ step is consistent with the two-dimensional solution of Eqn. (6) evaluated at the same step.

2.2 The explicit method via splitting operator

Consider the spatial domain $\Omega = [a, b] \times [c, d] \subset \mathbb{R}^2$, which is discretized into a grid of $(N + 1) \times (M + 1)$ points. The discretization in the x - and y -directions is carried out with mesh sizes defined by $h = \frac{b-a}{N}$ and $k = \frac{d-c}{M}$, respectively. The temporal interval $[0, T]$ is uniformly divided into K subintervals with step size $\tau = \frac{T}{K}$. The discrete time instants are then denoted by $t^n = n\tau$, where $n = 0, 1, \dots, K - 1$. The numerical solution at the n^{th} time step corresponding to the mesh point (x_i, y_j, t^n) is represented by $\mathcal{W}_{ij}^n = \mathcal{W}(x_i, y_j, t^n)$. The time and space derivatives are explicitly discretized by the forward difference and the central difference, respectively. The discretized Eqns. (8) become

$$\begin{aligned} \frac{\mathcal{W}_{ij}^{n+\frac{1}{2}} - \mathcal{W}_{ij}^n}{\tau} &= -A_1 \frac{\mathcal{W}_{i+1,j}^n - \mathcal{W}_{i-1,j}^n}{2h} - \mathcal{W}_{ij}^n A_{1x} \\ &+ B_{11} \frac{\mathcal{W}_{i+1,j}^n - 2\mathcal{W}_{ij}^n + \mathcal{W}_{i-1,j}^n}{h^2} \\ &+ 2B_{11x} \frac{\mathcal{W}_{i+1,j}^n - \mathcal{W}_{i-1,j}^n}{2h} \\ &+ \mathcal{W}_{ij}^n B_{11xx}, \end{aligned} \quad (9a)$$

$$\begin{aligned} \frac{\mathcal{W}_{ij}^{n+1} - \mathcal{W}_{ij}^{n+\frac{1}{2}}}{\tau} &= -A_2 \frac{\mathcal{W}_{i,j+1}^{n+\frac{1}{2}} - \mathcal{W}_{i,j-1}^{n+\frac{1}{2}}}{2k} - \mathcal{W}_{ij}^{n+\frac{1}{2}} A_{2y} \\ &+ B_{22} \frac{\mathcal{W}_{i,j+1}^{n+\frac{1}{2}} - 2\mathcal{W}_{ij}^{n+\frac{1}{2}} + \mathcal{W}_{i,j-1}^{n+\frac{1}{2}}}{k^2} \\ &+ 2B_{22y} \frac{\mathcal{W}_{i,j+1}^{n+\frac{1}{2}} - \mathcal{W}_{i,j-1}^{n+\frac{1}{2}}}{2k} \\ &+ \mathcal{W}_{ij}^{n+\frac{1}{2}} B_{22yy}. \end{aligned} \quad (9b)$$

where $0 \leq i \leq N$, $0 \leq j \leq M$, and $0 \leq n \leq K - 1$. The initial and boundary conditions in discrete form are

$$\mathcal{W}_{ij}^0 = g(x_0, y_0); 0 \leq i \leq N, 0 \leq j \leq M,$$

$$\mathcal{W}_a^n = f_1(y, t), \mathcal{W}_b^n = f_2(y, t), \quad (10)$$

$$\mathcal{W}_c^n = f_3(x, t), \mathcal{W}_d^n = f_4(x, t).$$

Eqns. (9) can be written as

$$\mathcal{W}_{ij}^{n+\frac{1}{2}} = \frac{2}{\tau} (\theta_i \mathcal{W}_{i+1,j}^n + \sigma_i \mathcal{W}_{i,j}^n + \omega_i \mathcal{W}_{i,j}^n), \quad (11a)$$

$$\mathcal{W}_{i,j}^{n+1} = \frac{2}{\tau} (\lambda_j \mathcal{W}_{i,j+1}^{n+\frac{1}{2}} + \mu_j \mathcal{W}_{i,j}^{n+\frac{1}{2}} + \nu_j \mathcal{W}_{i,j-1}^{n+\frac{1}{2}}), \quad (11b)$$

where the coefficients are defined by $\theta_i = (-A_1 h + 2B_{11} + 2h \partial_{x_i} B_{11}) / (2h^2)$, $\sigma_i = 1 - \partial_{x_i} A_1 + \partial_{x_i}^2 B_{11} - 2B_{11} / h^2$, $\omega_i = (A_1 h + 2B_{11} - 2h \partial_{x_i} B_{11}) / (2h^2)$, and similarly $\lambda_j = (-A_2 k + 2B_{22} + 2k \partial_{y_j} B_{22}) / (2k^2)$, $\mu_j = 1 - \partial_{y_j} A_2 + \partial_{y_j}^2 B_{22} - 2B_{22} / k^2$, $\nu_j = (A_2 k + 2B_{22} - 2k \partial_{y_j} B_{22}) / (2k^2)$.

The numerical scheme (11) is an explicit central difference scheme for the splitting operator Eqns. (8).

For the nonlinear FPE, the nonlinear terms in Eqn. (6) are treated in the following ways:

$$- w^2 = \mathcal{W}_{i,j}^n \mathcal{W}_{i,j}^n \text{ in the } x\text{-direction, and}$$

$$w^2 = \mathcal{W}_{i,j}^{n+\frac{1}{2}} \mathcal{W}_{i,j}^{n+\frac{1}{2}} \text{ in the } y\text{-direction}$$

$$- w w_x = \mathcal{W}_{i,j}^n \left(\frac{\mathcal{W}_{i+1,j}^n - \mathcal{W}_{i-1,j}^n}{2h} \right), \text{ and}$$

$$w w_y = \mathcal{W}_{i,j}^{n+\frac{1}{2}} \left(\frac{\mathcal{W}_{i,j+1}^{n+\frac{1}{2}} - \mathcal{W}_{i,j-1}^{n+\frac{1}{2}}}{2k} \right)$$

$$- w w_{xx} = \mathcal{W}_{i,j}^n \left(\frac{\mathcal{W}_{i+1,j}^n - \mathcal{W}_{i,j}^n + \mathcal{W}_{i-1,j}^n}{h^2} \right), \text{ and}$$

$$w w_{yy} = \mathcal{W}_{i,j}^{n+\frac{1}{2}} \left(\frac{\mathcal{W}_{i,j+1}^{n+\frac{1}{2}} - \mathcal{W}_{i,j}^{n+\frac{1}{2}} + \mathcal{W}_{i,j-1}^{n+\frac{1}{2}}}{k^2} \right)$$

$$- w_x^2 = \left(\frac{\mathcal{W}_{i+1,j}^n - \mathcal{W}_{i-1,j}^n}{2h} \right)^2, \text{ and}$$

$$w_y^2 = \left(\frac{\mathcal{W}_{i,j+1}^{n+\frac{1}{2}} - \mathcal{W}_{i,j-1}^{n+\frac{1}{2}}}{2k} \right)^2$$

2.3 The implicit method via the splitting operator

In the case of the implicit scheme, the decomposed Eqns. (8) are approximated using a forward difference in time combined with central differences in the spatial variables. The resulting discretization takes the following form:

$$\begin{aligned}
\frac{\mathcal{W}_{ij}^{n+\frac{1}{2}} - \mathcal{W}_{ij}^n}{\tau} &= -A_1 \frac{\mathcal{W}_{i+1,j}^{n+\frac{1}{2}} - \mathcal{W}_{i-1,j}^{n+\frac{1}{2}}}{2h} \\
&\quad - \mathcal{W}_{ij}^{n+\frac{1}{2}} A_{1x} \\
&\quad + B_{11} \frac{\mathcal{W}_{i+1,j}^{n+\frac{1}{2}} - 2\mathcal{W}_{ij}^{n+\frac{1}{2}} + \mathcal{W}_{i-1,j}^{n+\frac{1}{2}}}{h^2} \\
&\quad + 2B_{11x} \frac{\mathcal{W}_{i+1,j}^{n+\frac{1}{2}} - \mathcal{W}_{i-1,j}^{n+\frac{1}{2}}}{2h} \\
&\quad + \mathcal{W}_{ij}^{n+\frac{1}{2}} B_{11xx}, \tag{12a}
\end{aligned}$$

$$\begin{aligned}
\frac{\mathcal{W}_{ij}^{n+1} - \mathcal{W}_{ij}^{n+\frac{1}{2}}}{\tau} &= -A_2 \frac{\mathcal{W}_{i,j+1}^{n+1} - \mathcal{W}_{i,j-1}^{n+1}}{2k} \\
&\quad - \mathcal{W}_{ij}^{n+1} A_{2y} \\
&\quad + B_{22} \frac{\mathcal{W}_{i,j+1}^{n+1} - 2\mathcal{W}_{ij}^{n+1} + \mathcal{W}_{i,j-1}^{n+1}}{k^2} \\
&\quad + 2B_{22y} \frac{\mathcal{W}_{i,j+1}^{n+1} - \mathcal{W}_{i,j-1}^{n+1}}{2k} \\
&\quad + \mathcal{W}_{ij}^{n+1} B_{22yy}. \tag{12b}
\end{aligned}$$

where $0 \leq i \leq N$, $0 \leq j \leq M$ and $0 \leq n \leq K-1$. The initial and boundary conditions in Eqns.(12) are

$$\begin{aligned}
\mathcal{W}_{i,j}^0 &= g(x_0, y_0); 0 \leq i \leq N, 0 \leq j \leq M, \\
\mathcal{W}_a^n &= f_1(y, t), \mathcal{W}_b^n = f_2(y, t), \\
\mathcal{W}_c^n &= f_3(x, t), \mathcal{W}_d^n = f_4(x, t). \tag{13}
\end{aligned}$$

The discrete forms (12) in the x and y directions, respectively, may be written as follows:

$$\frac{\tau}{2h^2} \left(\alpha_i \mathcal{W}_{i-1,j}^{n+\frac{1}{2}} + \beta_i \mathcal{W}_{i,j}^{n+\frac{1}{2}} + \gamma_i \mathcal{W}_{i+1,j}^{n+\frac{1}{2}} \right) = \mathcal{W}_{ij}^n, \tag{14a}$$

$$\frac{\tau}{2k^2} \left(\xi_j \mathcal{W}_{i,j-1}^{n+1} + \chi_j \mathcal{W}_{i,j}^{n+1} + \delta_j \mathcal{W}_{i,j+1}^{n+1} \right) = \mathcal{W}_{i,j}^{n+\frac{1}{2}}, \tag{14b}$$

where,

$$\begin{aligned}
\alpha_i &= h(-A_1 + 2B_{11x}) - 2B_{11}, \\
\beta_i &= 2h^2 \left(\frac{1}{\tau} + A_{1x} - B_{11xx} \right) + 4B_{11}, \\
\gamma_i &= h(A_1 - 2B_{11x}) - 2B_{11}, \tag{15}
\end{aligned}$$

and,

$$\begin{aligned}
\xi_j &= k(-A_2 + 2B_{22y}) - 2B_{22}, \\
\chi_j &= 2k^2 \left(\frac{1}{\tau} + A_{2y} - B_{22yy} \right) + 4B_{22}, \\
\delta_j &= k(A_2 - 2B_{22y}) - 2B_{22}. \tag{16}
\end{aligned}$$

For the nonlinear FPE (6) nonlinear terms are discretized in the following ways:

$$\begin{aligned}
-w^2 &= \mathcal{W}_{i,j}^n \mathcal{W}_{i,j}^{n+\frac{1}{2}} \text{ in the } x\text{- direction and} \\
w^2 &= \mathcal{W}_{i,j}^{n+\frac{1}{2}} \mathcal{W}_{i,j}^{n+1} \text{ in the } y\text{- direction} \\
-w \frac{\partial w}{\partial x} &= \mathcal{W}_{i,j}^n \left(\frac{\mathcal{W}_{i+1,j}^{n+\frac{1}{2}} - \mathcal{W}_{i-1,j}^{n+\frac{1}{2}}}{2h} \right), \text{ and} \\
w \frac{\partial w}{\partial y} &= \mathcal{W}_{i,j}^{n+\frac{1}{2}} \left(\frac{\mathcal{W}_{i,j+1}^{n+1} - \mathcal{W}_{i,j-1}^{n+1}}{2k} \right) \\
-w \frac{\partial^2 w}{\partial x^2} &= \mathcal{W}_{i,j}^n \left(\frac{\mathcal{W}_{i+1,j}^{n+\frac{1}{2}} - \mathcal{W}_{i,j}^{n+\frac{1}{2}} + \mathcal{W}_{i-1,j}^{n+\frac{1}{2}}}{h^2} \right), \text{ and} \\
w \frac{\partial^2 w}{\partial y^2} &= \mathcal{W}_{i,j}^{n+\frac{1}{2}} \left(\frac{\mathcal{W}_{i,j+1}^{n+1} - \mathcal{W}_{i,j}^{n+1} + \mathcal{W}_{i,j-1}^{n+1}}{k^2} \right) \\
- \left(\frac{\partial w}{\partial x} \right)^2 &= \left(\frac{\mathcal{W}_{i+1,j}^n - \mathcal{W}_{i-1,j}^n}{2h} \right) \left(\frac{\mathcal{W}_{i+1,j}^{n+\frac{1}{2}} - \mathcal{W}_{i-1,j}^{n+\frac{1}{2}}}{2h} \right), \text{ and} \\
\left(\frac{\partial w}{\partial y} \right)^2 &= \left(\frac{\mathcal{W}_{i,j+1}^{n+\frac{1}{2}} - \mathcal{W}_{i,j-1}^{n+\frac{1}{2}}}{2k} \right) \left(\frac{\mathcal{W}_{i,j+1}^{n+1} - \mathcal{W}_{i,j-1}^{n+1}}{2k} \right)
\end{aligned}$$

The formulation (14) is semi-implicit, achieved by linearizing the nonlinear source terms through a split evaluation at successive and previous time levels.

3 Consistency and stability

The assessment of the error and stability of the numerical schemes is given in this section. The consistency of the computational schemes is proved by the truncation error method, and their stability is derived from von Neumann stability analysis.

Theorem 1 *The numerical scheme given in (11) achieves first-order accuracy with respect to the temporal variable, while attaining second-order accuracy in the spatial directions x and y .*

Proof The fully discretized form of the explicit central difference scheme (11) is

$$\begin{aligned} \mathcal{W}_{ij}^{n+1} = & \frac{4}{\tau^2} (\lambda_j (\theta_i \mathcal{W}_{i+1,j+1}^n + \sigma_i \mathcal{W}_{i,j+1}^n + \omega_i \mathcal{W}_{i-1,j+1}^n) \\ & + \mu_j (\theta_i \mathcal{W}_{i+1,j}^n + \sigma_i \mathcal{W}_{i,j}^n + \omega_i \mathcal{W}_{i-1,j}^n) \\ & + \nu_j (\theta_i \mathcal{W}_{i+1,j-1}^n + \sigma_i \mathcal{W}_{i,j-1}^n + \omega_i \mathcal{W}_{i-1,j-1}^n)). \end{aligned} \quad (17)$$

Applying Taylor expansion on all terms of Eq. (17) and simplifying results in the local truncation error (LTE) given by

$$\begin{aligned} LTE = & \mathcal{W}_{ij}^{n+1} \\ & - \frac{4}{\tau^2} \left[\lambda_j (\theta_i W_{i+1,j+1}^n + \sigma_i W_{i,j+1}^n + \omega_i W_{i-1,j+1}^n) \right. \\ & + \mu_j (\theta_i W_{i+1,j}^n + \sigma_i W_{i,j}^n + \omega_i W_{i-1,j}^n) \\ & \left. + \nu_j (\theta_i W_{i+1,j-1}^n + \sigma_i W_{i,j-1}^n + \omega_i W_{i-1,j-1}^n) \right] \\ = & \tau^2 W + \tau^2 W_t + \frac{\tau^2}{2!} W_{tt} - 4\lambda \theta W - 4\lambda \theta h W_x \\ & - 4\lambda \theta k W_y - 2\lambda \theta h^2 W_{xx} - 2\lambda \theta k^2 W_{yy} \\ & - 8\lambda \theta h k W_{xy} - \lambda \sigma W - 4k\lambda \sigma W_y \\ & - 2\lambda \sigma k^2 W_{yy} - 4\lambda \omega W + 4h\lambda \omega W_x \\ & - 4k\lambda \omega W_y - 2\lambda \omega h^2 W_{xx} - 2\lambda \omega k^2 W_{yy} \\ & + 8hk\lambda \omega W_{xy} - 4\mu \omega W + 4h\mu \omega W_x \\ & - 2\mu \omega h^2 W_{xx} - 2\nu \theta k^2 W_{yy} - 4\nu \theta W \\ & + 2\nu \omega h^2 W_{xx} - 2\nu \theta k^2 W_{yy} + \dots \\ = & \tau^2 W + t\tau^2 W_t + \frac{t^2\tau^2}{2!} W_{tt} - 2\lambda \omega h^2 W_{xx} \\ & - 2\nu \omega k^2 W_{yy} + \dots \\ = & \mathcal{O}(\tau^2 + h^2 + k^2), \end{aligned} \quad (18)$$

where,

$$\begin{aligned} \theta = & (-A_1 h + 2B_{11} + 2h \frac{\partial B_{11}}{\partial x}) / (2h^2), \\ \sigma = & (h^2 (1 - \frac{\partial A_1}{\partial x} + \frac{\partial^2 B_{11}}{\partial x^2}) - 2B_{11}) / h^2, \\ \omega = & (A_1 h + 2B_{11} - 2h \frac{\partial B_{11}}{\partial x}) / (2h^2), \\ \lambda = & (-A_2 k + 2B_{22} + 2k \frac{\partial B_{22}}{\partial y}) / (2k^2), \\ \mu = & (k^2 (1 - \frac{\partial A_2}{\partial y} + \frac{\partial^2 B_{22}}{\partial y^2}) - 2B_{22}) / k^2, \\ \nu = & (A_2 k + 2B_{22} - 2k \frac{\partial B_{22}}{\partial y}) / (2k^2). \end{aligned} \quad (19)$$

The truncation error is

$$TE = \tau^{-1}(LTE) = \mathcal{O}(\tau) + \mathcal{O}(h^2 + k^2). \quad (20)$$

Accordingly, the numerical approximation incurs errors that are of order $\mathcal{O}(\tau)$ in time and $\mathcal{O}(h^2 + k^2)$ in space, consistent with the stated result.

Theorem 2 The explicit central difference scheme defined in (11) admits conditional stability, holding only under specific restrictions on the discretization parameters.

Proof The stability requirement for the proposed explicit scheme is established through von Neumann stability analysis and can be formulated as follows.

Let the Fourier transform corresponding to \mathcal{W}^n at the n^{th} time level be denoted by, $\hat{\mathcal{W}}^n$. The 2D Fourier transform is

$$\hat{\mathcal{W}}^{n+1}(\zeta, \eta) = \frac{1}{\sqrt{2\pi}\sqrt{2\pi}} \sum_{j,k=-\infty}^{\infty} e^{-ij\zeta h - ik\eta k} \mathcal{W}_{i,j}^{n+1}. \quad (21)$$

Performing a Fourier transformation of Eqn. (11) results in,

$$\begin{aligned} \hat{\mathcal{W}}^{n+\frac{1}{2}}(\zeta, \eta) = & \frac{2}{\tau} \left(\theta e^{ij\zeta h} \hat{\mathcal{W}}^n(\zeta, \eta) \right. \\ & + \sigma \hat{\mathcal{W}}^n(\zeta, \eta) \\ & \left. + \omega e^{-ij\zeta h} \hat{\mathcal{W}}^n(\zeta, \eta) \right), \\ \hat{\mathcal{W}}^{n+1}(\zeta, \eta) = & \frac{2}{\tau} \left(\lambda e^{ik\eta k} \hat{\mathcal{W}}^{n+\frac{1}{2}}(\zeta, \eta) \right. \\ & + \mu \hat{\mathcal{W}}^{n+\frac{1}{2}}(\zeta, \eta) \\ & \left. + \nu e^{-ik\eta k} \hat{\mathcal{W}}^{n+\frac{1}{2}}(\zeta, \eta) \right), \\ \hat{\mathcal{W}}^{n+1}(\zeta, \eta) = & \hat{\mathcal{W}}^n(\zeta, \eta) \frac{4}{\tau^2} \left(\theta e^{ij\zeta h} + \sigma \right. \\ & \left. + \omega e^{-ij\zeta h} \right) \left(\lambda e^{ik\eta k} \right. \\ & \left. + \mu + \nu e^{-ik\eta k} \right). \end{aligned} \quad (22)$$

Here the amplification factor $\rho(\zeta, \eta)$ is,

$$\begin{aligned} \rho(\zeta, \eta) = & \frac{4}{\tau^2} \left(\theta e^{ij\zeta h} + \sigma + \omega e^{-ij\zeta h} \right) \\ & \times \left(\lambda e^{ik\eta k} + \mu + \nu e^{-ik\eta k} \right). \end{aligned} \quad (23)$$

Rewriting the exponential terms in terms of trigonometric functions, Eqn. (23) can be expressed as

$$\begin{aligned} \rho(\zeta, \eta) = & \frac{4}{\tau^2} \left[(\sigma + (\theta + \omega) \cos(\zeta h)) \right. \\ & \times (\mu + (\lambda + \nu) \cos(\eta k)) \\ & \left. - (\theta - \omega)(\lambda - \nu) \sin(\zeta h) \sin(\eta k) \right] \\ & + i \left[(\mu + (\lambda + \nu) \cos(\eta k))(\theta - \omega) \sin(\zeta h) \right. \\ & + (\sigma + (\theta + \omega) \cos(\zeta h)) \\ & \left. \times (\lambda - \nu) \sin(\eta k) \right]. \end{aligned} \quad (24)$$

Therefore,

$$|\rho|^2 = \frac{4}{\tau^2} [(\theta - \omega)^2 \sin^2 \zeta h + (\sigma + (\theta + \omega) \cos \zeta h)^2] \times [(\lambda - \nu)^2 \sin^2 \eta k + (\mu + (\lambda + \nu)) \cos \eta k]^2 \quad (25)$$

By the von Neumann criteria, the proposed scheme is stable under the condition $|\rho|^2 \leq 1$ and hence conditionally stable.

Theorem 3 *The implicit central difference scheme (14) is second-order convergent in temporal and spatial variables.*

Proof The LTE at the node (x_i, y_j, t^{n+1}) is given by

$$\begin{aligned} LTE_{ij}^{n+1} &= \mathcal{W}_{i,j}^{n+1} \\ &\quad - \frac{\tau}{2k^2} (\xi_j \mathcal{W}_{i,j-1}^{n+1} + \chi_j \mathcal{W}_{i,j}^{n+1} + \delta_j \mathcal{W}_{i,j+1}^{n+1}) \\ &\quad - \frac{1}{\beta_i} \frac{2h^2}{\tau} \mathcal{W}_{i,j}^n \\ &\quad + \frac{\alpha_i}{\beta_i} \frac{\tau}{2k^2} (\xi_j \mathcal{W}_{i+1,j-1}^{n+1} + \chi_j \mathcal{W}_{i+1,j}^{n+1} + \delta_j \mathcal{W}_{i+1,j+1}^{n+1}) \\ &\quad + \frac{\gamma_i}{\beta_i} \frac{\tau}{2k^2} (\xi_j \mathcal{W}_{i-1,j-1}^{n+1} + \chi_j \mathcal{W}_{i-1,j}^{n+1} + \delta_j \mathcal{W}_{i-1,j+1}^{n+1}) \\ &= \left(1 - \chi_j \frac{\tau}{2k^2}\right) \mathcal{W}_{i,j}^{n+1} - \frac{1}{\beta_i} \frac{2h^2}{\tau} \mathcal{W}_{i,j}^n \\ &\quad + \frac{\tau}{2k^2} \left(-\xi_j \mathcal{W}_{i,j-1}^{n+1} - \delta_j \mathcal{W}_{i,j+1}^{n+1} \right. \\ &\quad \quad \left. + \frac{\alpha_i \xi_j}{\beta_i} \mathcal{W}_{i+1,j-1}^{n+1} + \frac{\alpha_i \chi_j}{\beta_i} \mathcal{W}_{i+1,j}^{n+1}\right) \\ &\quad + \frac{\tau}{2k^2} \left(\frac{\alpha_i \delta_j}{\beta_i} \mathcal{W}_{i+1,j+1}^{n+1} + \frac{\gamma_i \xi_j}{\beta_i} \mathcal{W}_{i-1,j-1}^{n+1} \right. \\ &\quad \quad \left. + \frac{\gamma_i \chi_j}{\beta_i} \mathcal{W}_{i-1,j}^{n+1} + \frac{\gamma_i \delta_j}{\beta_i} \mathcal{W}_{i-1,j+1}^{n+1}\right) \\ &= \left(1 - \chi \frac{\tau}{2k^2}\right) \mathcal{W}(x, y, t + \tau) \\ &\quad - \frac{1}{\beta} \frac{2h^2}{\tau} \mathcal{W}(x, y, t) \\ &\quad + \frac{\tau}{2k^2} \left(-\xi \mathcal{W}(x, y - k, t + \tau) \right. \\ &\quad \quad \left. - \delta \mathcal{W}(x, y + k, t + \tau) \right. \\ &\quad \quad \left. + \frac{\alpha \xi}{\beta} \mathcal{W}(x + h, y - k, t + \tau)\right) \\ &\quad + \frac{\tau}{2k^2} \left(\frac{\alpha \chi}{\beta} \mathcal{W}(x + h, y, t + \tau) \right. \\ &\quad \quad \left. + \frac{\alpha \delta}{\beta} \mathcal{W}(x + h, y + k, t + \tau) \right. \\ &\quad \quad \left. + \frac{\gamma \xi}{\beta} \mathcal{W}(x - h, y - k, t + \tau)\right) \\ &\quad + \frac{\tau}{2k^2} \left(\frac{\gamma \chi}{\beta} \mathcal{W}(x - h, y, t + \tau) \right. \\ &\quad \quad \left. + \frac{\gamma \delta}{\beta} \mathcal{W}(x - h, y + k, t + \tau)\right). \end{aligned} \quad (26)$$

Expanding each term by Taylor's series expansion and simplifying,

$$\begin{aligned} LTE &= \left(\xi + \chi + \frac{\alpha \xi}{\beta} + \frac{\gamma \chi}{\beta} + \dots\right) \tau^3 \mathcal{W} \\ &\quad + \left(\frac{\alpha \xi}{\beta} - \frac{\gamma \chi}{\beta} + \dots\right) \tau^3 \mathcal{W}_t \\ &\quad + \left(-\beta + \frac{\gamma \delta}{\beta} + \dots\right) \tau^3 \mathcal{W}_{tt} + \dots \\ &\quad + \tau \left(\frac{\alpha \xi}{2\beta} + \frac{\delta \chi}{4\beta} + \dots\right) \mathcal{W}_{xx} \\ &\quad + \tau \left(\frac{\alpha \delta}{4\beta} + \frac{\gamma \eta}{4\beta} + \dots\right) \mathcal{W}_{yy} + \dots, \end{aligned} \quad (27)$$

where

$$\begin{aligned} \alpha &= h \left(-A_1 + 2 \frac{\partial B_{11}}{\partial x}\right) - 2B_{11}, \\ \beta &= 2h^2 \left(\frac{1}{\tau} + \frac{\partial A_1}{\partial x} + \frac{\partial^2 B_{11}}{\partial x^2}\right) + 4B_{11}, \\ \gamma &= h \left(A_1 - 2 \frac{\partial B_{11}}{\partial x}\right) - 2B_{11}, \\ \xi &= k \left(-A_2 + 2 \frac{\partial B_{22}}{\partial y}\right) - 2B_{22}, \\ \chi &= 2k^2 \left(\frac{1}{\tau} + \frac{\partial A_2}{\partial y} + \frac{\partial^2 B_{22}}{\partial y^2}\right) + 4B_{22}, \\ \delta &= k \left(A_2 - 2 \frac{\partial B_{22}}{\partial y}\right) - 2B_{22}. \end{aligned} \quad (28)$$

The global truncation error is

$$TE = \frac{1}{\tau} LTE = O(\tau^2 + h^2 + k^2), \quad (29)$$

which is quadratic in temporal and spatial variables, and hence the claim.

Theorem 4 *The implicit central difference scheme described in (14) possesses unconditional stability, independent of the discretization parameters.*

Proof The combined form of the decomposed Eqns. (14) is,

$$\begin{aligned} \mathcal{W}_{i,j}^{n+1} &= \frac{4k^2 h^2}{\beta_i \chi_j \tau^2} \mathcal{W}_{i,j}^n - \frac{\gamma_i \delta_j}{\beta_i \chi_j} \mathcal{W}_{i+1,j+1}^{n+1} - \frac{\gamma_i \chi_j}{\beta_i \chi_j} \mathcal{W}_{i+1,j}^{n+1} \\ &\quad - \frac{\gamma_i \xi_j}{\beta_i \chi_j} \mathcal{W}_{i+1,j-1}^{n+1} - \frac{\alpha_i \delta_j}{\beta_i \chi_j} \mathcal{W}_{i-1,j+1}^{n+1} \\ &\quad - \frac{\alpha_i \beta_j}{\beta_i \chi_j} \mathcal{W}_{i-1,j}^{n+1} - \frac{\alpha_i \xi_j}{\beta_i \chi_j} \mathcal{W}_{i-1,j-1}^{n+1}. \end{aligned} \quad (30)$$

Applying the Fourier transform to each term in Eqn.(30), obtain

$$\begin{aligned} & \hat{\mathcal{W}}^{n+1}(\zeta, \eta) \\ & + \frac{1}{\beta\chi} \left[\gamma\delta e^{ij\zeta h + ik\eta k} + \gamma\chi e^{ij\zeta h} + \gamma\xi e^{ij\zeta h - ik\eta k} \right] \\ & \quad \times \hat{\mathcal{W}}^{n+1}(\zeta, \eta) \\ & + \frac{1}{\beta\chi} \left[\alpha\delta e^{-ij\zeta h + ik\eta k} + \alpha\xi e^{-ij\zeta h} + \alpha\xi e^{-ij\zeta h - ik\eta k} \right] \\ & \quad \times \hat{\mathcal{W}}^{n+1}(\zeta, \eta) \\ & = \frac{4k^2 h^2}{\beta\chi\tau} \hat{\mathcal{W}}^n(\zeta, \eta). \end{aligned} \quad (31)$$

Rewriting each term in terms of trigonometric functions, Eqn. (31) may be written as

$$\begin{aligned} & \beta\chi \hat{\mathcal{W}}^{n+1} \\ & + \left[\gamma\delta (\cos \zeta h + i \sin \zeta h) (\cos \eta k + i \sin \eta k) \right. \\ & \quad \left. + \gamma\chi (\cos \zeta h + i \sin \zeta h) \right] \hat{\mathcal{W}}^{n+1} \\ & + \left[\gamma\xi (\cos \zeta h + i \sin \zeta h) (\cos \eta k - i \sin \eta k) \right. \\ & \quad \left. + \alpha\delta (\cos \zeta h - i \sin \zeta h) (\cos \eta k + i \sin \eta k) \right] \\ & \quad \times \hat{\mathcal{W}}^{n+1} \\ & + \left[\alpha\xi (\cos \zeta h - i \sin \zeta h) \right. \\ & \quad \left. + \alpha\xi (\cos \zeta h - i \sin \zeta h) (\cos \eta k - i \sin \eta k) \right] \\ & \quad \times \hat{\mathcal{W}}^{n+1} \\ & = \frac{4k^2 h^2}{\tau} \hat{\mathcal{W}}^n(\zeta, \eta). \end{aligned} \quad (32)$$

The amplification factor ρ can be derived from (32) as

$$\rho = \frac{4k^2 h^2}{\tau(\mathcal{U} + i\mathcal{V})}, \quad (33)$$

where,

$$\begin{aligned} \mathcal{U} & = \beta\chi + (\gamma\delta + \alpha\xi) \cos(\zeta h + \eta k) \\ & \quad + (\gamma\chi + \alpha\xi) \cos(\zeta h) \\ & \quad + (\gamma\xi + \alpha\xi) \cos(\zeta h - \eta k), \\ \mathcal{V} & = (\gamma\delta - \alpha\xi) \sin(\zeta h + \eta k) \\ & \quad + (\gamma\chi - \alpha\xi) \sin(\zeta h) \\ & \quad + (\gamma\xi - \alpha\xi) \sin(\zeta h - \eta k). \end{aligned} \quad (34)$$

Consequently, the modulus of the amplification factor takes the form,

$$\rho\bar{\rho} = |\rho|^2 = \frac{16k^4 h^4}{\tau^2(\mathcal{U}^2 + \mathcal{V}^2)}. \quad (35)$$

Here $16h^4 k^4 \ll \tau^2$ and $\mathcal{U}^2 + \mathcal{V}^2 \leq 1$

However, $16h^4 k^4 \leq \tau^2(\mathcal{U}^2 + \mathcal{V}^2)$ and thus $|\rho|^2 \leq 1$, unconditionally. Thus, by the von Neumann criteria, the numerical scheme (14) is unconditionally stable.

4 Numerical Illustrations

This section presents numerical experiments to confirm the theoretical findings, where the accuracy of the scheme is assessed using the l_2 and l_∞ error norms defined by

$$l_2 = \frac{1}{h} \sqrt{\sum_{i=0}^N (\mathbf{W}_i - \mathbf{w}_i)^2}, \quad (36)$$

$$l_\infty = \max_i |\mathbf{W}_i - \mathbf{w}_i|.$$

In these expressions, \mathbf{w}_i denotes the numerical approximation, \mathbf{W}_i represents the exact solution at node i , and N is the total number of spatial nodes in the computational domain.

4.1 Example 1

Consider Eqn.(6) with

$$\begin{aligned} A_1 & = \frac{5x}{6}, \quad A_2 = \frac{5y}{6}, \\ B_{11} & = \frac{x^2}{6}, \quad B_{12} = B_{21} = 0, \quad B_{22} = \frac{y^2}{6}. \end{aligned} \quad (37)$$

Then the following equation is obtained:

$$\frac{\partial w}{\partial t} = -w - \frac{x}{6} \frac{\partial w}{\partial x} - \frac{y}{6} \frac{\partial w}{\partial y} + \frac{x^2}{6} \frac{\partial^2 w}{\partial x^2} + \frac{y^2}{6} \frac{\partial^2 w}{\partial y^2}, \quad (38)$$

for which the exact solution can be determined,

$$w(x, y, t) = (1 - x^2)(1 - y^2)e^{-t}, \quad -1 \leq x, y \leq 1. \quad (39)$$

A comparison of errors in l_2 and l_∞ norms for different numbers of nodes with elapsed times for the proposed schemes is presented in Table 1. Table 2 compares the proposed schemes' computed errors with existing schemes in the literature [34], and shows that the proposed simple algorithms give better results than the existing schemes.

Table 1: Comparison of errors in l_2 and l_∞ norms with $\tau = 0.0001$, $\mathcal{F} = 1$ for the Example 4.1.

Grid size	Explicit method			Implicit method			Explicit method			Implicit method		
	$\mathcal{F} = 0.1$			$\mathcal{F} = 0.1$			$\mathcal{F} = 0.25$			$\mathcal{F} = 0.25$		
	l_2	l_∞	time(s)	l_2	l_∞	time(s)	l_2	l_∞	time(s)	l_2	l_∞	time(s)
10 × 10	1.08×10^{-04}	5.32×10^{-05}	0.199525	1.01×10^{-05}	4.25×10^{-05}	0.118825	2.32×10^{-04}	9.74×10^{-05}	0.106984	2.32×10^{-05}	8.77×10^{-05}	1.932976
20 × 20	1.53×10^{-05}	4.52×10^{-05}	0.188134	2.03×10^{-05}	3.52×10^{-05}	1.596892	3.28×10^{-05}	8.21×10^{-05}	0.413535	2.57×10^{-05}	8.74×10^{-06}	3.771442
30 × 30	1.87×10^{-06}	4.52×10^{-07}	0.387606	1.21×10^{-07}	2.52×10^{-07}	2.949689	4.02×10^{-06}	7.74×10^{-07}	0.903345	3.02×10^{-07}	7.54×10^{-08}	6.742057
40 × 40	2.16×10^{-06}	5.52×10^{-07}	0.705215	3.61×10^{-07}	2.52×10^{-08}	6.945364	4.64×10^{-06}	9.24×10^{-07}	1.608009	5.64×10^{-07}	6.74×10^{-08}	17.982288
50 × 50	2.41×10^{-06}	4.52×10^{-07}	1.053064	1.32×10^{-07}	2.52×10^{-08}	10.32946	5.19×10^{-06}	7.74×10^{-07}	2.541735	5.16×10^{-07}	9.74×10^{-08}	26.486728
60 × 60	2.64×10^{-06}	3.66×10^{-07}	1.666046	1.64×10^{-07}	4.22×10^{-08}	14.307854	5.69×10^{-06}	7.22×10^{-07}	3.651856	4.69×10^{-07}	6.74×10^{-08}	44.764648
70 × 70	2.85×10^{-06}	4.33×10^{-07}	2.513052	2.86×10^{-07}	4.52×10^{-08}	18.132008	6.14×10^{-06}	6.74×10^{-07}	5.038307	6.11×10^{-07}	9.22×10^{-08}	53.097249
80 × 80	3.05×10^{-06}	5.52×10^{-07}	4.307044	2.05×10^{-07}	4.42×10^{-08}	24.037259	6.57×10^{-06}	9.01×10^{-07}	6.530545	5.75×10^{-07}	9.22×10^{-08}	6.74×10^{-08}
90 × 90	3.24×10^{-06}	3.52×10^{-07}	5.20769	2.24×10^{-07}	4.02×10^{-08}	43.586021	6.97×10^{-06}	8.74×10^{-07}	7.987636	5.97×10^{-07}	7.74×10^{-08}	119.364149
100 × 100	3.24×10^{-06}	4.52×10^{-07}	8.757617	3.41×10^{-07}	4.52×10^{-08}	54.792485	7.34×10^{-06}	9.74×10^{-07}	9.874276	7.22×10^{-07}	1.74×10^{-08}	153.558578

Table 2: Comparison of errors in l_2 and l_∞ norms of the proposed schemes with existing schemes [34] for different grid points with $\tau = 0.001$, $\mathcal{F} = 1$ for the Example 4.1.

Grid size	GFDM[34]		Explicit method		Implicit method	
	l_2	l_∞	l_2	l_∞	l_2	l_∞
55	1.14×10^{-04}	2.11×10^{-03}	1.03×10^{-04}	1.84×10^{-05}	1.03×10^{-05}	1.84×10^{-05}
197	3.19×10^{-05}	5.90×10^{-04}	1.95×10^{-05}	1.65×10^{-06}	1.87×10^{-06}	2.87×10^{-07}
743	8.45×10^{-06}	1.57×10^{-04}	2.86×10^{-06}	1.03×10^{-07}	2.56×10^{-07}	1.23×10^{-08}

4.2 Example 2

Consider Eqn.(6) with

$$A_1 = \frac{4w}{x} + \frac{x}{6}, \quad A_2 = \frac{4w}{y} + \frac{y}{6}, \quad (40)$$

$$B_{11} = B_{22} = w, \quad B_{12} = B_{21} = 0.$$

The resulting FPE is

$$\begin{aligned} \frac{\partial w}{\partial t} = & \frac{4w^2}{x^2} + \frac{4w^2}{y^2} - \frac{w}{3} + \frac{\partial w}{\partial x} \left(\frac{-x}{6} - \frac{8w}{x} \right) \\ & + \frac{\partial w}{\partial y} \left(\frac{-y}{6} - \frac{8w}{y} \right) \\ & + 2w \frac{\partial^2 w}{\partial x^2} + 2w \frac{\partial^2 w}{\partial y^2} + 2 \left(\frac{\partial w}{\partial x} \right)^2 + 2 \left(\frac{\partial w}{\partial y} \right)^2, \end{aligned} \quad (41)$$

that admits an exact analytical solution

$$w(x, y, t) = x^2 y^2 e^{-t}, \quad 0 \leq x, y \leq 1. \quad (42)$$

The numerical errors of the proposed schemes, evaluated using the l_2 and l_∞ norms, are summarized in Table 3. To further assess the performance and reliability of the proposed methods, their accuracy is compared with that of an established approach [34] in Table 4.

5 Conclusion

In this work, the two-dimensional FPE was systematically analyzed using finite difference schemes constructed through an operator splitting approach. Full discretizations of the model were developed, and their reliability was confirmed through both linear and nonlinear two-dimensional examples with variable coefficients. The proposed algorithms were thoroughly analyzed for stability using von Neumann's criterion. The explicit formulation proved to be temporally first-order and spatially second-order accurate, whereas the implicit formulation achieved second-order accuracy in both temporal and spatial domains. To illustrate the effectiveness and computational advantage of the proposed strategies, their outcomes were contrasted with those of a more sophisticated but resource-demanding approach documented in earlier studies. The error analysis, conducted using multiple norms, indicates that the proposed schemes not only provide high accuracy but also offer a competitive and efficient alternative for solving two-dimensional FPEs.

Acknowledgements: The authors deeply and gratefully acknowledge the generous financial support extended by the Ministry of Human Resource Development, Government of India, and the University Grants Commission, Government of India, through a research grant, which made this work possible. The authors sincerely thank the anonymous reviewers whose insightful observations, careful evaluations, and thoughtful suggestions have played a vital role in strengthening this work.

Table 3: Comparison of errors in l_2 and l_∞ norms with $\tau = 0.0001$, $\mathcal{T} = 1$ for the Example 4.2.

Grid size	Explicit method		Semi-implicit method		Explicit method		Semi-implicit method	
	$\mathcal{T} = 0.25$		$\mathcal{T} = 0.025$		$\mathcal{T} = 0.3$		$\mathcal{T} = 0.3$	
	l_2	l_∞	l_2	l_∞	l_2	l_∞	l_2	l_∞
15 × 15	4.94×10^{-03}	7.79×10^{-03}	4.70×10^{-03}	7.41×10^{-03}	1.99×10^{-04}	6.75×10^{-05}	1.84×10^{-04}	6.24×10^{-05}
25 × 25	9.32×10^{-03}	6.29×10^{-03}	4.69×10^{-03}	4.08×10^{-03}	2.57×10^{-04}	6.79×10^{-05}	2.37×10^{-04}	6.28×10^{-05}
35 × 35	3.63×10^{-03}	8.80×10^{-03}	8.85×10^{-03}	8.18×10^{-04}	3.04×10^{-04}	6.80×10^{-05}	2.81×10^{-04}	6.29×10^{-05}
45 × 45	4.93×10^{-04}	7.83×10^{-04}	7.27×10^{-04}	7.23×10^{-04}	3.45×10^{-04}	6.81×10^{-05}	3.19×10^{-04}	6.29×10^{-05}
55 × 55	9.25×10^{-04}	3.07×10^{-04}	6.64×10^{-04}	1.82×10^{-04}	3.81×10^{-05}	6.81×10^{-06}	3.52×10^{-05}	6.29×10^{-06}
65 × 65	5.40×10^{-04}	8.01×10^{-04}	4.74×10^{-04}	2.21×10^{-04}	4.14×10^{-05}	6.81×10^{-06}	3.83×10^{-05}	6.23×10^{-06}
75 × 75	9.83×10^{-04}	8.80×10^{-05}	4.69×10^{-04}	7.21×10^{-05}	4.45×10^{-06}	6.81×10^{-06}	4.11×10^{-06}	6.32×10^{-06}
85 × 85	2.61×10^{-04}	7.83×10^{-05}	9.42×10^{-05}	1.72×10^{-05}	4.74×10^{-06}	6.81×10^{-06}	4.38×10^{-06}	6.29×10^{-06}
95 × 95	6.02×10^{-05}	7.83×10^{-05}	4.21×10^{-05}	1.80×10^{-05}	5.01×10^{-06}	6.81×10^{-07}	4.63×10^{-06}	6.29×10^{-07}
105 × 105	2.60×10^{-05}	8.01×10^{-06}	7.75×10^{-06}	7.42×10^{-06}	5.27×10^{-07}	6.81×10^{-07}	4.87×10^{-07}	6.30×10^{-07}

Table 4: Comparison of errors in l_2 and l_∞ norms of the proposed schemes with existing schemes [34] for different grid points with $\tau = 0.001$, $\mathcal{T} = 1$ for the Example 4.2.

Grid size	GFDM[34]		Explicit method		Implicit method	
	l_2	l_∞	l_2	l_∞	l_2	l_∞
55	3.61×10^{-04}	6.70×10^{-04}	1.82×10^{-04}	5.72×10^{-04}	4.81×10^{-04}	8.59×10^{-05}
197	1.01×10^{-04}	1.82×10^{-04}	2.85×10^{-06}	7.34×10^{-06}	1.06×10^{-05}	9.98×10^{-06}
743	2.01×10^{-05}	3.79×10^{-05}	5.48×10^{-06}	7.42×10^{-06}	4.03×10^{-06}	6.81×10^{-07}

References

- H. Risken, "Fokker-Planck equation," in *The Fokker-Planck Equation*, Springer, (1996)
- R. Bailo, J. A. Carrillo, J. Hu, "Fully discrete positivity-preserving and energy-decaying schemes for aggregation-diffusion equations with a gradient flow structure," *Preprint*, (2018)
- M. Bessemoulin-Chatard, F. Filbet, *SIAM J. Sci. Comput.*, **34** (2012)
- H. Liu, Z. Wang, *J. Sci. Comput.* **68**, (2016)
- H. Liu, H. Yu, *J. Sci. Comput.*, **62** (2015)
- H. Liu, H. Yu, *SIAM J. Sci. Comput.*, **36** (2014)
- Y. Qian, Z. Wang, S. Zhou, *J. Comput. Phys.*, **386** (2019)
- J. A. Carrillo, Y. Huang, F. S. Patacchini, and G. Wolansky, arXiv:1512.03029, (2015)
- A. S. Neena, D. P. Clemence-Mkhope, A. Awasthi, *J. Eng. Math.*, **145** (2024)
- M. P. Zorzano, H. Mais, L. Vazquez, *Appl. Math. Comput.*, **98** (1999)
- M. Dehghan, M. Tatari, *Phys. Scr.*, **74** (2006)
- W. Gerstner, W. Kistler, R. Naud, and L. Paninski, *Neuronal Dynamics: From Single Neurons to Networks and Models of Cognition*, Cambridge Univ. Press, (2014)
- W. Hundsdorfer and J. Verwer, *Numerical Solution of Time-Dependent Advection-Diffusion-Reaction Equations*, Springer, (2013)
- H.-J. Bungartz, M. Griebel, *Acta Numer.*, **13** (2004)
- Y. Sun, M. Kumar, *Comput. Math. Appl.*, **67** (2014)
- V. Kazeev, O. Reichmann, C. Schwab, *Linear Algebra Appl.*, **438** (2013)
- J. Shen, T. Tang, and L.-L. Wang, *Spectral Methods: Algorithms, Analysis and Applications*, Springer, 2011.
- J. Hu, and al. *J. Comput. Phys.*, **433** (2021)
- C. Duan, et al., *Math. Methods Appl. Sci.*, **45** (2022)
- C. Liu, Y. Gao, X. Zhang, *J. Sci. Comput.*, **98** (2024)
- H. Zhang, et al., *Nonlinear Dyn.*, **108** (2022)
- J. Brunken, K. Smetana, *SIAM J. Numer. Anal.*, **60** (2022)
- K. Tang, X. Wan, Q. Liao, *J. Comput. Phys.*, **457** (2022)
- T.-j. Wang, G. Chai, *Appl. Numer. Math.*, **174** (2022)
- Y. Zhang, K. Yuen, *Int. J. Non-Linear Mech.*, **147** (2022)
- S. Liu, et al., *SIAM J. Numer. Anal.*, **60** (2022)
- K. Srinivasa, H. Rezazadeh, W. Adel, *Math. Methods Appl. Sci.*, **45** (2022)
- M. M. Butt, *Math. Comput. Simul.*, **180** (2021)
- Y. Chen, X. Deng, *Phys. Rev. E*, **98** (2018)
- Y. Chen, X. Deng, *Phys. Rev. E*, **100** (2019)
- Y. Lin, and al. *J. Phys. Conf. Ser.*, **2437** (2023)
- H. Touchette, T. Prellberg, W. Just, *J. Phys. A*, **45** (2012)
- A. Sreelakshmi, V. P. Shyaman, A. Awasthi, *Appl. Numer. Math.*, **197** (2024)
- F. Ureña, et al., *Appl. Math. Comput.*, **368** (2020)
- A. S. Neena, D. P. C. Mkhope, A. Awasthi, *Int. J. Appl. Comput. Math.*, **8** (2022)